THESIS

DEPOSITIONAL SYSTEM, FACIES RELATIONS & RESERVOIR CHARACTERISTICS OF THE CODELL SANDSTONE, COLORADO

Submitted by

Donna C. Caraway

Department of Earth Resources

In partial fulfillment of the requirements

for the degree of Master of Science

Colorado State University

Fort Collins, Colorado

Summer, 1990

COLORADO STATE UNIVERSITY

January 20, 1990

WE HEREBY RECOMMEND THAT THE THESIS PREPARED UNDER OUR SUPERVISION BY DONNA C. CARAWAY ENTITLED DEPOSITIONAL SYSTEM, FACIES RELATIONS & RESERVOIR CHARACTERISTICS OF THE CODELL SANDSTONE, COLORADO BE ACCEPTED AS FULFILLING IN PART REQUIREMENTS FOR THE DEGREE OF MASTER OF SCIENCE.

Committee on Graduate Work

[redacted]

[redacted]

[redacted]

Adviser

[redacted]

Department Head

ABSTRACT

DEPOSITIONAL SYSTEM, FACIES RELATIONS & RESERVOIR CHARACTERISTICS OF THE CODELL SANDSTONE, COLORADO

Deposition of the Turonian Codell Sandstone member of the Carlile Shale in north-central Colorado occurred along the western margin of the Cretaceous Epeiric Seaway. Abrupt and irregular facies relationships, gross sheet-like geometry with internal linear thickness trends, ichnofacies arrangement, and stratigraphic positioning suggest an inner shelf depositional origin. The Codell sandstone is initially sourced from Frontier equivalent delta systems in Wyoming during the 90 m.y.a. lowstand and is thought to represent the shelf component of a transgressive system tract which developed during the subsequent Niobrara cycle transgression. Storm processes operating along the inner shelf margin produced amalgamated storm sheet deposits of mid-late Turonian age. Deepening of the seaway restricted sediment influx onto the shelf which resulted in the cannibalization of the previously deposited shelf sediments. This change is marked by a marine flooding surface which separates the inner shelf sediments from the winnowed condensed section above. The silica or calcite-cemented uppermost bed of the Codell Sandstone represents the winnowed cap of a condensed section produced by this starved basin condition. Further deepening of the seaway placed the shelf floor beyond the reach of epidsodic storm processes and is marked by an abrupt litholgic transition into marine limestone deposits. This contact is referred to as a basinal sequence boundary.

Production from the Codell Sandstone consists predominantly of Volatile Oil (GOR between 1000 and 5000 SCF/STBO) or Retrograde Gas Condensate (high API gravities and GOR between 5,000-100,000 SCF/STBO). Distribution of the production patterns depends primarily upon proximity to the faulted basin axis and thicker Codell Sandstone intervals. High GOR's created from the increased thermal gradients and fluid conductivity associated with the major basin-syncline bounding faults charged the system with solution driven gas. This produces an extremely mobile hydrocarbon environment. Because the Codell Sandstone is porous, but fairly impermeable, any reversal in dip direction or en-echelon arranged fault system updip from the down-dropped basin axis, provides a potential site for hydrocarbon accumulation. Correspondence of better production rates near fault systems in areas of slightly thicker sandstone indicates that the trapping mechanism is both a fuction of stratigraphy and structural relationships (a combination trap).

Secondary porosity, developed from the dissolution of unstable framework constituents (plagioclase feldspar grains and rock fragments), allows hydrocarbon accumulation in an interval that would otherwise contain too much clay to be normally productive. The Codell Sandstone contains quartz grains and layered phyllosilicates (illite, illite/smectite, and chlorite). Subsidiary amounts of plagioclase feldspar and pyrite are also present. The abundant distribution of detrital clay in this interval, is due in part, to extensive bioturbation. Dissolution of calcite cement also enhances the development of secondary porosity in the Codell Sandstone. Extensive artificial fracturing techniques and weakly acidic delivery systems are the most efficient completion practices yet developed for this interval.

Donna Cathryn Caraway
Department of Earth Resources
Colorado State University
Fort Collins, CO 80523
Summer, 1990

ACKNOWLEDGEMENTS

It is is difficult to summarize the help, support and inspiration given me (and my thesis) over the last three years of academic pursuit. First, my advisor Frank G. Ethridge, deserves many thanks for his prodding, thoughtful discussions, and loud-voiced encouragement. Both myself and consequently my work greatly benefited from the close association with fellow graduate students Wendy Sumner, Maria Wood, Jim Haerter, Ana Vargo, Terri Craig, and John Evans. Their boundless curiosity, late-night discourses, and mutual support made the whole experience worthwhile. Three other professors in the Department of Earth Resources; Lary Burns, Eric Erslev, and Michael Harvey provided enthusiastic, insightful, and thought-provoking tutelage.

Logistical and technical support has been provided by Dave Ferderer, Don Johnson, and Bob Marolda of Energy Minerals Corporation; Paul Thompson, Boettcher Quarry, Ideal Cement Company; and ARCO Oil and Gas Company. Without their willingness to supply subsurface data, access to outcrop, and technical assistance, this study would not have reached fruition. I am very grateful for their help.

There are a number of people I need to thank outside of the university environment. John Barwis, Shell Development Company and Kristian Meisling, ARCO Oil & Gas Company willingly made time in their busy schedules to review and critique portions of this manuscript. My writing improved because of their thoughtful comments. Laura Helsel of ARCO Oil & Gas Company stepped in at the last minute to assist me in physically putting together the manuscript. Without her help, I would still be pasting figure captions in 1990. John Balsley, AAPG Field Seminar Program provided the

opportunity for me to examine strandline/shelf systems in outcrop and core. His knowledgeable field observations, wry humor, and passion for sedimentology and nature in general, helped me again realize the joy and satisfaction in trying to piece together a small portion of the earth. Jack and Barb Grace of Leadville, Colorado adopted me as one of their own which helped ease the difficulties of becoming a student again.

Finally, I am most grateful to my family; parents, Perry and Martha Caraway, grandmother, Mrs. L.E. Rambo, and aunt and uncle, Betty and Frank Tandy who provided financial assistance through my schooling. Their faith in me and support of an endeavor which seemed to have more 'lows' than 'highs', reaffirms my belief in what a family can be.

To everyone mentioned above, and those people I have unintentionally overlooked - Thank you.

I have no doubt at all the Devil grins,
As seas of ink I splatter.
Ye gods, forgive my 'literary' sins -
The other kind don't matter.

Robert Service (1907)

DEDICATION

In Memory of

Mrs. Katherine Finch

Mrs. Ruby Adams Gentry

TABLE OF CONTENTS

LIST OF TABLES

LIST OF FIGURES

CHAPTER I

Introduction

Purpose and Methodology

Recognition of the Upper Cretaceous Codell Sandstone as a new exploration target in an extensively drilled portion of the Denver-Julesburg basin (D-J basin), Colorado occurred in 1979 and 1980. Previous to that time, exploration and production in the west-central portion of the D-J basin was confined to the lower Cretaceous Dakota Group which includes the "D" and "J" fluvial/deltaic sandstones; and in the Upper Cretaceous shallow marine sandstone bodies of the Hygiene interval. Subsequent drilling in 1982 - 1984 proved that the interval contained significant reserves because of its broad lateral continuity in northeastern Colorado. Plunging oil prices in 1985 and 1986 induced waning interest in exploration efforts, although in-field development drilling continues at the present time. Approximately thirty exploration firms completed gas/condensate wells in the Codell Sandstone or have acquired an acreage position in anticipation of future exploration in this zone. Despite these efforts, no detailed surface/subsurface study integrating the geometry, depositional environment, facies relationships and diagenesis has been published in the area of established Codell production in northeastern Colorado (Figure 1).

With the exception of a thermal maturation and source rock study, previous investigations dealing with the Codell Sandstone are generally confined to the southwestern portion of the Denver-Julesburg basin. In the area of established production in northeastern Colorado, the unit has been scrutinized in detail by in-house

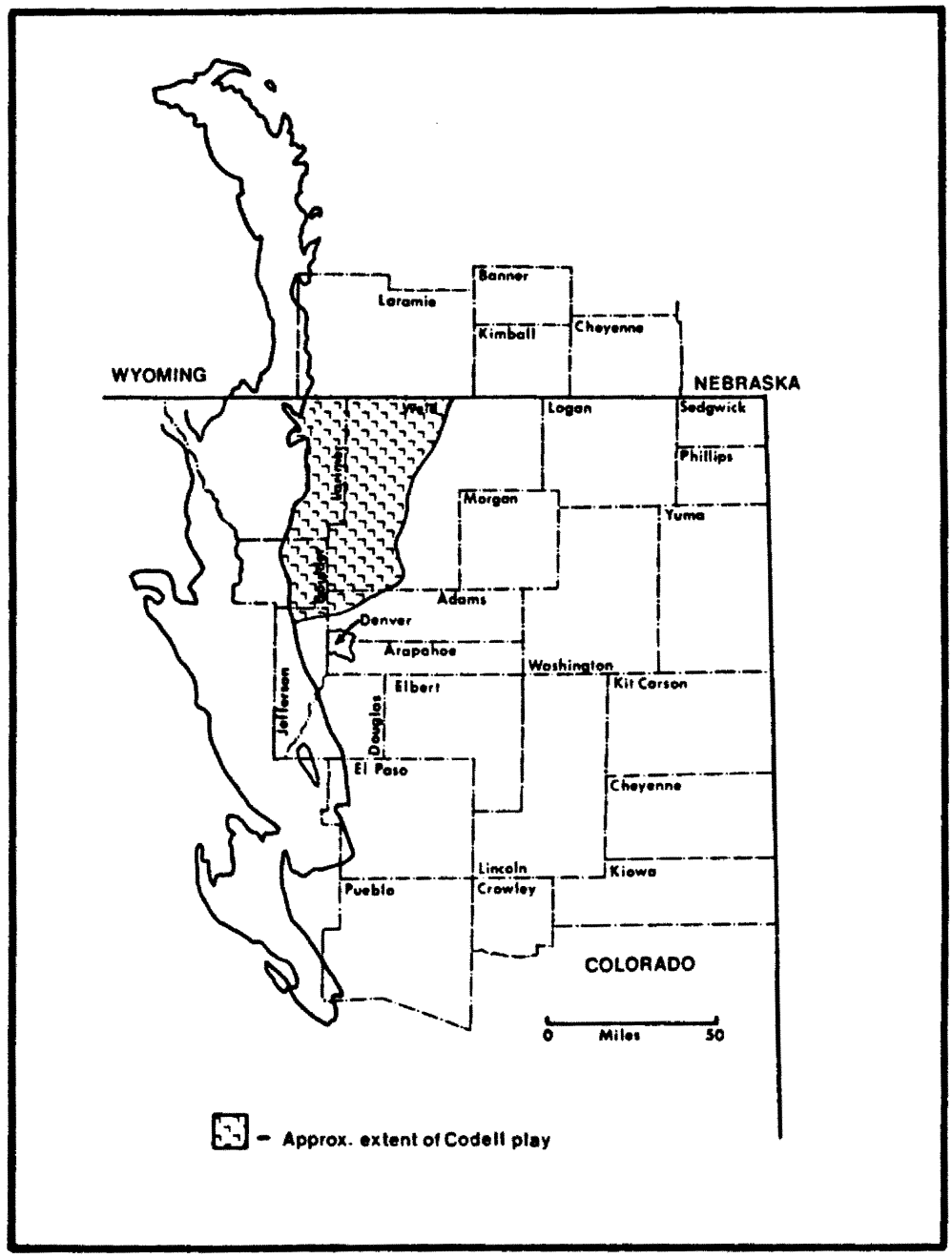

Figure 1. Location of the present extent of the Codell play in the north central Denver-Julesburg basin, Colorado.

geologists affiliated with oil and gas firms whose findings are mostly proprietary in nature. The objectives of this study were:

I. Determination of the depositional system and facies relationships of the Codell Sandstone in northcentral Denver-Julesburg basin, Colorado using subsurface and outcrop data.

II. Delineation of reservoir geometry, production trends, structural and stratigraphic relationships so that future exploration and development in this interval will be optimized.

III. Analyze the compositional elements of the Codell Sandstone and their effects on diagenesis and hydrocarbon recovery in the play area.

Construction of a model of deposition and diagenesis will facilitate future exploration efforts and aid in the efficient use of appropriate completion techniques. In addition, knowledge gained from the study of the Codell Sandstone can be used to understand analogous very fine-grained offshore, marine sandstone intervals which are common in Cretaceous sediments of the Rocky Mountain region.

Standard methodologies were used to investigate the characteristics and distribution of the Codell Interval. In addition, trend-surface analyses were utilized to analyze the stratigraphy and unconformity relationships. The methodology and techniques listed below were used in achieving the overall purpose of this study.

I. Lithologic profiles of outcrops and stratigraphic cross-sections along the western margin of the D-J basin were constructed.

II. Core, subsurface log information, and stratigraphic profiles were integrated and correlated using cross-sections and photographs to document different lithologies, geometry, and facies relationships.

III. Over 500 subsurface wireline logs were analyzed and isopach, isolith, and structure contour maps were constructed to delineate geometry, production trends, and structural controls on the sandstone. In addition, initial production and formation pressure data

were correlated to identify the highest quality reservoir facies in the Codell.

IV. Petrographic, SEM, and X-ray diffraction techniques were used to determine composition and textural relationships which affect the reservoir quality. Data on texture, grain composition, types and amounts of porosity, and distribution and types of clays and cements were collected during this phase of the study.

V. Computer assisted, trend-surface software was utilized to construct three-dimensional trend surfaces. These plots helped to investigate the hydrocarbon accumulation patterns and overall stratigraphy of the Codell interval.

Location

Surface sections of the Codell Sandstone were measured in T6N and T7N - R69W, Larimer County, Colorado (Figure 2). These sections are located along the steeply dipping western flank of the D-J basin (Figure 3). Three sections along a three mile discontinuous outcrop, oriented in a north-south direction, were measured along the foothills of the Front Range of Colorado (Figure 2). These sections were correlated with over 500 wells in Weld, Larimer, and Boulder counties of northeastern Colorado. Subsurface log information from wells in T3N - T6N, R69W - R65W, were integrated into maps. Figure 4 depicts major fields located in or near the Codell play. In addition, the specific location of outcrop and core sections correlated in this study are depicted numerically. The area studied covers approximately 1/2 of the Codell play, in which both active exploration efforts continue and established production exists.

General Stratigraphy

The middle-late Turonian Codell Sandstone member of the Carlile Shale is a widespread sandstone interval in the west-central portion of the D-J basin. In a generalized stratigraphic column for the D-J basin, Pearl (1980) gave the unit formation status (Figure 5). However, most workers believe the sandstone to be the one of the

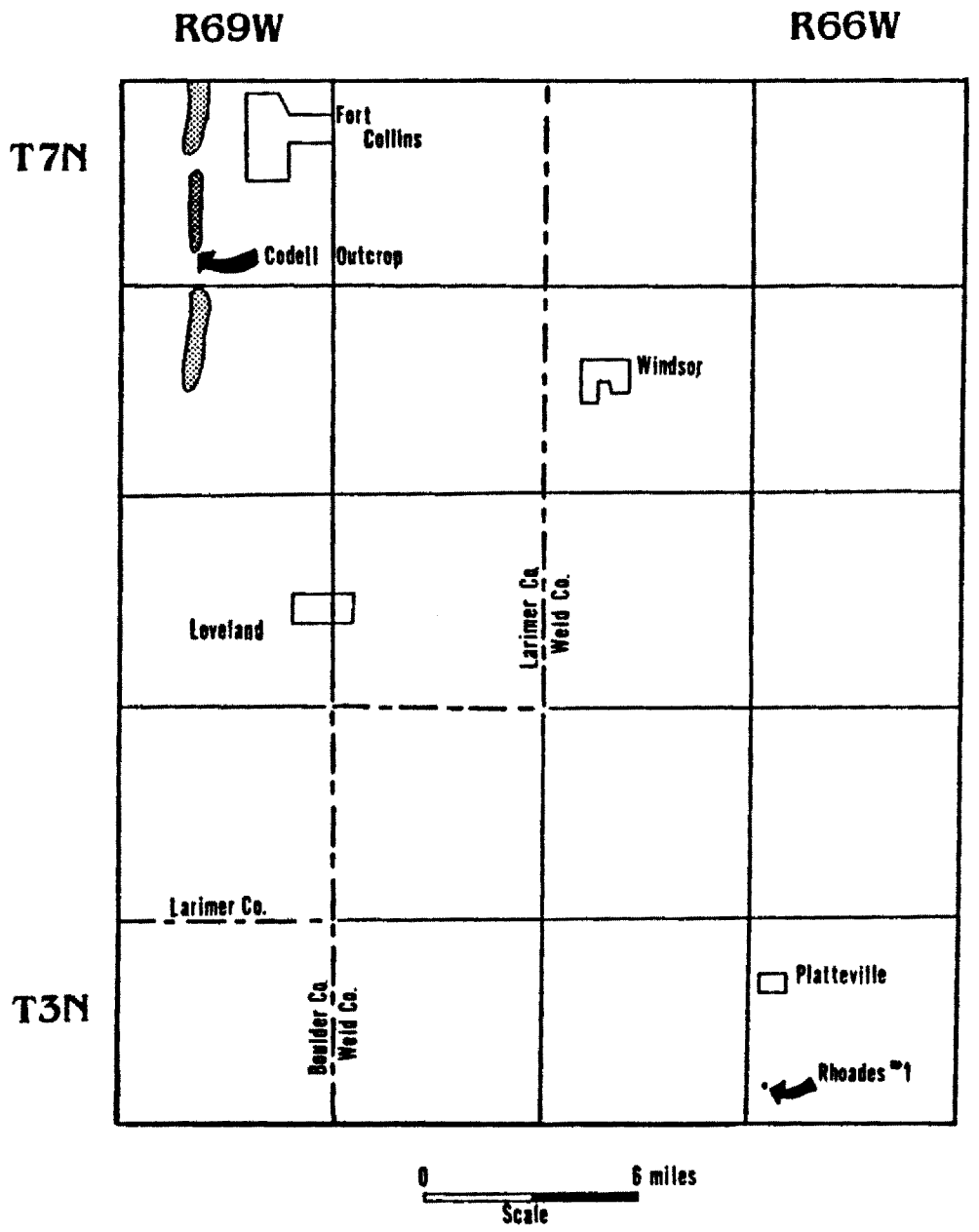

Location of Codell Outcrop in relation to cored interval in Rhoades #1 - north-central Denver-Julesburg Basin, Colorado

Figure 2. Location of surface sections measured along the extreme western edge of the Denver-Julesburg basin, Colorado.

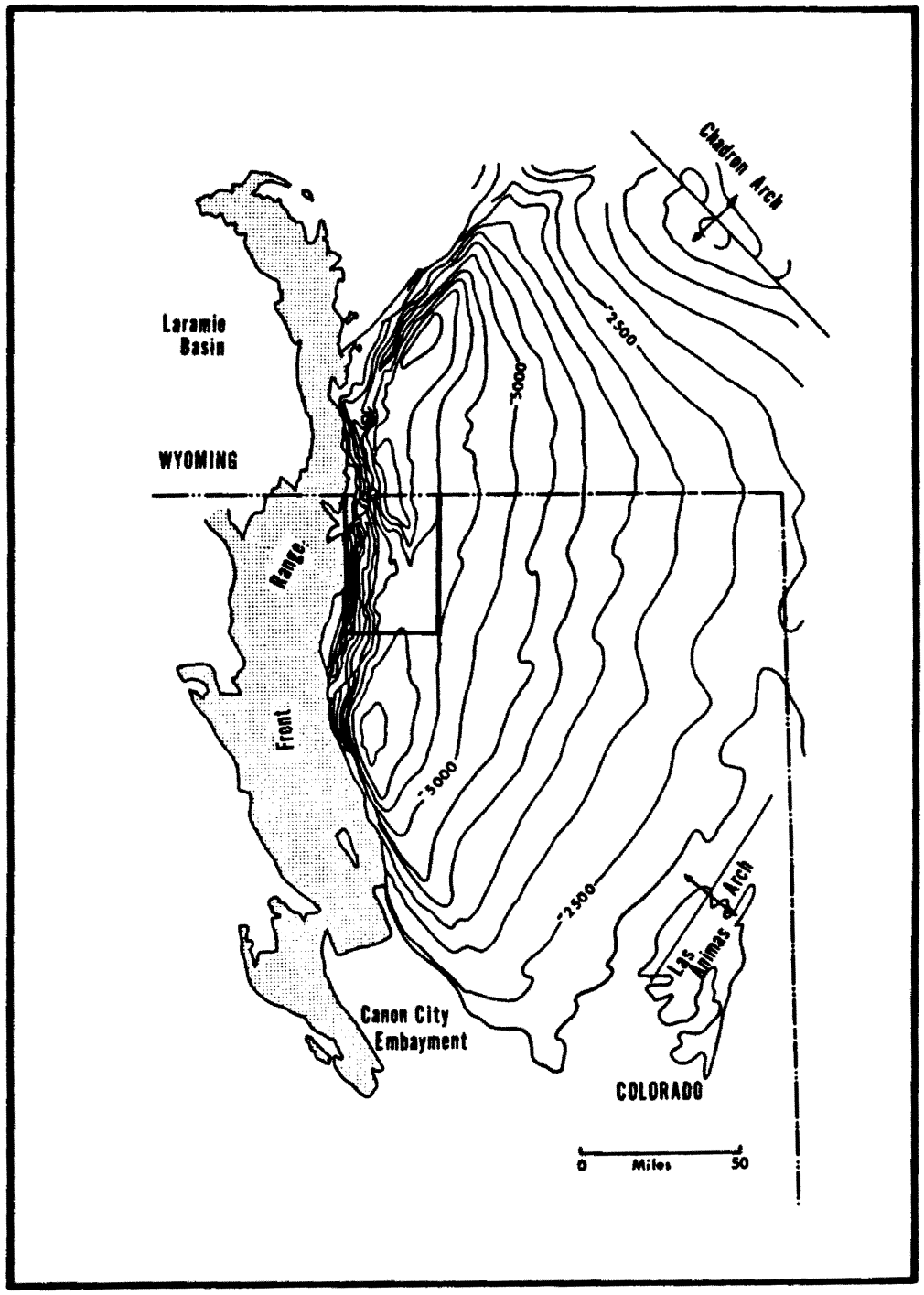

Figure 3. Approximate extent of study area outlined by rectangle, superimposed on the Denver-Julesburg basin structure contour map. Contoured on the Precambrian basement surface (modified from Martin, 1965).

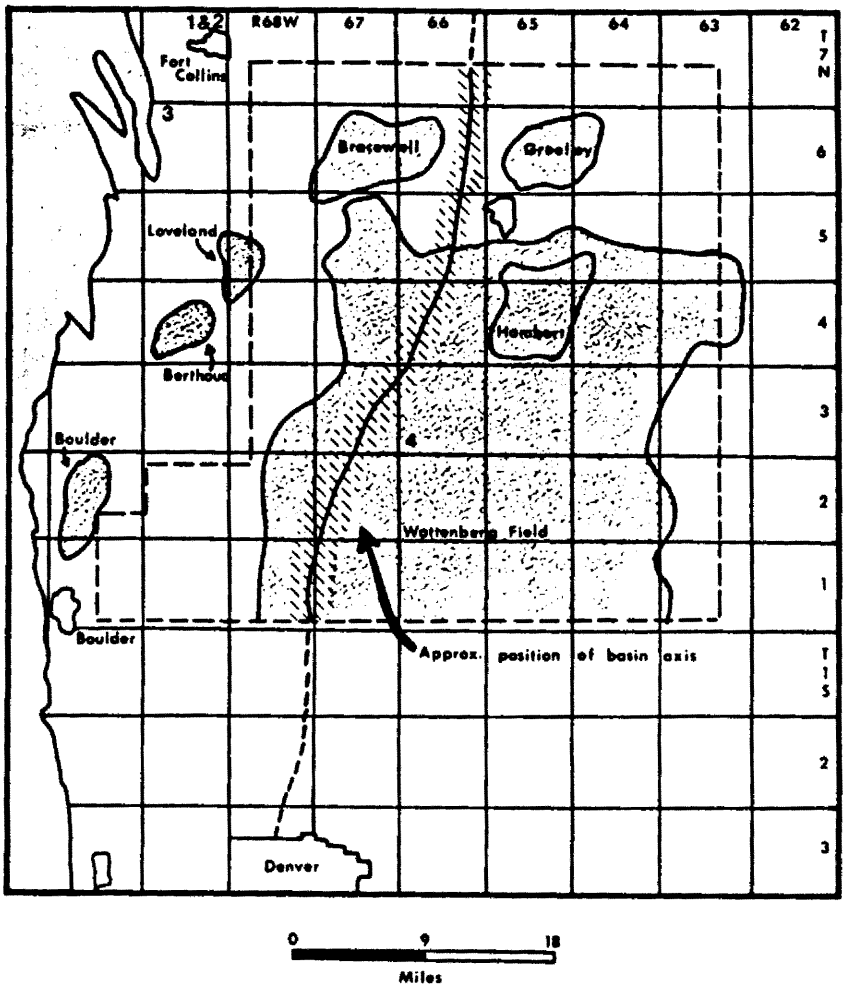

Figure 4. Position of basin axis in the dashed outline of the Codell play. Field outlines are portrayed and outcrop/core locations are listed numerically.

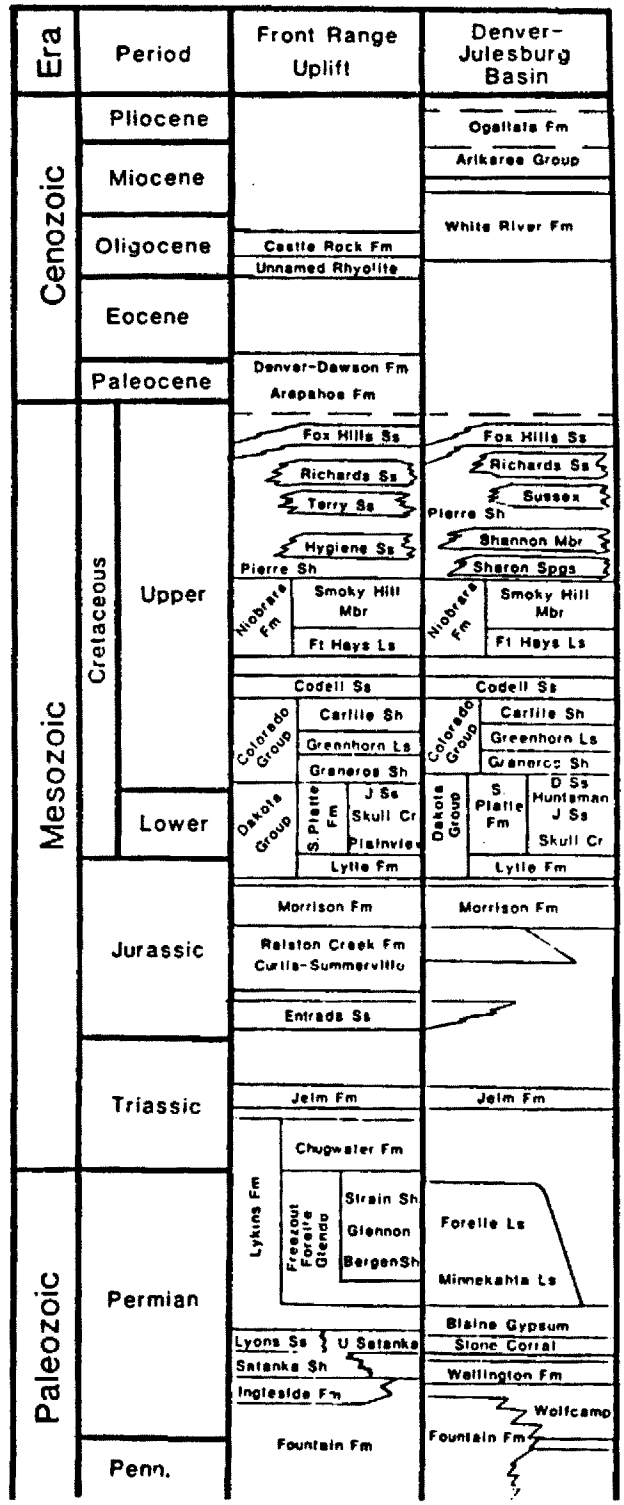

Figure 5. Stratigraphic nomenclature for late Paleozoic, Mesozoic, and Cenozoic eras for the Front Range Uplift and Denver-Julesburg basin of Colorado (modified after Pearl, 1980).

uppermost members of the Carlile Shale (Figure 6). Marine processes account for over 6500 feet (1981 m) of shale, shaly sandstone, and limestone accumulation in the basin during the middle-late Cretaceous. These sediments represent Upper Cretaceous sedimentation in and along the western margin of the Cretaceous Epeiric Seaway which divided the North American continent into western and eastern parts (Figure 7). The Carlile Shale interval, which contains the Codell is part of a regionally extensive Upper Cretaceous marine shale sequence over 350 feet (106.7 m) thick, variously named the Benton or Colorado Group (Figure 6).

Lower Cretaceous sediments in this portion of the basin consist of fluvial/deltaic sandstones and shales of the Dakota Group (Figure 5), whose terrigenous clastic sediment source was located both to the east and west of the seaway (Aulia, 1982; Weimer, 1960). During late Cretaceous time the dominant source of sediment influx shifted to the west in response to the Sevier Orogenic Uplift in what is presently western Utah and Wyoming (Lowman, 1977; Weimer, 1960). As the interior seaway enlarged in response to major eustatic transgressions and tectonic downwarping, the Benton Group sediments were deposited in the following order; first, the Graneros Shale, followed by the Greenhorn Limestone, and finally, the Carlile Shale interval (Figure 5). The Carlile Shale is subdivided into the Fairport, Blue Hill, Codell, and Juana Lopez members (Figure 6). The Fairport and Blue Hill members are composed of dark gray to black silty, shale which was deposited under normal marine conditions. Stratified to burrowed fine-grained sandstone, siltstone, and shale sequences comprise the Codell and Juana Lopez members of the Carlile Shale.

In the northern part of the D-J basin, the basal contact of the Codell Sandstone appears gradational into the underlying Blue Hill Shale. However, some workers suggest that a disconformable relationship exists based on missing faunal zones in time equivalent sandstone/shale sequences in Wyoming and a progressive westward truncation of the lower Carlile from Kansas and Nebraska (Weimer, 1983; Merewether, Cobban, & Cavanaugh, 1979).

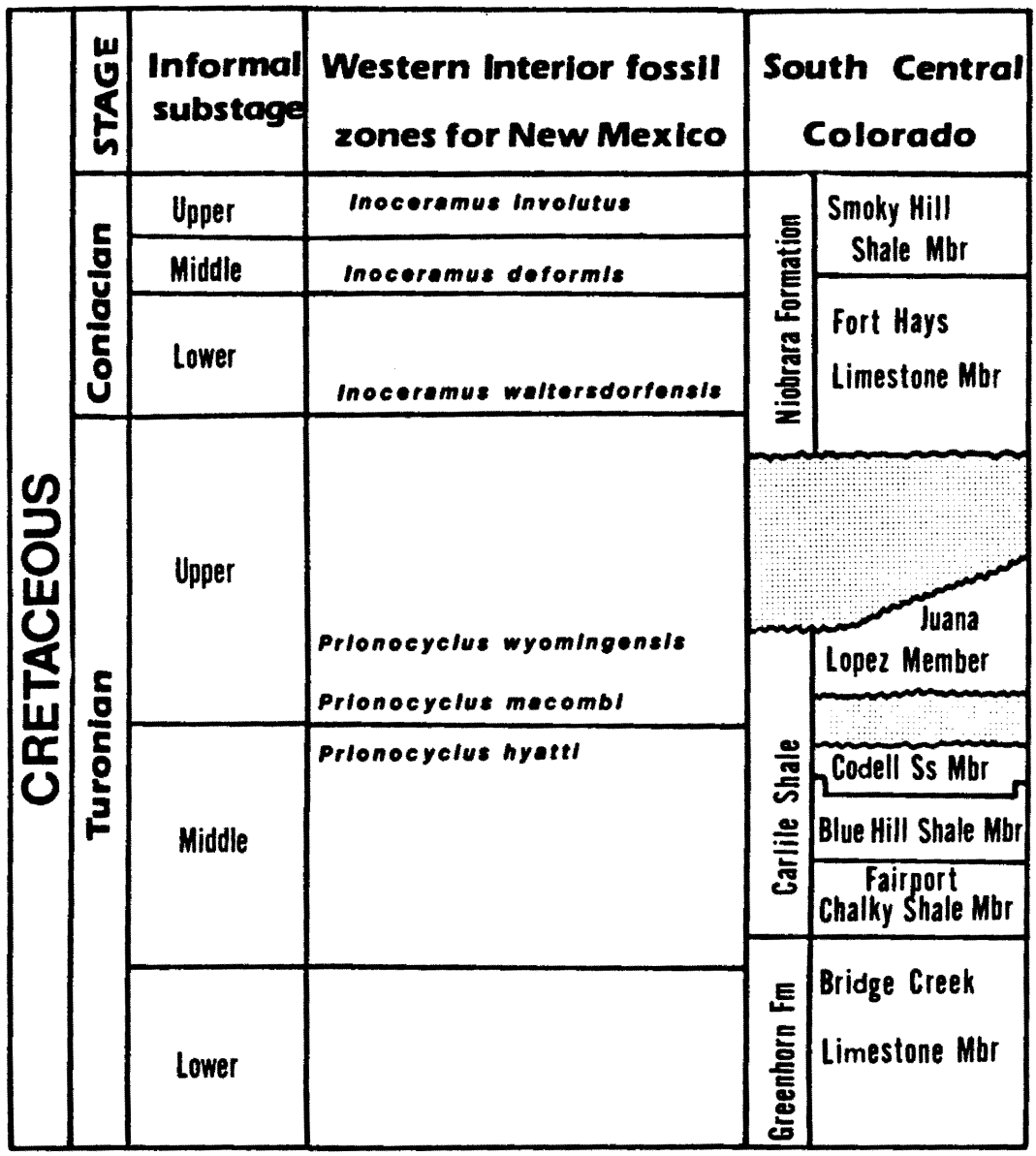

After Cobban, Merewether, Molenaar, 1983

Figure 6. Time-stratigraphic relationships of the Carlile Shale and Niobrara Formation for south central Colorado.

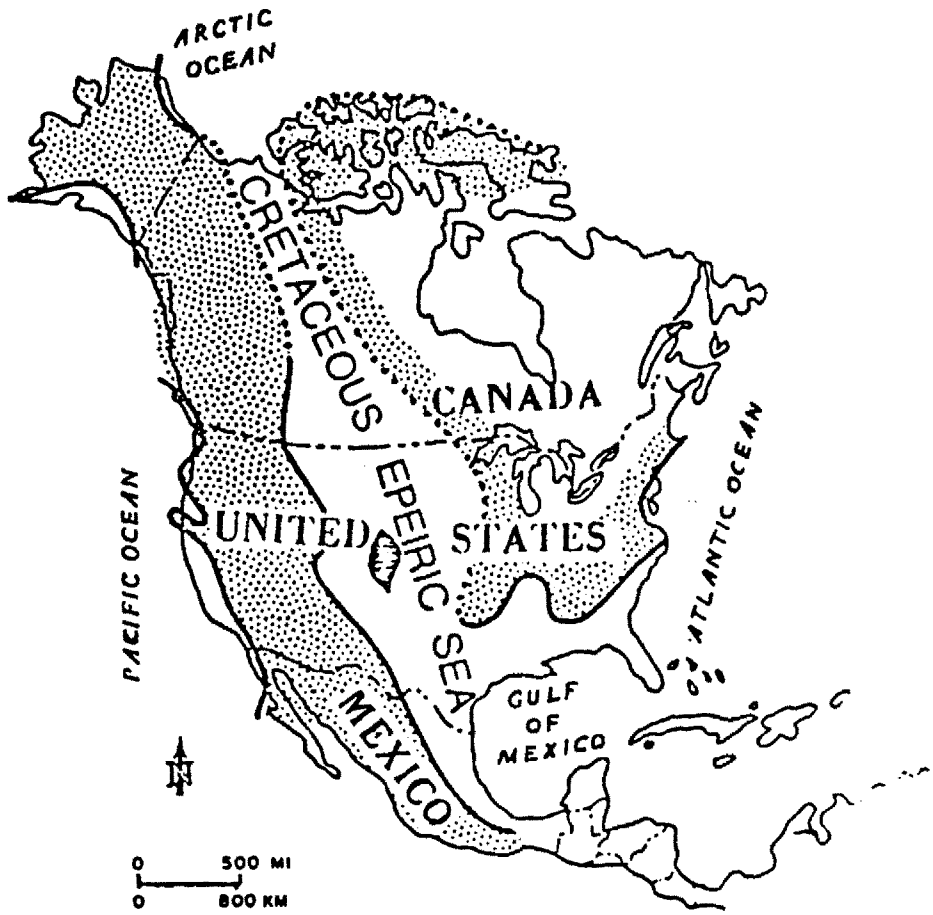

Figure 7. Probable distribution of land and sea in North America during late Cretaceous time showing the geographic position of the epeiric seaway that divided the continent into eastern and western parts. The Denver-Julesburg basin is located in the west central portion of the seaway (modified from Gill & Cobban, 1973).

The Codell is unconformably overlain by the Fort Hays limestone member of the Niobrara Formation in the north-central portion of the basin and unconformably overlain by the Juana Lopez member of the Carlile Shale in the south-central part of the basin, approximately south of Denver (Weimer, 1983; McClane, 1982; Pinel, 1977). Some confusion exists as to whether the uppermost Codell in the study area is actually part of the Juana Lopez (Lowman, 1977; Weimer, 1983). At any rate, a major basin-wide unconformity is postulated between uppermost Carlile and lowermost Niobrara strata in Colorado and adjacent states on the basis of 2-5 missing faunal zones and abrupt lithology changes.

Following Codell deposition, the overlying Niobrara limestone and Pierre Shale were deposited in the Cretaceous Seaway. The thick pile of interbedded shale, sandstone, and limestone deposits in the D-J basin created the conditions needed for subsequent hydrocarbon generation and emplacement. For generation and entrapment of hydrocarbon, several requirements are necessary; 1) accumulation of thick sequences of source rock (i.e. organic rich shales or limestones, 2) adequate depth of burial, 3) the existence of potential reservoir facies in the basin, 4) trapping mechanisms and seals (i.e. stratigraphic pinch-out, anticlinal structures, faulting, etc.), and 5) proper timing of hydrocarbon maturation, and migration. In addition, an advantageous diagenetic overprint in the potential reservoir is usually helpful (i.e. increased porosity). Both Lower and Upper Cretaceous sediments in the Denver-Julesburg basin meet these requirements and have proven to be a prolific source of gas/condensate and to a lesser degree, moderate-high gravity, 'sweet' oil.

Regional Structural Setting

The D-J basin is bounded on the west by the Front range of Colorado and the Laramie Range of Wyoming, on the northeast by the Chadron Arch, and on the southeast by the Las Animas Arch (Figure 3). The basin spans most of eastern Colorado, southeastern Wyoming and southwestern Nebraska. Contours of the Precambrian basement surface produce a decidedly asymmetric basinal trough bounded by a steeply dipping western flank and a gently dipping easter flank (Figure 3). Codell production straddles both sides of the basin axis, however, 60-65% of established production is concentrated east of the axis (Figure 4).

Precambrian basement rocks form the core of the Front Range Uplift adjacent to the basin, and are composed of schists and gneisses which are intruded by granitic batholiths and complex granitic dike swarms. Structural relief across the abrupt edge of the uplift as measured by displacement of basement rock is approximately 20,000 feet (6096 m) (LeMasurier, 1970). Axes of both the Front Range and the D-J basin are subparallel and trend northward. Early mapping along the Front Range between Longmont, Colorado and the state line of Wyoming, distinguished the belt of north-to-northwest trending faults and en echelon folds that mark the edge of the uplift (Figure 8). Typically, the faults dip to the northeast at a high angle and have been mapped as either high angle reverse or normal faults. The en echelon, north-south trending folds are of two kinds: south-plunging asymmetrical folds which are steeper on the west (e.g. Loveland anticline), and doubly plunging symmetrical box folds (e.g. Bellvue Dome). Hogback ridges of exposed Pennsylvanian-Permian and Cretaceous sedimentary strata which dip to the east at a high angle flatten out rapidly eastward into the basin. These ridges flank the uplift and form the topographic break which defines the western extent of the basin.

According to Tweto, 1975; Warner, 1956; and others, a northwesterly-trending uplift occupied an area that approximates the present Front Range during the

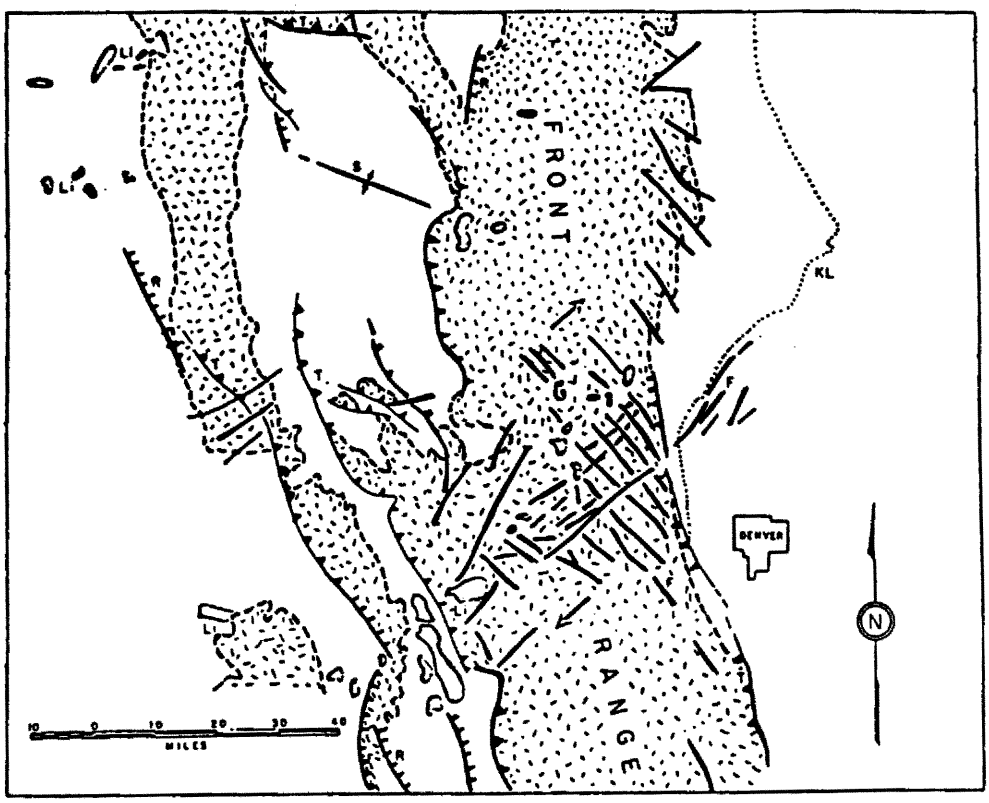

Figure 8. Arrangement of Front Range thrust faults and en echelon fold/fault systems which define the western extent of the Denver-Julesburg basin (from Warner, 1956).

Pennsylvanian and much of the Permian. Generally, this uplift has been referred to as the Ancestral Rocky Mountain highland. Triassic and Jurassic deposits are relatively thin in Colorado and are covered by a thick package of Cretaceous sediments which indicate fairly continuous basinal or basin margin sedimentation to account for the thick accumulation. During latest Cretaceous and early Eocene time, the Laramide Orogeny uplifted and deformed basement rock producing most of the present Rocky Mountain configuration in Wyoming and Colorado. Timing of movement on the foreland uplifts range from Campanian (late Cretaceous) through mid Eocene. Some areas underwent several episodes of tectonic uplift and deformation during this span of time (Gries, 1983). Figure 9 depicts the regional trend of uplift patterns during late Cretaceous, Paleocene, and Eocene time. Evidently as time progressed during the Laramide Orogeny, predominantly east-west compression caused by the collision of the North American and Pacific (Farallon) plates shifted into north-south directed compression (causing east-west trending uplifts) in response to the opening of the Arctic Ocean (Gries, 1983). According to the interpretation presented by Gries (1983), the Front Range was deformed during latest Cretaceous and earliest Paleocene by thrusting from the west.

The formation of the major structural elements of the Front Range of Colorado has been the subject of some controversy during the 1970's and early 1980's. Shortening in the foreland due to compressive forces initiated by plate collision has been attributed to compression in the basement, but also to vertical uplift of the basement (Lowell, 1983). Anticlinal folding, monoclinal drape folding, and high angle faulting present along the eastern edge of the Front Range was attributed to basement block faulting from literature published in the 1970's. Wedges of basement were upthrust by high angle faulting which steepened with depth to produce the tilted basement blocks. This movement induced draping of overlying, layered sedimentary deposits over the uplifted basement core, subsidiary high angle normal faulting, and a resultant diminished distance of

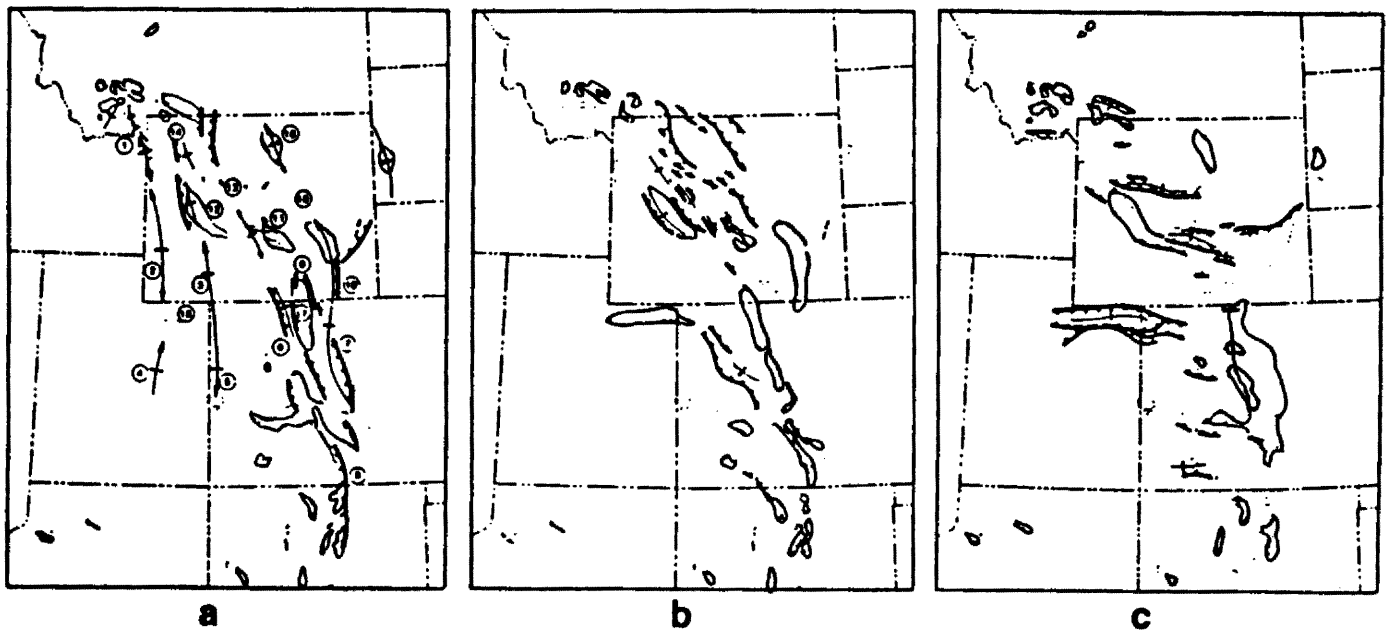

Figure 9. The time of movement on foreland uplifts is not the same for all uplifts in the Rocky Mountain region.
a. North to south-trending arches and uplifts are early Laramide features and are progressively younger from the west (Campanian) to the east (Paleocene).
b. Northwest-trending features are most dominant in the northern foreland and are associated with Paleocene movement.
c. East-west trending structures are the youngest Laramide features (Eocene) and are associated with the strongest period of compression in the foreland (from Gries, 1983).

basement overhang (Stearns, 1978). Initial work completed in the 1950's along the Front Range proposed thrusting as a mechanism for the structures observed instead of forced folding vertical uplift (Warner, 1956). Subsequent research has suggested that a larger horizontal component of compression associated with thrusting dovetails with surface data, strain analyses, and geometrically constrained, balanced cross-sections in a better manner than the vertical uplift hypothesis. E. Erslev, J. Rogers & M. Harvey (1988) propose that back thrusting associated with a blind detachment at depth accounts for the basin-side up shear sense markers, steeply northeast dipping faults and fold systems, and the west-vergent asymmetries of the Wellington and Fort Collins oil field structures.

Lowell, 1983 considers three observations pertinent to the problem of a dominantly horizontal vs. vertical component of foreland uplifts. He concludes that the mechanism of horizontal shortening associated with compression is the most influential parameter in the construction of foreland uplifts. First, on many mountain front faults which mark the lead edge of the thrust; the fault surface between the lead edge and a subsurface well behind the lead edge which drilled through basement indicate fault dips of much less than 45°. Secondly, the dip of the fault mountainward from drilled wells (usually from high quality reflection seismic lines) reveal low-angle basement thrusts and thrust overhangs of 10 miles or more (Lowell, 1983). This argues strongly against vertical, rigid block tectonic uplift. Finally, the presence of overturned section beneath the basement thrust for significant distances is most easily accomplished by low angle thrusting. In addition, associated asymmetrical anticlines common in seismic sections beneath thrusted Precambrian blocks are not predicted by a forced fold vertical uplift model (Gries, 1983).

Whether the Front Range has been thrusted of uplifted vertically significantly affects exploration strategies in the adjacent Denver-Julesburg basin. Gravimetric evidence, surface mapping, and seismic surveys from an area between Castle Rock and Boulder,

Colorado along the Front Range indicates significant thrust overlap from the west of Precambrian rocks over younger Paleozoic and Mesozoic sediments to the south. The overlap decreases in dimension to the north with a coincident steepening of fault dips (Bieber, 1983; Jacob, 1983). Potential wedges of hydrocarbon bearing strata would then be predicted under the Precambrian overhang. In addition to the indirect evidence, oil seeps are present in portions of the Front Range and flow out of fractures in gneissic rock, an indication of hydrocarbon migration from sediments below (Jacob, 1983).

Beside the deformation associated with the Laramide Front Range Uplift, a positive element called the Transcontinental Arch was postulated to be active during late Cretaceous time and caused a thinning to occur in the Niobrara stratigraphic sequence (Weimer, 1978; Hann, 1981). The arch trends northeast through eastern Colorado and into Nebraska. Weimer also suggests that this influenced Codell deposition and caused erosion and preservation of multiple unconformities above and below Codell strata over the arch in northeastern Colorado and southwestern Nebraska (Figure 10). Duration of this positive element through the Cretaceous would have provided sites of hydrocarbon accumulation in strata both younger and older than the Codell (Weimer, 1983). According to an hypothesis proposed by Weimer the Wattenberg Field which straddles the basin axis in northeastern Colorado, was created by the influence of the Transcontinental arch (Figure 4). Early migration of hydrocarbons into structurally positive reservoir sandstone bodies accounts for production from basin lows in the D-J basin.

Codell production is influenced by proximity to areas of intense faulting and structural controls affect the stratigraphic relations significantly. These associations will be examined later in this study under the subsurface analyses chapter.

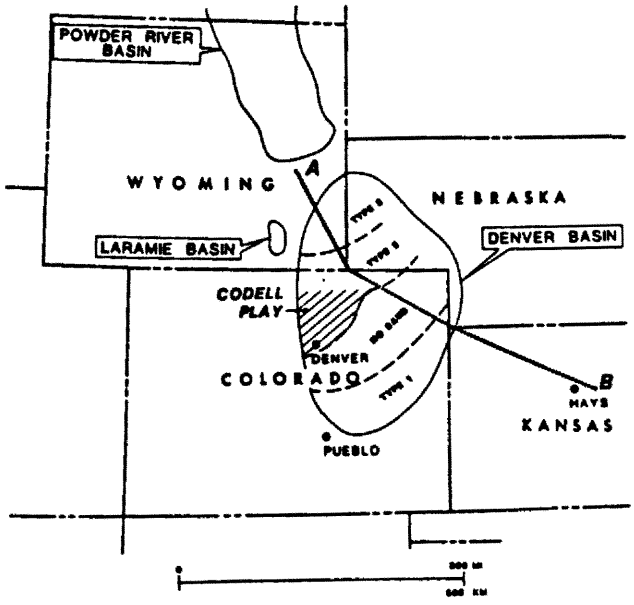

Distribution of Codell Sandstone

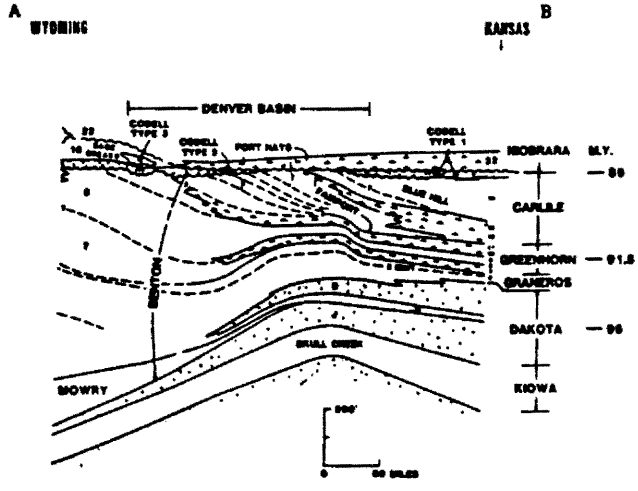

Restored stratigraphic section

Figure 10. Arrangement of the Codell Sandstone over the Transcontinental arch (from Weimer, 1983).

Field History of the Codell Sandstone

In 1980, the Upper-Cretaceous Codell Sandstone was recognized as a new exploration target in the west-central portion of the D-J basin between Denver and Fort Collins, Colorado. Development of the Codell was stalled for a long period of time because of its muted log characteristics and poor sample quality in drill hole cuttings. High percentage clay volumes in the Codell accounts for this problem. Production was first established in 1955 with the discovery of the Soda Lake field just southeast of Morrison, Colorado. Initial production topped 100 barrels of oil/day but rapidly dwindled and was abandoned after producing only 15,275 bbls of oil (Kennedy, 1983). Through the 1960's and early 1970's, the Codell was sporadically tested and perforated in conjunction with Niobrara, Sussex, and Shannon completions. Generally, it was only tested if other primary targets were non-economic.

The #1 Ertl (Martin Exploration Management Corp.), drilled in section 17-1N-69W, Boulder County in 1979 was the catalyst for the Codell play in the D-J basin (Kennedy, 1983). The Codell and 'J' Sandstones were commingled with initial production reported at 1.6 MMcf of gas, 250 bbls of condensate, and 47 bbls of water per day. Over a year later, Toltek Drilling and Centennial Petroleum in a joint venture, drilled the #1 Futhey located in section 26-1N-69W, also in Boulder County. Initial production of the Codell following acidization and fracture treatment was 262 bbls of 52 gravity condensate and 1.3 MMcf gas per day. The newly-evolving Codell play up to this time had been limited to the disturbed western flank of the D-J basin. In 1981, Energy Minerals Corporation and Energy Oil drilled and completed wells in the Codell Sandstone in or near the Wattenberg Field area located adjacent to the basin axis. Previous to that time, Wattenberg Field produced hydrocarbons from the lower Cretaceous 'J' sandstone and upper Cretaceous Sussex interval. To accommodate further exploration efforts in an already established field, 40 acre offset drilling was approved by the Colorado State Oil and Gas Commission.

By that time, it was obvious that the Codell was present over a large area of the basin in northeastern Colorado and could contain large reserves. The dwindling number

of new exploration targets in the basin coupled with the Natural Gas Policy Act of 1978 and the subsequent decontrol of oil in 1981, brought prices up enough for the Codell to become economic (Kennedy, 1983). Drilling and completion costs are higher for the Codell than the typical 'D', 'J', and Hygeine wells because it is slightly overpressured, tighter, more clay rich, and more vulnerable to fluid damage.

Despite warnings of falling oil/condensate prices and shrinking markets for Codell gas, exploration continued un-abated in 1983 and well into 1984. Operators began a more cautious approach in 1984 and 1985 when it became obvious that pipeline companies were denying hook-ups for new Codell gas. The market was saturated and when oil prices fell dramatically in 1985 and early 1986 to $10-12/barrel of oil, rapid expansion of the Codell play ceased. In 1986 and 1987, drilling was confined to in-field development and holding leased acreage. Until prices increase and stabilize, preferably around $20-24/barrel, exploration and production from the Codell is marginally economic (Wright & Fields, 1988). However, the Codell Sandstone is an excellent example of a secondary of tertiary target objective. Completing thin, relatively "tight" sandstone intervals which are common in Cretaceous sequences in the Rocky Mountain region, can provide efficient use of drilling dollars. Commingled production or later up-hole completions can increase the return on investment ratio considerably.

CHAPTER II

Literature Review

Previous work

Stratigraphic studies of the Codell Sandstone have been confined predominantly to the southern portion of the Denver-Julesburg basin. A number of workers in this region have studied both the Codell Sandstone and its relationship with the overlying Juana Lopez Member of the Carlile Shale and Fort Hays Member of the Niobrara Formation (Krutak,1970; Reisser, 1976; Pinel, 1977 & 1983; McLane, 1982 & 1983; Aulia, 1982). Their analyzes help to provide the regional framework in which to study the Codell Sandstone in the northern portion of the basin. Initial investigations by Krutak (1970) concluded that deposition of the Codell sequence occurred on stable mud bottoms of a shelf-lagoon area which in the rock record were bounded above and below by provincial disconformities. In addition, he described a laterally continuous calcarenite zone which capped the Codell Sandstone and attributed it to a rise in sea level (transgression).

Pinel (1977) called the calcarenite zone the Juana Lopez Member of the Carlile Shale. From his detailed descriptions, the Juana Lopez is a sandy bioclastic, marly limestone which is occasionally cross-stratified by high-angle, planar foreset laminae. According to his interpretation, the Juana Lopez Member is a transgressive deposit which overlies shoreface to sub-shoreface deposits of the Codell Sandstone. The two members are separated by a scour surface paved with lag debris (chert pebbles, shell fragments, rounded clay clasts, and coarse quartz sand). Gently undulatory in character, the surface locally scours over 1 ft. (34 cm) into the underlying Codell

Sandstone. He concludes that the progressive coarsening-upward nature of the sequence reflects the transition from marginal marine shelf sedimentation through shoreface/strandline environments which are capped by a subaerial erosion surface. Subsequent transgression reworked the surface deposits, (the bioclastic Juana Lopex Member) which grade upward into onlap deposits of the deeper neritic Fort Hays Limestone. According to Pinel (1977), a regressive pulse (sea level drop) resulted in an increased sediment influx into the southern portion of the D-J basin. Codell deposition followed and this same sediment source was shut off by the subsequent transgression.

McLane (1982) concluded that the Codell represented deposition in a complex strandline network of low wave-energy, microtidal, coastal marine environments which occurred during a minor regressive episode in the late Turonian. His conclusions were based on outcrop data collected between Canon City and Pueblo, Colorado, in the extreme southwestern portion of the Denver-Julesburg basin. Through the use of vertical stratigraphic profiles he demonstrated a northwest to southeast progression of shoreface and tidal delta environments which interfinger with offshore, marine bar complexes. Facies relationships suggest that the strandline orientation was northeast-southwest and the sediment source were probably from the west. He proposed the hypothesis that Codell sediments deposited in the southeastern portion of the basin may have been recycled from previously deposited sediments to the north that were subaerially eroded as the strandline progressed southward. In addition, he concluded that the Juana Lopez Member resulted from a transgressive episode which slightly reworked the underlying Codell Sandstone, forming a lag deposit of calcareous sandstone and limestone containing abraded fragments of bivalves, shark teeth, and rounded bone fragments.

Aulia (1982) studied the Codell in an area near Colorado Springs, Colorado using both outcrop and subsurface data. He proposed that the interval represents an offshore, marine shelf sandstone deposit which coarsens upward in response to shoaling water

conditions during a marine regression. In his interpretation, Codell sediments were never subaerially exposed, and water depths remaining largely below fair-weather wave base. As a consequence, the Juana Lopez Member is a transgressive, palimpsest deposit derived from slight subaqueous reworking of the underlying Codell sediments. Storm-intensified and/or storm-generated shelf currents generally flowed to the southeast, providing the hydrodynamic conditions necessary to entrain and winnow sediment. He suggested that the stratigraphic distribution of upper Carlile deposits was controlled by recurrent movement of the Transcontinental Arch, Ute Pass fault, and the horst blocks in the Red Creek Arch. Thin Codell Sandstone deposits are present on structural highs, but are relatively 'clean' due to winnowing effects of accelerating currents converging around areas of positive topographic relief. Structurally 'low' areas contain Codell deposits which are much thicker but predominantly composed of shale and silt deposited primarily by suspension processes.

In the north-central portion of the basin, the interval has been investigated primarily through geologic reconnaissance by Fenneman (1905), Henderson (1908), and by Chronic (1957). These studies primarily focused on the development of Cretaceous stratigraphy in the region. However, between Boulder and Lyons, Colorado, Lowman (1977) completed a detailed study of the Codell/Fort Hays contact using outcrop correlations. Present delineation of the Codell play include the outcrops used in Lowman's study (T2-3N, R71-70W) in the extreme southwestern margin. According to her interpretations, deposition of the interval occurred in an offshore, marine setting by storm-intensified currents which resulted in a heavily bioturbated, clay-rich, fine-grained sandstone. In this area, the lower Codell Sandstone consists of alternating stratified to burrowed sequences in which low angle tabular-planar cross-stratified sandstones (hummocky cross stratification?) are interbedded with thinner units of ripple cross-laminated sandstone. The stratified beds are lenticular in nature and tend to pinch and swell. Sandstone composition of this upper unit is a very fine-grained quartz arenite

which is clay-cemented at the base and calcite-cemented near the top. In the upper portion of the Codell, intense bioturbation has destroyed any original stratification which gives the unit a massive appearance. As was present in the southern part of the D-J basin, a thin, discontinuous calcarenite unit tops the Codell and is composed of rounded carbonate hash containing *Inoceramid* prisms, phosphate nodules, and shark teeth with abundant angular quartz grains set in a carbonate mudstone matrix. It is faintly ripple cross-laminated. Lowman (1977) refers to this interval as the Juana Lopez Member of the Carlile Shale Formation. Lowman's interpretations of the depositional framework of the Codell suggest that the Codell Sandstone is a marine shelf deposit which formed during a regressive episode of the epicontinental seaway. Sediment influx was from the west and northeast, with sand transported south from a northeastern source by episodic, storm-generated currents.

As early as the late 1950's and early 1960's, attempts were made to recognize the significance of sediment packages bounded above and below by unconformities or lithologic disconformities in the Denver-Julesburg basin. Weimer (1960) recognized four major Late Cretaceous transgressive cycles each followed by a regressive pulse of shorter duration. These are called the Greenhorn, Niobrara, Claggett and Bearpaw cycles (McGookey, et al., 1972). How these cycles fit into the refined sequences and nomenclature of sequence stratigraphy will be discussed later in the discussion and conclusions of this study. Lowman (1977) suggested that the incipient Niobrara transgressive cycle produced an essentially starved shelf condition which resulted in calcarenite deposition produced by winnowing of the underlying upper portion of the Codell Sandstone. Further deepening resulted in deposition of the Fort Hays Limestone under restricted marine conditions. Alternatively, Hann (1981) suggested that the Fort Hays Member was deposited under moderately shallow, normal marine conditions. The lack of benthic fauna in the interval was due to soft substrate conditions rather than poorly oxygenated, restricted marine conditions. The abundance and diversity of trace

fossils (especially in the lower Fort Hays) suggests well-aerated sediments (Hann, 1981). In any event, a major change in depositional regime is reflected in the transition from predominantly clastic to carbonate deposition in this portion of the seaway.

Lowman (1977) mapped regional lithofacies patterns for the *Prionocyclus hyatti* faunal zone which roughly corresponds to the time of Codell deposition. Figure 11 illustrates the distribution of sandstone and shale dominated zones in the western portion of the epeiric seaway with deltaic depocenters to the west and northeast introducing terrigenous clastic sediment. An area of erosion or nondeposition covered portions of northwestern Colorado and central Wyoming. Presumably, erosional processes occurred under subaqueous conditions. This distribution roughly coincides with regional paleogeographic maps published by Merewether *et al.*, (1983). During the *Prionocyclus wyomingensis* faunal zone (Figure 12), deposition of the calcarenite (?Juana Lopez) was roughly contemporaneous with the Turner Sandstone of the Black Hills and Frontier Formation of northwestern Colorado. Following the initial stages of transgression, the northeastern sediment supply evidently terminated, resulting in the deposition of the Sage Breaks and Cody Shale Formations (Figure 13). A western sediment source was still present, the strandline position shifting to the northwest, 150-250 kilometers from the present geographical position of northeastern Colorado. As a result of the decreased sediment input and water deepening associated with the Niobrara transgressive cycle, the Fort Hays Limestone was deposited in a deeper neritic basinal setting of the epeiric seaway (Figure 13).

In the actual boundaries of the present Codell play, only one published study has been completed concerning the interval. Ritchie (1986) conducted a thermal maturation and source rock evaluation of the Codell Sandstone and underlying Carlile Shale and determined that the dominant hydrocarbon source in this interval is from the Carlile Shale. Both units are past peak thermal maturity and are near the upper limit of petroleum generation. Type III kerogen is contained in the Codell and was chiefly

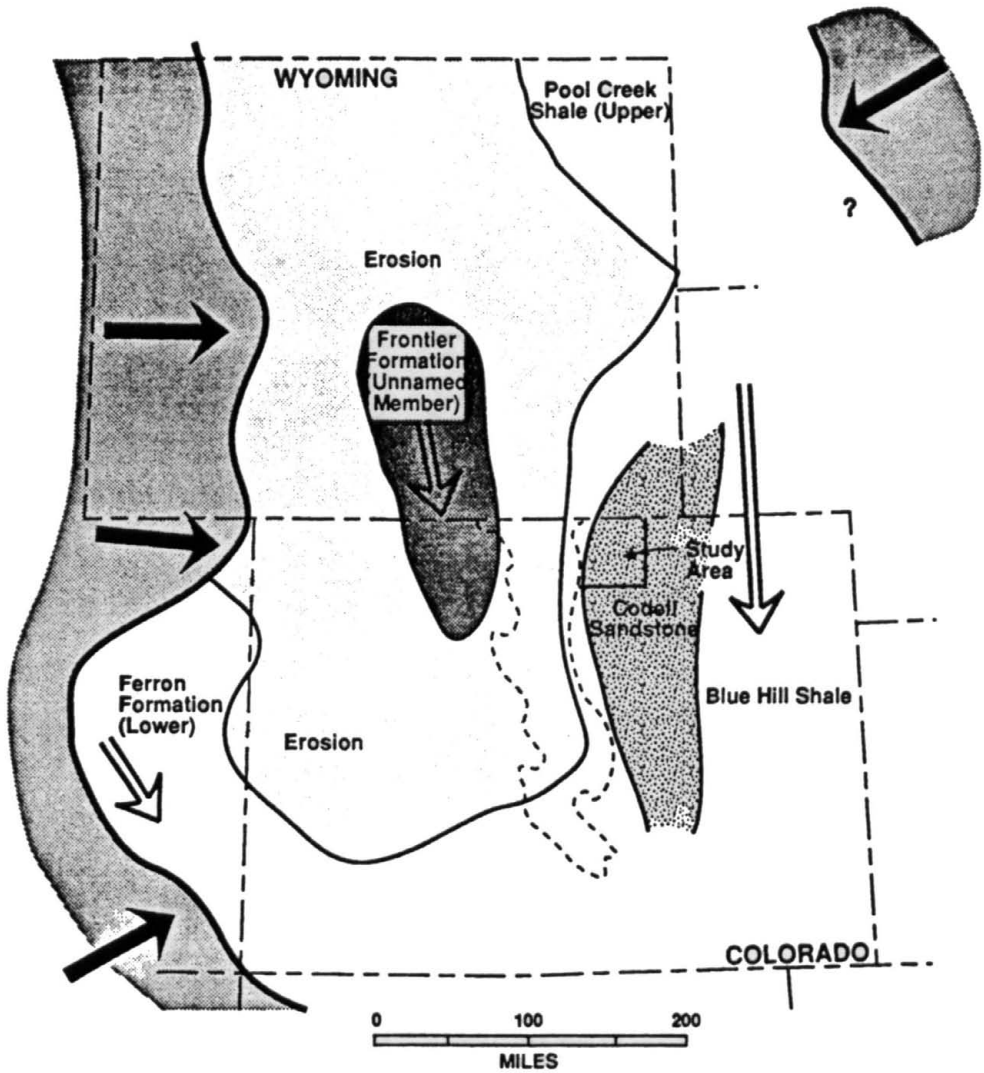

Figure 11. Regional lithofacies pattern during *Prionocyclus hyatti* range zone (middle Turonian). Large black arrows indicate deltaic depocenters. Large open arrows indicate offshore current pattern (documented from paleocurrent orientations). Area of erosion took place under subaqueous conditions (modified from Lowman, 1977).

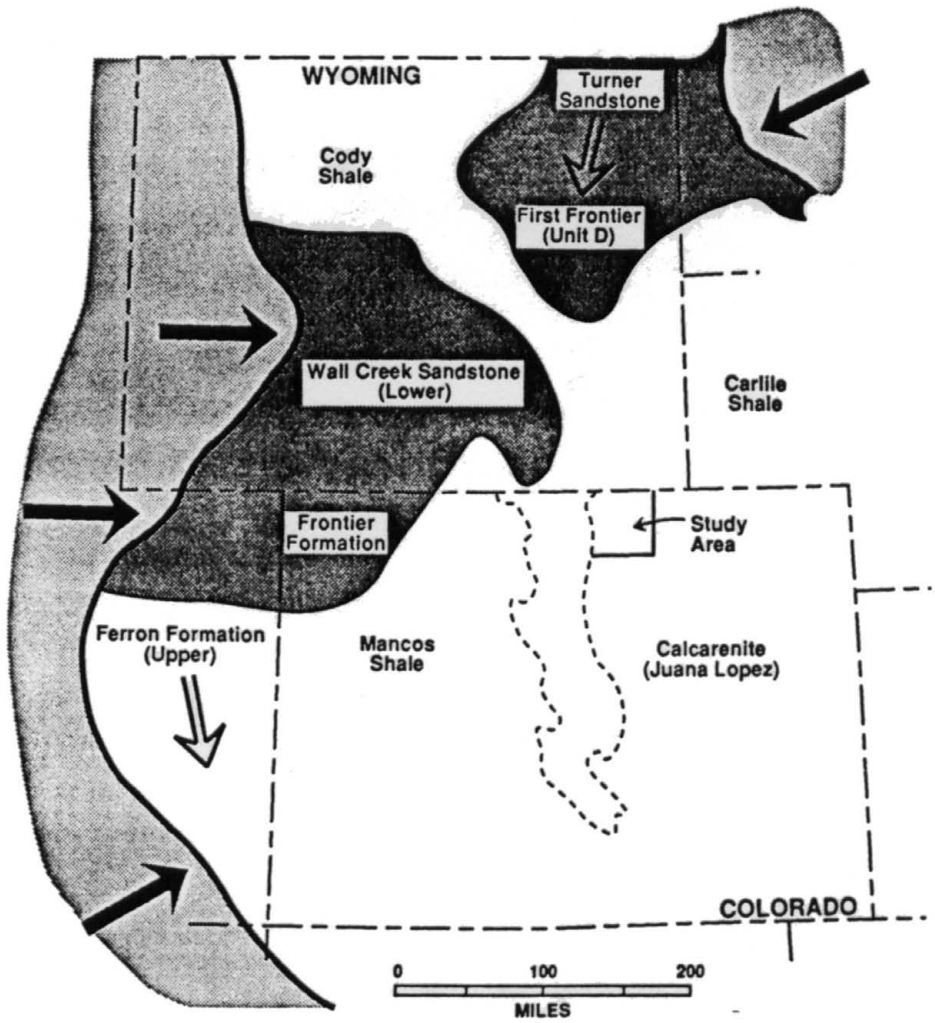

Figure 12. Regional lithofacies during *Prionocyclus wyomingensis* range zone (upper Turonian). Symbols the same as for figure 11 (modified from Lowman, 1977).

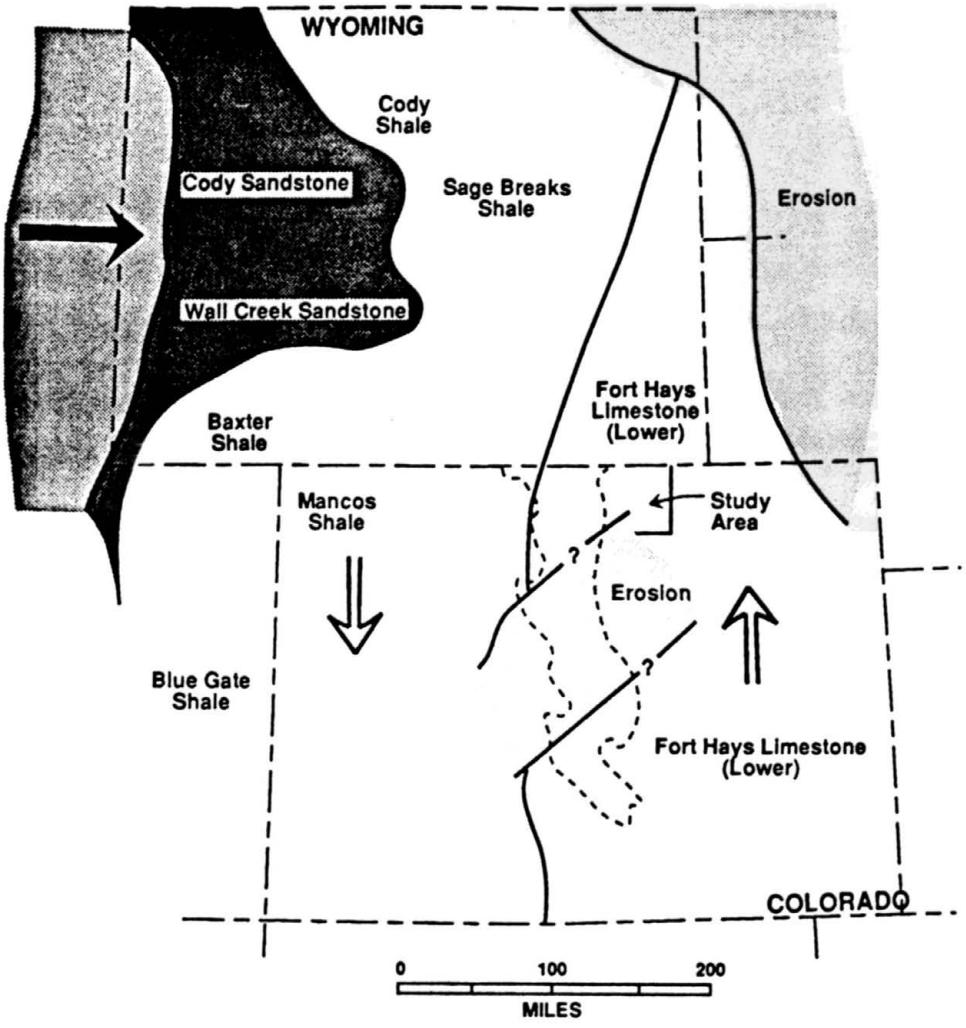

Figure 13. Regional lithofacies pattern during *Inoceramus erectus* range zone. Symbols the as for figure 11. Northeast-trending region of erosion is related to the Transcontinental arch (modified from Lowman, 1977).

derived from the constituents of higher continental plants and subsidiary amounts of marine planktonic organisms. Characteristics of this gas prone kerogen include low H/C ratios, high O/C ratios, and relatively low oil potential (Perrodon, 1988). In contrast, the underlying Carlile contains more Type II kerogen, an oil prone source which is generated predominantly from marine constituents. Natural gas and condensate produced from the Codell Sandstone are thermogenic in origin and produced by extreme catagenesis bordering on metagenesis. Rice and Threlkeld (1983) also completed a study on the character and origin of natural gas from both the Codell and 'J' sandstones of the Denver-Julesburg basin and concluded that it was thermogenic and not biogenic in origin.

Scott and Cobban (1965),Fassett (1976), Dane *et al.* (1968), and Hattin (1975) completed detailed studies on portions of the upper Carilie and lower Niobrara Formations in other parts of Colorado, Wyoming, and New Mexico. Kauffman (1969), Merewether *et al.* (1979), and Evetts (1976) published faunal studies concerning the upper Carlile. Regional correlation of the upper Carlile and lower Niobrara contact has been attempted by Kauffman (1969), Hattin (1975), and Weimer (1983).

In conclusion, previous interpretations for the depositional environments of the Codell Sandstone span the range from shoreface/beach deposits seaward into offshore marine bar complexes. In the northern portion of the basin, the Codell seems to exhibit more marine affinities. The general consensus among most workers indicates that a regressive-transgressive couplet accounts for the stratigraphic relationships of the Codell Sandstone and overlying Fort Hays Limestone. A regional unconformity separates the upper Carlile and lower Niobrara Formations and may be referred to as a sequence boundary.

Synthesis of Sedimentological Studies

Before an attempt is made to describe and detail a physical entity, it is critical to know know what characteristics to look for that best describe its form. As a corollary to the multiple working hypothesis approach of the scientific method; the determination of what something might be is at times best facilitated by finding out what it is not. Previous studies of the Codell Sandstone in the Denver-Julesburg basin suggest a depositional origin ranging from strandline/shoreface and tidal inlet environments to an offshore, shallow marine setting. Volumes of literature have been written on the morphological and hydrodynamic aspects of the barrier island/shoreface systems. However, study of the shelf environment is still very much in its infancy. Because of the complex nature of hydrodynamic processes associated with the shelf, I have chosen to investigate the literature regarding its characteristics. This will result in an objective comparison of strandline/shelf environments.

Shelf Processes: A Brief Overview

Geometry and facies architecture of the Codell Sandstone in the northern Denver-Julesburg basin of Colorado suggest as one possibility an offshore marine shelf environment of deposition. Facies characteristics demonstrate that the currents needed to entrain and subsequently deposit sediment in this shelf setting were dependent upon water depth, proximity to shoreline, tectonic setting, bathymetry of the shelf, and the intensity and duration of meteorological disturbances which impinge upon it. These parameters have a causal affect on hydrodynamic conditions in the inner-outer shelf environment. This literature review will first examine modern shelf processes including shelf sediment transport, and then summarize by integrating bedform and hydrodynamic relationships in both the modern and ancient rock record.

Figure 14 illustrates the general classification of marine topographic features. The continental shelf is generally described as that area bracketed by the landward, littoral shoreline zone and the seaward continental shelf break (Kennett, 1982). Further classification of the continental shelf zone has been attempted by Tillman *et al.* (1985a),

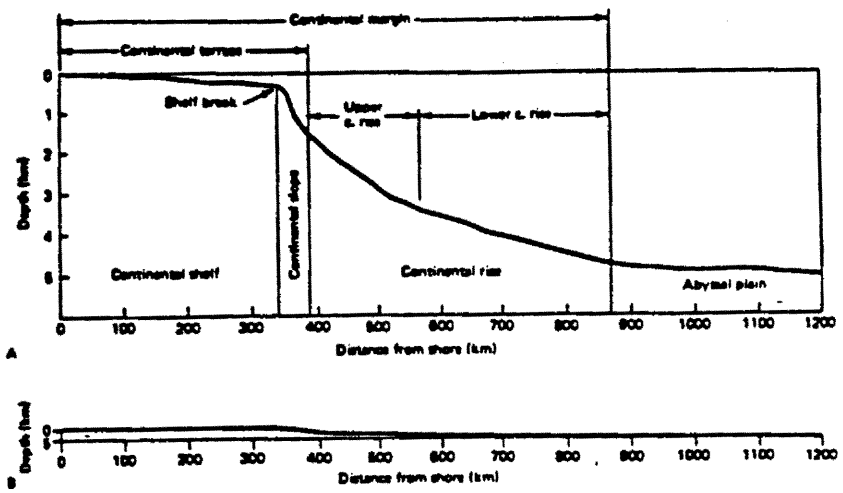

SHELF SUBDIVISIONS

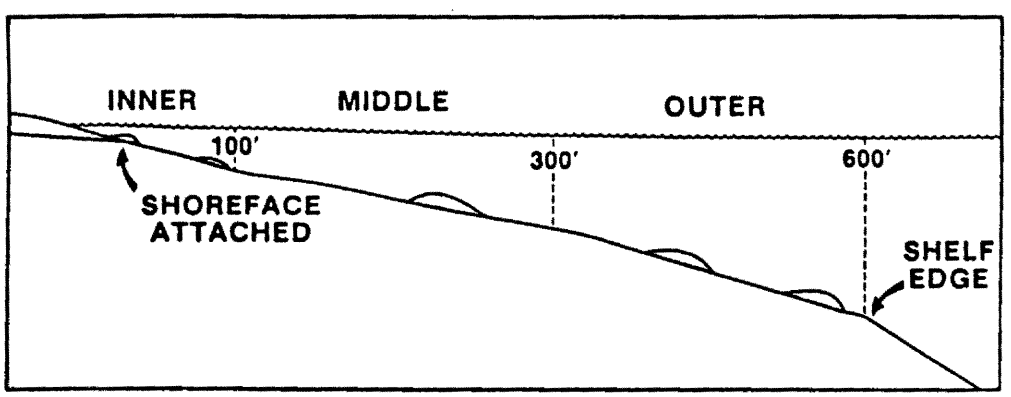

Figure 14. Principal features of the continental margin. A: vertical exaggeration 1/50. B: no vertical exaggeration. From Kennett, 1982.

Figure 15. Subdivisions of the shelf where sand may accumulate based on distance from shoreline and water depths (from Tillman, 1985).

Swift (1976), Johnson (1978) and others. Figure 15 illustrates the designation of inner, middle, and outer portions of the shelf based on water depth. This classification is useful because it attempts to delineate preferred sites of sand accumulation based on the relationship between water depth and distance from shoreline. Hydrodynamic processes are sensitive to this relationship. Kreisa (1988) contends that a distinction needs to be made between 'shelf' and the 'shallow marine' environments based primarily on the depositional slope of each. He suggests that the 'shelf' designation refer to a fairly flat, shallow-water area analogous to much of today's continental freeboard and the term 'shallow-marine' refer to a sloping depositional surface in 0 - 200 meter water depths.

Shelf dimensions can vary greatly according to the associated tectonic setting, thus influencing the distribution and arrangement of sediment packages. Along passive continental margins, the shelf is broad and generally associated with barrier island, lagoon, and beach ridge complexes. Typically, continental shelves associated with collision edge margins are much narrower in extent and exist in conjunction with landward coastal terraces and mountains (Gorsline & Swift, 1977). In both cases, the slope of the shelf can be imperceptible. Slopes range from 1/4° - 4° and are commonly between 1/4° - 1° (Tillman, 1985a). Modern shelves exhibit low topographic relief in addition to very gradational slope.

Modern shelf configuration cannot be used as a direct analog for many ancient 'shelf' and 'shallow-marine' deposits. During late Paleozoic and Mesozoic time, broad portions of mid-continent areas were inundated and epeiric seas developed. In these epicontinental shelf zones, clearly defined shelf breaks, continental rises, and abyssal plains were usually absent. Asquith (1970), using bentonite markers correlated throughout Wyoming, demonstrated the existence of a shelf/slope configuration in the northern portion of the Western Interior Cretaceous Seaway. However, by condensing the horizontal scale of the basinal profile, the cross-sections were hung with significant vertical exaggeration, greatly enhancing the topographic profile of the shelf/slope break.

The modern Bering Sea and southern North Sea shelf areas have been proposed as partial analogs of epicontinental shelf sedimentation. Care must be taken in making that comparison because of their limited areal extent (when compared to ancient epeiric seaways) and unusually strong tidal influence on deposition and transportation of sediment.

In addition to shelf configuration, the amount of sediment input onto the shelf from extrabasinal sources influences the distribution and type of shelf sedimentation. Shelves which are essentially starved of a modern supply of terrigenous clastics because of the Holocene sea-level rise have complex sand/mud geometries. The mid-Atlantic shelf of the United States has been proposed as a partial analog for ancient transgressive shelf sequences. Continental shelf areas such as western Louisiana and the Texas Gulf coast, which have been subject to rapid sediment aggradation by fluvial/deltaic progradational pulses in early Miocene to Pliocene, have been used as possible analogs for ancient regressive shelf deposits. However, preserved ancient and modern shelf sequences are not correlative. Ancient shelf deposits contain abundant inclined foreset laminae consisting of small to medium-scale trough cross-stratification, small-large scale planar cross-stratification, gently undulating parallel lamination, and hummocky cross-stratification. The depositional fabric of modern shelves contain relatively small amounts of inclined foreset laminae, instead, horizontally-laminated, normally-graded sand and parallel-laminated muds and silts compose the bulk of the shelf. This difference may be just the limitations of the modern historical record versus the selectively preserved ancient rock record. More on this dichotomy will be discussed later in this chapter.

Hydrodynamic processes operating on the shelf consist of tidal currents, wind-generated longshore currents, wave-modified currents, storm currents permanent or semi-permanent global circulation patterns, and turbidity currents (Tillman, 1985a). Because of the shelf configuration of the Western Interior Cretaceous Seaway (i.e.

gentle topographic profiles, large areal extent of shallow platforms, and microtidal to mesotidal tidal ranges), episodic storm-generated unidirectional currents probably are the most important factor in the generation of shelf sequences such as the Codell Sandstone. These long period surface gravity currents are sheared by shorter-period wave orbital currents inducing a combined-flow hydrodynamic regime. Locally, mass movement phenomena and density flows (turbidity currents) usually associated with sediment influx from depocenters along the shoreline, account for some shelf sedimentation. However, the limited areal extent of turbidity current impact contribute to its subsidiary importance in shelf construction and modification. By studying modern storm processes and current patterns, a broad understanding of shelf sedimentation can be accomplished.

Modern storms (U.S. classification) are either classified as tropical storms (wind speed > 35 mph), hurricanes (wind speed > 75 mph) or extratropical winter storms. At the center of tropical storms and hurricanes is an intense low pressure system. The pressure drop occurs over a relatively small region and the consequent steep pressure gradient produces extremely strong winds. Waves produced by the winds radiate from the storm in all directions; but the maximum wave energy flux is directed towards land, parallel to the track of the storm (Kennett, 1982). Because of pressure gradients and fluid dynamics, storms generated in offshore areas will generally follow a track towards the nearest land mass.

The reduced central pressure and strong rotating winds associated with the storm or hurricane cause an increase in sea level elevation within the storm called a 'storm surge'. This surge can become a 'forced wave' as it moves across the continental shelf towards shore (Nummendal & Fischer, 1978). The height of the storm surge depends upon 1) the central pressure index of the disturbance (difference between pressure in the center of the storm and that of the ambient atmosphere at its fringe), 2) the path of the storm relative to land, 3) the elapsed time that the storm spends over water (the slower it

moves, the higher the surge), 4) lateral extent of the storm, 5) configuration of the shoreline (the surge increases in height when forced into funnel-shaped embayments), and 6) the bathymetry of the continental shelf (Nummendal and Fischer, 1978). A broad, shallow continental shelf will generally produce a higher storm surge than a shelf which is narrow and steep. Most workers consider the Western Interior Epeiric Seaway to have a gentle topographic profile and shallow shelf platform (av. water depth between 40 - 80 m). Tides can augment or detract from the storm surge depending upon the timing of the event. It is likely that low-lying coastal areas of micro-mesotidal tidal ranges adjacent to the Cretaceous Seaway would be inundated by storm surges much in the same way as storms affect the Texas Gulf coast. Magnitudes of recorded storm surges range around a few meters. Usually what is actually measured by instrumentation is the 'storm tide', which is the surge plus effects of the astronomical tide. Hurricane Carla (1961), which affected the Gulf coast of Texas, is one of the largest storms recorded in U.S. history. Carla had a 7 meter (23 ft.) storm tide associated with it (Hayes, 1967). Hurricane Allen (1980), an 'average' hurricane event, produced a peak storm tide of about 3 meters (9.8) at Padre Island, Texas (Morton, 1981).

These storm surges help to establish current patterns which may modify the inner-outer shelf setting. Hayes (1967) first proposed the concept of storm-surge ebb to account for normally graded sand deposits found on the Texas Gulf shelf following the passage of Hurricane Carla. He suggested that storm surges ponded in bays and lagoons generate strong gravity-induced currents which flowed seaward through washover channels back onto the shelf. However, subsequent investigations produced evidence which argued against the storm-surge ebb hypothesis. Morton (1979) also reviewed hydrologic, photographic, and sedimentological data from the effects of Hurricane Carla. He documented an extensive area of graded bed deposits seaward of a barrier island segment in which vegetated and stabilized dunes prevented the dissection

of the barrier island segment through the formation of washover channels. Also, by reviewing instrumentation records, the water levels measured along the Laguna Madre portion of the Gulf were actually below normal as a result of wind circulation. He suggests that the broad, sub-aerial plain of the back-barrier environment of Padre Island (typical of most of the Texas Gulf coast) dissipated the hydraulic head of the storm surge(tide) by causing considerable frictional resistance to flow; and this greatly retarded the current flow back to the Gulf.

Morton (1981) introduced an alternative hypothesis regarding the formation of normally graded sand and mud couplets after the passage of major storm events which involved unidirectional bottom currents created by wind forcing. Wind velocities and direction, surge height, its angle of approach to the shoreline, shelf slope, and shoreline orientation affect the magnitude, direction, and duration of these bottom currents. According to field instrument data collected during the passage of several storm events, a single-layer or two-layer current system is generated in the water column adjacent to the shoreline (Morton, 1981). The entire water column moves longshore in the same direction as the wind, in a single-layer system. In the two-layer system, bottom water masses generally move offshore in a direction opposite to that of the wind. Therefore, when wind-forced surface water layers move onshore at relatively high angles, strong offshore directed bottom currents are set up.

Under a more rigorous quantitative analysis, wind, tide, and wave data collected during Hurricane Carla also concluded that the wind-induced hydrostatic pressure gradient was critical in establishing strong bottom current velocities (Snedden & Nummedal, 1989). They also postulated that as surface flow was largely oriented onshore, bottom current motion was likely oriented along-shelf. From mathematical simulation, wind-driven surface currents peaked at 46 cm/sec just prior to hurricane landfall, while the calculated geostrophic currents were likely six times that in magnitude, up to 300 cm/sec (Snedden & Nummedal, 1989).

Velocities of bottom layer currents measured during several other storm events (Camille (1969), Delia (1973), etc.) range from 1.6m/sec to 2m/sec (Nummendal *et al.*, 1980). The maximum bottom velocities occur shortly after maximum wind stress is applied but before the passage of the storm's center and landfall. Butman *et al.* (1979) also demonstrated that direct wind-driven 'slab flow' enters the current configuration pattern in shallow water. How far out onto the shelf these currents retain their integrity is open to interpretation. Field *et al.* (1988) made the distinction between storm currents and flood currents and their resultant deposits produced by major storm events affecting the northern California coast. Storm current patterns, velocity vectors, and resultant depositional facies tract are much different in arrangement and orientation when compared to currents supplied seaward from flood-swollen fluvial/deltaic systems.

Swift *et al.* (1976, 1984, 1985) and others expanded upon the concept of wind-forced, unidirectional storm currents and introduced the concept of geostrophic flow. The storm-induced set-up of the sea surface against a coast will cause a seaward-directed pressure gradient (Swift, 1976). This pressure gradient will induce a seaward-directed movement of water at depth (Swift & Rice, 1984). As soon as movement begins, the Coriolis force will deflect the surface layer of moving water to the right (northern hemisphere) and bottom friction will act in an opposite direction to that of the flow (Figure 16). According to the geostrophic flow hypothesis, the Coriolis and friction force vectors contained in the bottom layer will balance the driving pressure gradient force under equilibrium conditions. To sustain this current configuration, water is supplied by down welling along the shoreface of the coastline which is in turn fed by on-shore flow in the upper part of the water column (Swift & Rice, 1984). In the middle of the water column, where the friction of the bottom boundary layer has essentially no effect, the Coriolis force must itself balance the pressure gradient force. The resulting core, geostrophic flow will be oriented exactly parallel to shore, along the shelf. As a consequence of this balance of forces, a three-cored circulation

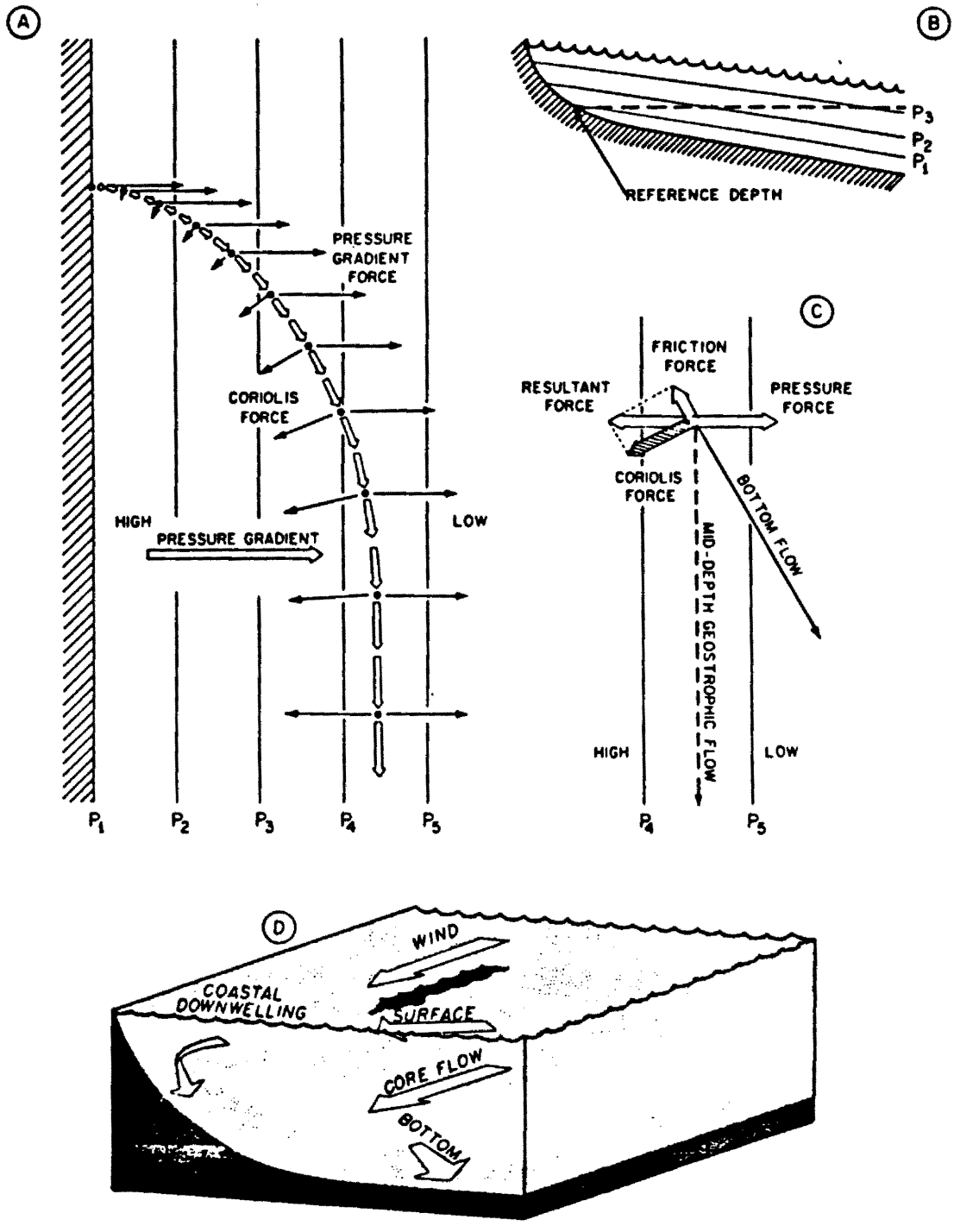

Figure 16. Geostrophic flow on the continental shelf. (A) in this plan view, a parcel of water at a reference depth moves seaward (to the right) in response to pressure-gradient force. As it accelerates, it experiences a Coriolis force impelling it to the right of its trajectory. (B) cross-section of hypothetical shelf experiencing geostrophic flow illustrating relation of sea surface slope, isobaric surfaces and reference depth. (C) relation between geostrophic flow and flow in bottom boundary layer. (D) block diagram of geostrophic flow, showing landward moving upper boundary layer (stippled), fluid interior (clear), and seaward veering boundary layer (stippled). From Swift & Rice, 1984.

configuration will be set up in the shelf setting (Figure 16). According to Swift *et al* .(1984, 1985) the geostrophic core flow will always be oriented exactly parallel to the shore regardless of the relative angle between wind and shoreline. This relationship is produced by the interaction of the current driven shore-normal pressure gradient force, not directly be wind stress (Figure 16). Because depth to the core flow is highly variable in response to storm magnitude, measurements documenting the flow are suspect. Velocities cited in literature range from .35m/sec to 1.6m/sec. This hypothesis regarding nearshore current flow is therefore different from mechanisms proposed by Morton (1981).

On closer inspection, the dynamic core zones hypothesized by Swift *et al.* (1984, 1985) are constrained by water depths and shelf configuration, and so a geostrophic core flow is probably not possible in shallow water (5 - 25 m). Those layers of the water column where flow is significantly affected by boundary conditions (air-sea interface or the water-sediment interface) are referred to as boundary layers. In shallow water where the upper and lower boundary layers overlap, one has a friction dominated zone (i.e. shoreface seaward to include breaker zone. This friction dominated zone expands in areal extent when external stress is applied to the system (i.e. wind-forcing and pressure gradients associated with storm events). Where the water is deep enough to clearly separate the two boundary layers, creation of the geostrophic core flow has been postulated. The extent of the two-layer or three-layer current zonation clearly depends upon storm magnitudes.

In moderate to shallow water depths (5 - 40 m), the interaction between the friction dominated bottom layer currents and the oscillatory shear stress associated with movement of long period, low-moderate amplitude storm waves can result in an intense mixing of the normally stratified water column. This mixing has been lumped under the term of 'combined flow'. Madsen & Grant (1976) conclude that bed shear stress under combined flow is a non-linear combination of the stresses associated with unidirectional

current and oscillatory wave motion. Therefore in relatively shallow shelf areas affected by large magnitude storm events, superposition of oscillatory stress vectors on unidirectional current patterns occur. This results in bottom water particle trajectories which follow extremely complex paths. In addition, storm events generate multiple wave trains with slightly different directional orientation which complicate already complex water particle trajectories (Nummendal & Fischer, 1978). Because of these reasons, bed configurations produced under marine shelf conditions differ from what has been produced from experimental devices such as flumes and wave tanks (Harms *et al.*, 1982).

Geostrophic flow is not only constrained by combined flow mechanisms and water depths, it depends upon the coastal downwelling of water along the shoreface to constantly replenish the water column over the shelf (Figure 16). During the passage of high magnitude storm cells along a shoreline of low relief (i.e. Texas Gulf coast, portions of the Atlantic coast, and most likely shoreline areas of the Western Interior Seaway), inundation of low lying areas may occur and extend as far landward as 5 to 10 km (3.2 to 6.2 miles). Because of the low topographic relief, vegetation, and the volumetrically large areal extent of inundation, a 'set-up' of an elevated storm surge(tide) against the coastline would be dissipated and the coastal downwelling of flood waters along the shoreline retarded. Except in shelf areas fronting large river systems, the forces needed to constantly feed the geostrophic core flow are probably not available. Much as Hayes (1967) storm-surge ebb hypothesis, geostrophic flow adjacent to the shoreline in shallow-water settings is not possible.

Morton (1981), Swift *et al.* (1984,1985) and others conclude that wind-driven storm currents in addition to generating offshore-oriented bottom return flows, create currents which are usually parallel or nearly parallel to the shoreline, the shelf edge, and the contours of the shelf floor. These flows are not necessarily directly driven by wind stress oriented in the same direction. Because of the concept of continuity, based on the

law of conservation and mass, water cannot flow away from the shoreface (flow seaward) in large volumes because more water cannot easily flow in and replace it. Conversely, water cannot flow landward toward the shoreface zone in large volumes because it would pile up. Therefore, wind-induced current movement will primarily drive water along the shelf in an longshore direction.

Shelf Sediment Kinematics

Estimates of current strength and sediment entrainment thresholds in and along the shelf setting tend to be constrained more in a qualitative framework than based on actual measured data. Therefore, some broad generalizations can be made regarding patterns and types of flow. Because movement in the water column produces boundary layers or surfaces, numerical simulations can try to understand which forces predominate in and along the shelf area (Niedoroda, *et al.*, 1989).

Along a storm-dominated shelf, four overlapping zones occur (fig. 17): the surf, friction-dominated, transition, and geostrophic zones (Snedden & Nummedal, 1989). In general, the breaking waves of the surf zone generate along shore currents. The friction-dominated zone is where the interplay of boundary layers in the water column become complex. This zone contains the overlap of the upper (wind-influenced) boundary zone and the lower (friction-dominated) boundary layer (Snedden & Nummedal, 1989). Obviously this zone will expand seaward or shrink landward depending upon the magnitude of the storm event. The transition interval displays both aspects of the friction-dominated and geostrophic zones. In parts of the shelf in which depths are adequate to contain the wind-driven surface stresses to the upper boundary layer, significant separation between upper and lower boundaries occurs and produces a core zone. Motion in the interior zone is responsive to the sea surface slope, which is part of the pressure gradient force of the total water column (Csanady, 1982).

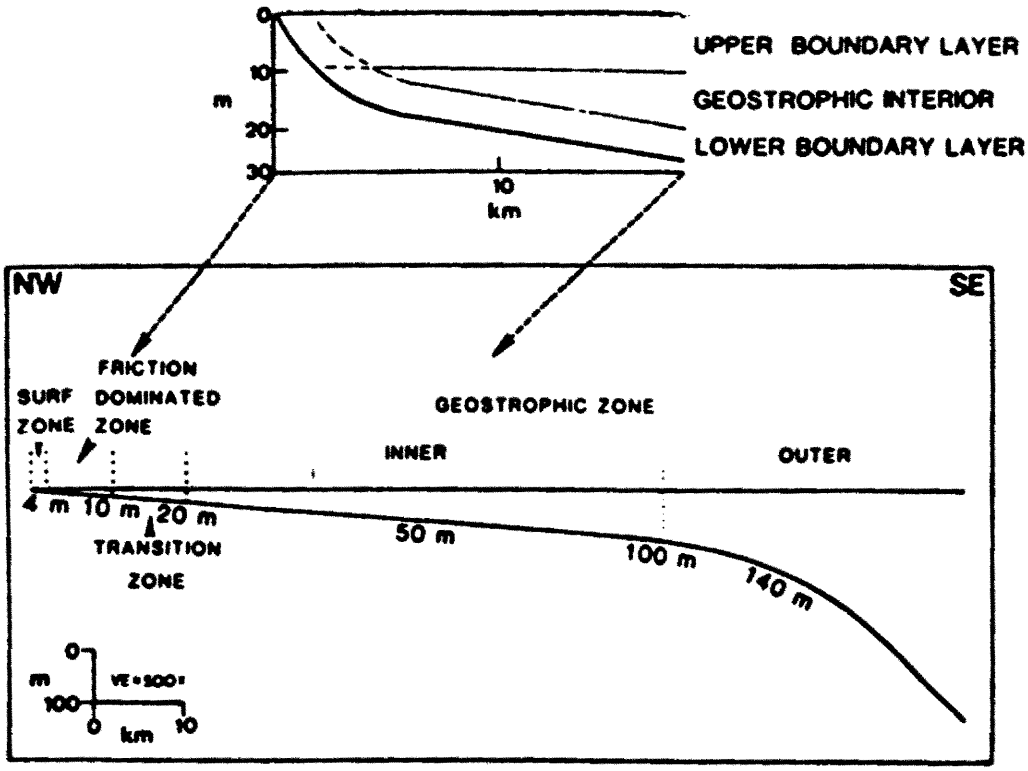

Figure 17. Coastal ocean dynamic zones. Inset shows an expanded view with schematic representation of boundary layers and frictionless (geostrophic) interior. From Snedden & Nummedal, 1989.

Using several empirical relationships based upon unidirectional flow models, Snedden & Nummedal (1989) attempted to derive estimates of current strength associated with Hurricane Carla. After factoring in wind-driven surface current speed and the strength of barotropically forced currents, which are the internal hydrostatic pressure field associated with wind-induced sea level set-up at the coast. From this, the boundary shear stress at the water/shelf bottom interface is estimated. Entrainment of clastic particles is controlled by the magnitude of this stress. Field studies concluded that entrainment of 100 micron sand would occur at shear stressed greater than 1.4 dynes/cm^2 or a current speed (at 1 meter off bottom) of 35 cm/sec (Snedden, 1985). According to this study, the calculated interior velocities of the water column approached 300 cm/sec. It is likely that the current strengths near the shelf bottom/water interface were somewhat lower. However, it is probable that the transport threshold of 100 micron sediment was easily surpassed during the passage of Hurricane Carla over Texas Gulf shelf areas.

Strong currents associated with storm events undoubtedly alter portions of the inner shelf. However, current velocities and fluid behavior are more complex in the shelf setting than the empirically-based unidirectional flow models would indicate. Gelfenbaum & Smith (1986) demonstrated the critical importance of suspended sediment concentrations on fluid flow behavior. Using velocity and suspended-sediment profiles, they concluded that as more sediment is put into suspension, the amount of turbulent mixing decreases as the fluid becomes stably stratified. This results in an increase in upper boundary layer velocities. Because of this damping effect, as more sediment is put into suspension, it is more difficult for the higher velocity fluid near the surface to mix with the lower velocity fluid below. This effectively decouples the upper flow from the lower flow. They used a wide spectrum of sand sizes ranging from very fine to coarse-grained to conduct their experiments. Suspended sediment concentrations obviously affect the internal configuration of preserved sedimentary structures and their associated facies tract. As most preserved shelf sand packages

(especially in the Cretaceous) are composed of very fine to medium-grained sandstone, it is likely that during major storm events, suspended sediment concentrations in the overlying water column were high and are partially responsible for the fabric we see today.

The presence of inclined foreset laminae in the shelf setting indicates that some traction movement of sediment occurs. There is some controversy as to whether traction movement can occur in fair weather conditions or only in episodic, storm-related current systems (Harms, *et al.* 1982). In the shoreface environment, velocity asymmetry of wave orbital shear stresses in the breaker and swash zone create a streaming carpet of sediment movement. Some workers contend that the gravity-induced bottom return flows associated with major storm events produce traction currents which scour and ultimately deposit sediment great distances seaward of the shoreface environment. Others invoke combined flow mechanisms to re-work sediment *in-situ* wherever current systems are set-up by meteorological disturbances (Walker, 1984, Snedden & Nummedal, 1989). Ultimately, the basic question is whether traction movement of bed load material can occur on the shelf floor under normal marine current conditions. In any event, Myrow & Southard (1988) created a combined-flow mechanism model which integrates both unidirectional and oscillatory movement resulting in a range of energy levels and stratification types. This allows the application of a practical treatment of complex flow parameters in the shelf setting. It should be noted that traction movement of bedload material is also affected by the amount of suspended wash load material in the same water column. How this affects the resultant stratification type is poorly understood.

In an effort to try and understand the effects of episodic, time-constrained flow events on the shelf, Swift & Rice (1984), concluded that two kinds of hydrodynamic models affect shelf sedimentation and the depositional framework. In a 'temporal acceleration' model the shelf is assumed to be very flat with little to no topographic relief

and sand to silt-size sediment already present on the shelf floor. Storm currents accelerate and decelerate in time due to the episodic nature of the meteorological disturbances. The current velocities shift abruptly from low (fair-weather) to high storm-generated velocities. As the current magnitude increases, erosion takes place on the shelf floor and places previously deposited mud and fine sand in suspension. Since an elevated shear stress needs to be applied before muds go into suspension, larger storm magnitudes are needed before large amounts of fine-grained sediment are entrained. Generally, the storm-induced currents can erode only a few inches (7-8 cm) into the shelf floor because of the mud entrainment threshold and carpet of coarser sand and shell debris which blanket most continental shelves. These sediment properties effectively armor the shelf floor against further erosion. As the current wanes, the sand falls out of suspension first, followed by silt and clay-size particles as fair-weather conditions return. This normally graded sand/mud couplet is common in both modern and ancient shelf sequences (Morton, 1981; Porter, 1976; Hobday & Morton, 1984; Swift *et al.* 1984, 1985). Bioturbation by feeding organisms may totally re-mix the sediment during the fair-weather lull in current activity. Because of this 'winnowing effect', shelves can be constructed in part by the slow process of storm-stratified sand and mud couplets. Generally speaking, it is difficult to envision short-term net shelf aggradation and accumulation of a thick sediment pile only under this hydrodynamic condition.

In reality however, shelf surfaces are areas of broad, gentle topographic gradients which are swept by wind-forced and barotropic currents whose regional velocity gradients will change over time. In a qualitative approach, Swift & Rice (1984) propose a spatial acceleration/deceleration model in which any shelf irregularities become self-perpetuating zones of sand accumulation during successive storm events. As flow accelerates and converges over a topographic 'bump', the shear stresses will be highest up the flank (stoss-side) of the feature and erosion will take place. On the crest and lee-

side of the bump, flow deceleration takes place and deposition results. This model is based on flow oriented perpendicular to the topographic form. If the current is oblique, areas of sediment entrainment and deposition are not as predictable. As a consequence of higher velocities and shear stresses, the coarsest grain sizes will collect on the stoss side of the form and finer sediment will fall out and accumulate on the lee-side. Therefore, 'highs' induced by topographic 'bumps' on the shelf floor (small-scale) or induced by tectonic warping (large-scale), will become zones of continued sand accumulation until such time as the hydrodynamic regime changes and/or sediment input onto the shelf ceases. It is important to note that these models can only be viewed as simplistic end-member examples of shelf construction and aggradation. Shelf sand bodies are known to be preserved (both in the ancient and modern) in topographic lows as well as on 'highs'. Net sand aggradation can occur on all sides of the topographic feature, not just the lee side, depending upon the amount of sediment input in the shelf setting. Also, winnowing works as long as coarse sediment is available to begin with. If not, it is impossible to create coarse lag deposits from fine sediment by only 'winnowing' the shelf floor. According to their models, the 'normal' model for shelf sedimentation (temporal acceleration) must precede the sand-accumulation model (spatial acceleration/deceleration). In other words, as the shelf becomes sand-rich due to winnowing processes, it becomes ripe for the formation and net accumulation of large, discrete sand bodies on the shelf floor. This may be true in part, but it is common to encounter sand lenses totally encased in mudstone in the rock record. For example, the Codell Sandstone of northern Colorado has a sharp basal contact with the underlying Carlile Shale; if 'winnowing' processes create the availability for sand entrainment and subsequent deposition, a gradational envelope of coarse sand, silt, and mud couplets should encase the sand body.

In another attempt to understand shelf kinematics, Boyles and Scott (1982) proposed a model of sediment transport and accretion for the Cretaceous Duffy Mountain shelf

sequence located in northwestern Colorado. They propose that the interaction of fair-weather and storm process created the shelf sequence and caused the bar to migrate and accrete. Sand waves migrated across the bar during fair-weather conditions. During successive storm events, erosion and breaching of the bar occurred producing spillover lobes of sediment to be deposited on the back bar. This model requires that the sediment forming the bar be in very shallow water depths (just seaward of the shoreface). In addition, the bar must have significant topographic relief to produce the flanking washover aprons and avalanche deposits. Basically, breaching of the shelf ridge deposit during high magnitude storm events is invoked to account for the facies tract. This hypothesis is very similar to the progradation and migration of barrier island complexes. It is likely that subaqueous conditions in the shelf setting are much different than the subaqueous/subaerial processes responsible for the formation of barrier islands.

All of these models of shelf sedimentation should produce an overall coarsening-upward textural trend of facies architecture. In the rock record, most sandstone bodies interpreted to be shelf sequences do show a discernible coarsening-upward textural trend (e.g. Sussex and Shannon Sandstone members of the Cody Shale, Hygeine member of the Pierre Shale, and the Duffy Mountain Sandstone member of the Mancos Shale). However, some shelf sandstone intervals fine upward or portray no discernible and/or highly variable textural trends (e.g. Terry Sandstone member of the Pierre Shale, Codell Sandstone member of the Carlile Shale, and portions of the Tocito sandstone member of the Mancos shale). The variability and complexity of shelf sandstone sequences in the rock record is undoubtedly due, in part, to the effect of combined flow mechanisms and episodic nature of the hydrodynamic regime. None of the models discussed adequately addresses the problem of sediment entrainment in the complex interface of unidirectional current flow and oscillatory current interference. In addition, recent investigations of ancient shelf sequences propose that the arrangement of sand complexes is genetically related to sea level and base level controls (Barwis, 1989; Rice, 1988). Sequence

bounding erosional surfaces are commonly located at the base and/or top of shelf sandstone intervals and their relationship may be eustatic, tectonic, or both. Because of these reasons, the rock record preserves a history of shelf sedimentation that is much more varied and complex than was first suspected by modern, coastal studies.

Bedforms and Hydrodynamic Relationships: Modern and Ancient

Correlation between modern and ancient shelf sand sequences is difficult at best because of several factors, the most important factor being the problem of time. Ancient shelf sequences preserve a punctuated and fragmented record as a result of selected preservation of catastrophic events. For example, a catastrophic storm event would undoubtedly modify both the shoreface and adjacent shelf setting, while a severe storm event would affect the shoreline but may not dramatically alter the shelf floor. As a result the catastrophic event would be totally encased by normal marine suspension deposition of muds and silts until the next major event. For this reason, it is easy to envision a progression of shelf sequences from nearshore to outer shelf which reflect not only a decrease in sediment influx, but also a decrease in 'average' storm influence and an increase in 'catastrophic' storm effects. Therefore, our historical record of modern shelves is limited to a severely restricted time frame when compared to the historical rock record. Even with this restriction, it is useful to study shelf processes today and extrapolate what is relevant into the rock record.

A majority of modern shelf studies document a progression of nearshore, normally graded sand, silt, and mud couplets which grade seaward into offshore mud deposits. However, along tidally dominated coastlines and wave-dominated shelves, 5-.5 km (3.1 - .3 mi) long and several hundred meter wide sand ridges have been documented (Martin & Fleming, 1986; Swift, 1986). These ridges may accrete seaward from headlands as submerged spit bars, grow in response to transgression of the shoreline as shoal retreat massifs, or enlarge in response to infragravity waves in areas of high wave energy

(Boczar-Karakiewicz & Bona, 1986). The internal structure of sand ridges are composed predominantly of large, transverse bed forms 1-4 meters (3.3-13 ft) high with an average wavelength between 40 to 80 meters (131-262 ft) (Martin & Fleming, 1986). Mechanisms for sediment transport, velocity vectors, and current patterns are poorly understood. In addition, how these ridges respond to major storm events; whether they wash out or aggrade is also poorly understood. These areas of extreme tidal energy are volumetrically of subsidiary importance in shelf construction when compared to other continental shelves.

A large percentage of modern shelf studies (even along storm-dominated shelves) document an intricate network of sand lenses which can be rippled, massively bedded, or infrequently cross-bedded by inclined foreset laminae (Luternauer, 1986; Cacchione, 1988). These sand lenses are surrounded by parallel-laminated mud and silt deposits. Volumetrically, these interlaminated sand/mud couplets are important in the construction and composition of the proximal portion of the inner shelf. Silty mud and cohesive mud patches comprise distal inner shelf and mid-shelf deposits (Nittrouer, et al., 1986). The sand/mud sequences are very susceptible to mixing by benthic organisms. Preservation of these stratified shelf deposits depends on the rate of sand accumulation, frequency and duration of storm events, and concentration of silt and clay in the water column under normal marine conditions. In addition, preservation of rippled and transverse bed forms depends, in part, upon the size of the sediment particles. Storm-generated oscillatory wave motion can produce symmetrically rippled bedforms in fine gravel in water depths of up to 60 meters (Luternauer, 1986). Inclined foreset lamination is rare in areas which contain nothing but fine sediment. The general consensus among most workers is that the interaction of short period wind-waves and long period swell waves induced by storm events; coupled with unidirectional wind-driven bottom currents (also created by storm events), produce the normally graded and rippled sand, silt, and mud deposits along the shelf (Kachel & Smith, 1986; Vincent, 1986).

Ancient shelf deposits interpreted to have been deposited in areas of low-moderate tidal energy consist of a complex assemblage of sand/shale couplets, small to large-scale trough cross-stratification, small-scale planar cross-stratification, rippled sandstone deposits, rip-up clasts, erosional lag deposits, and hummocky cross-stratification (Tillman & Martinsen, 1984; Rice, 1984; Walker, 1984; Porter, 1976). Inferred ancient shelf sequences contain more inclined foreset lamination than what has been observed in modern shelf deposits. Interpretation of ancient shelf sequences and deduction of energy levels and current patterns responsible for their formation is an inexact science at best. Most of the preserved Cretaceous shelf sediments in the United States and Canada contain fine to medium sand and large amounts of silt and clay. According to Clifton (1986), in this grain size range, 1) low energy levels are documented by siltstone and mudstone sequences which may or may not be bioturbated 2) moderately low energy levels indicated by ripple laminated and interlaminated sandstone and shale, 3) moderately high-energy levels indicated by rippled or planar laminated medium to fine-grained sandstone, and 4) high energy movement documented by horizontally laminated sandstone. This progression of energy levels is based on theoretical derivations of orbital velocities. Currents in the shelf setting are not only dependent upon orbital shear stresses but also on combined flow mechanisms generated by the interaction of unidirectional current flow and storm-generated wind-waves and swells (Clifton, 1986; Arnott, 1988).

Generalizations of energy levels are helpful but complicated by numerous factors. Extremely large storm events probably affect sediment deposition (and subsequent preservation) more in deeper shelf environments than shallow areas nearer the coastline which are re-worked more frequently by smaller storm events. It may not always be clear whether the size of a sediment particle reflects the maximum competence of the fluid motion or the maximum size of sediment particles available to be moved. Also, in an area which receives a high discharge of suspended fine sediment, the subsequent

deposition of mud may be more reflective of the concentration of suspended sediment rather than of energy level.

Association of sedimentary structures and orientations of foreset laminae can provide valuable clues regarding the type and configuration of the paleoshelf environment. Bioturbated shale layers which are truncated near the top, then capped by normally graded sand units probably reflect the episodic effects of storm-generated current acceleration and deceleration. Planar forests that dip in an onshore direction and the presence of symmetrical ripples are probably solely due to oscillatory current movement which reflect deposition within the zone of breaking waves. Forests which dip longshore or in an offshore direction probably document the influence of unidirectional currents (Clifton, 1986). Amalgamated sequences of planar or hummocky cross-stratified sandstone which contain little or no interlaminated shale deposits, may reflect deposition in shallow shelf areas which are affected frequently by storm events that scour the shelf floor, winnowing out the fine sediment and keeping it in suspension.

Hummocky cross-stratification has been used as a water depth estimator and as a definitive indicator of deposition in the shelf environment (Walker, 1984). In a general sense, the presence of hummocky stratified sandstone suggests deposition below fair-weather wave base but above storm wave base. However, recent studies indicate that the bedform can also be produced under very shallow conditions in the breaker and surf zone (Greenwood & Sherman, 1986). Along the storm-wave dominated coastline of the Canadian Great Lakes, hummocky bedforms have been observed in fine-grained sands in water depths of less than 2 meters (6.7 ft) where the interaction of breaking waves and longshore currents is strong. Greenwood & Sherman (1986) concluded that hummocky stratification is produced by an actively growing bedform with little or not lateral migration coupled with rapid vertical accretion of undulatory laminations. Alternatively, Nottvedt & Kreisa (1987) developed a bed-form phase diagram which indicated that most hummocky cross-stratification is related in a fundamental way to

low-relief megaripple bed forms produced in fine-grained sand under combined-flow conditions. They suggest that higher vertical aggradation rates, the superposition of bed sets formed during the same event but in different orientations, and low migration rates produce the morphology of hummocky cross-stratification which is much different from typical large-scale, low-angle trough cross-stratification.

Combined flow induced by the primary influence of wave oscillation and a secondary component of a 'steady' longshore (unidirectional) current produce the bedform. From observations of modern processes, hummocks seem to form under conditions close to that expected for upper flat bed stratification (Greenwood & Sherman, 1986; Nottvedt & Kreisa, 1987). Near-bed oscillatory flows were measured at 1.1 m/sec. and longshore currents had velocities around .27 m/sec. As these currents waned, rapid fallout of suspended sediment triggered the vertical growth of the hummocky bedform. Recent flume studies also have tried to examine the genetic structure of the hummocky bedform. Arnott & Southard (1988) altered the amounts and proportions of unidirectional and oscillatory current movement in a flow-duct experiment and observed the resultant form types. As expected, under oscillatory conditions, symmetrical bedforms developed. However, even at large oscillatory current velocities, a small introduction of a unidirectional velocity component produced a decided asymmetry to the form and triggered slow migration. This suggests that combined flow conditions can produce atypical bedforms even when the oscillatory component is large.

Figure 18 illustrates the typical hummocky bedform, portraying the downward curving hummocky sets truncating low-angle laminations of swaly sets. Harms *et al.* (1975, 1982) first introduced the term of hummocky cross-stratification to describe low-angle foreset laminations which pinch and swell. According to his observations, these laminations were abundant in some stratigraphic sequences and defied the normal bedform classification scheme. Even at that time, before rigorous study of the form

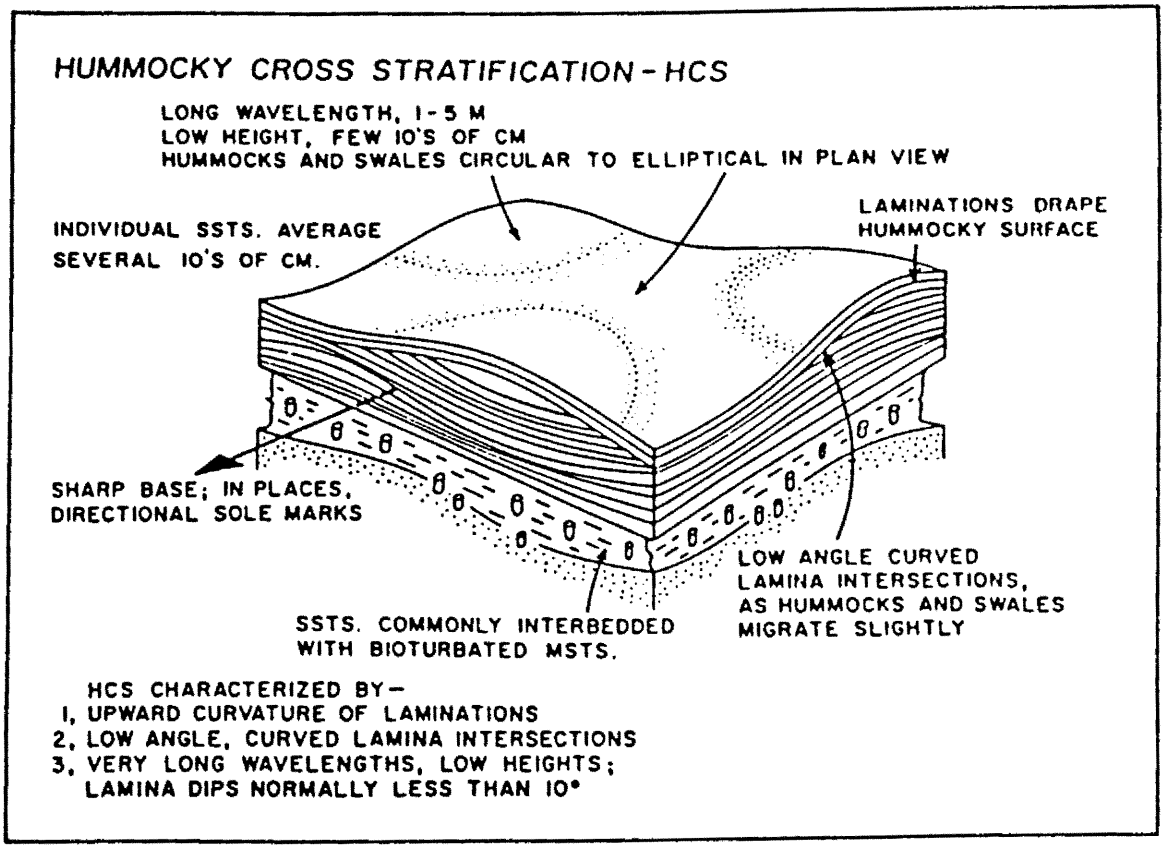

Figure 18. Block diagram depicting hummocky cross-stratification in a typical interbedded sandstone/bioturbated mudstone facies (from Walker, 1984).

both in ancient and modern deposits, the general consensus among workers that an oscillatory current component was needed in conjunction with a unidirectional flow to produce the bedform (Hunter & Clifton, 1981; Harms *et al.*, 1982). Some workers concluded that to produce the parallel to sub-parallel laminations which drape the hummocky form, rapid sediment aggradation is needed. Alternatively, Bourgeois (1984) suggested that the hummocks are not actively aggrading bedforms but are the end result of erosive storm-related processes which scoured the sea floor leaving behind a hummocky topography which was subsequently infilled by sediment. In all hypotheses, current regimes associated with storm events are the most likely causative agent for the production of the bedform.

In conclusion, most of the sedimentary structures preserved in ancient shelf sequences seem to be genetically related to the episodic effects or storm-generated currents. Both oscillatory and unidirectional current flow are needed to account for the internal configuration of bedforms in the shelf setting. These combined flow mechanisms are poorly understood and ancient shelf sequences reflect this complexity. By relating bedform, stratification types, and facies associations with hydrodynamic energy levels and processes, interpretation and identification of shelf sequences is possible.

CHAPTER III

Descriptive Stratigraphy

Carlile Shale

The Blue Hill Shale Member of the Carlile Shale Formation is poorly exposed in the foothills outcrop belt along the Front Range, between Longmont and Fort Collins, Colorado (T3N-T7N, R69-68W). Lower and Upper Cretaceous strata are exposed in eastward dipping hogback ridges oriented in an approximately north-south strike direction. These ridges are composed of resistive strata which include formations from the Dakota Group, Colorado Group, and Niobrara Formation (Figure 5). The Carlile Shale is typically a valley former located between the Dakota Formation hogback and a smaller ridge composed in part of Niobrara strata. Upper portions of the Carlile Shale which include the uppermost Blue Hill Shale Member, are usually only exposed when gullied or excavated by quarrying activities.

The Carlile is composed of slightly calcareous, fissile, bluish gray to grayish black shale which coarsens upward in response to increased silt content near the contact with the overlying Codell Sandstone. The contact between the two can appear gradational or sharp; variability in the nature of the contact is a distinctive characteristic along the outcrop belt in north central Colorado. In the northern part of the Boettcher Quarry (Sec. 1), the contact appears sharp due to an abrupt color change (Figure 19). Bluish gray shale is abruptly overlain by a light tan to brown siltstone which is in turn overlain by thin, lenticularly bedded sandstone. In this section, the Blue Hill/Codell contact is picked at this color change. However, 1250 feet (382 m) south of Section 1, near the extreme southern end of the Boettcher Quarry outcrop belt (Section 2), the contact

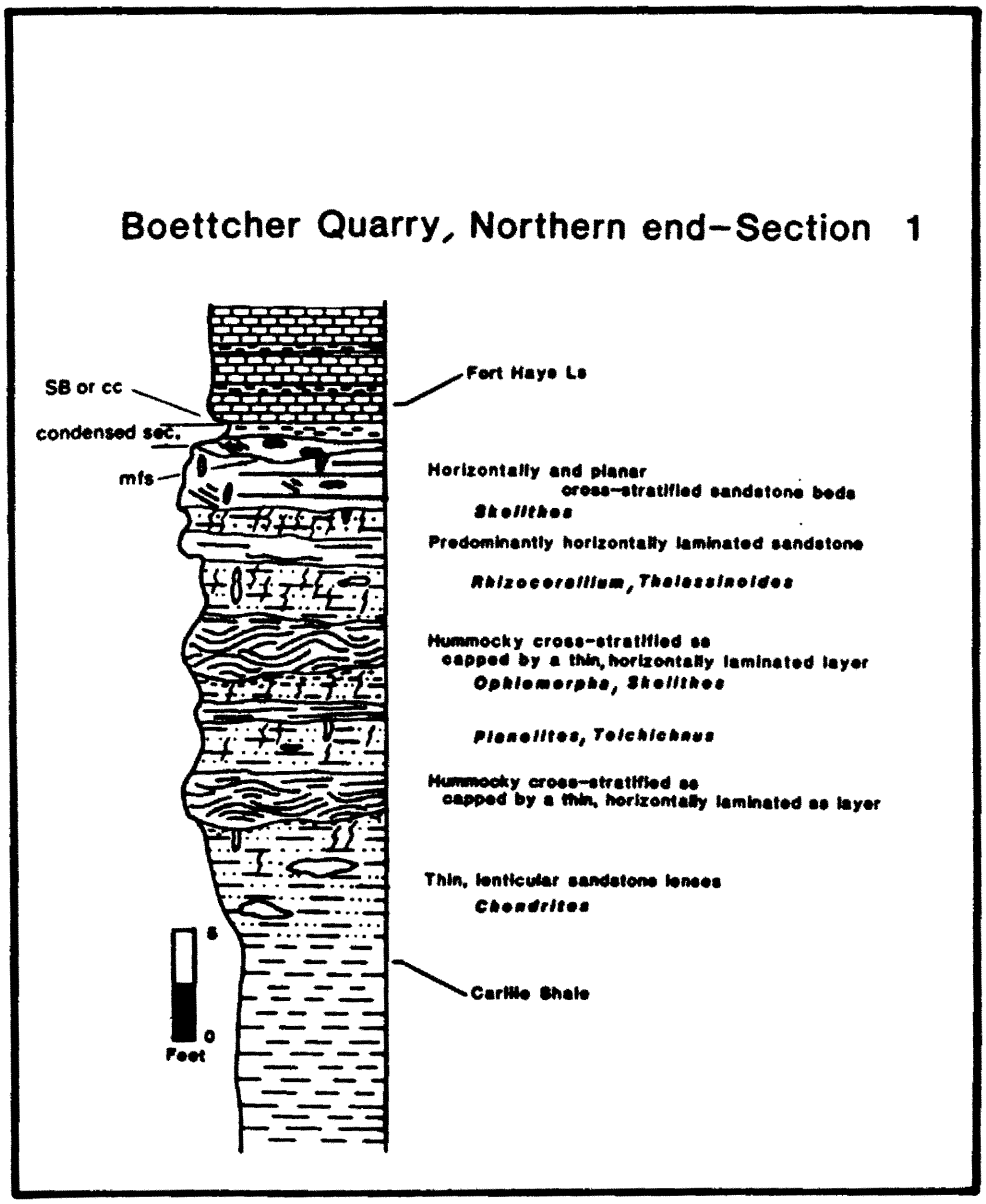

Figure 19. Section 1 - Measured outcrop at northern end of Boettcher Quarry. mfs - marine flooding surface, SB - sequence boundary, and cc - correlative conformity.

appears gradational and as a consequence, more difficult to pick (Figure 20). The color change is gradational, and reflects the gradual upward increase in silt content. Figure 20 also depicts an increase in bioturbation intensity as the Blue Hill Shale grades into the Codell Sandstone. In this area, thin < 2 in. thick (5 cm) lenticularly bedded very fine-grained sandstone lenses are common near the contact. The contact was picked at the base of the last lenticularly bedded sandstone lens < 1.5 in. (4 cm) thick, and in the absence of sandstone lenses, the contact was picked at the siltstone/ silty shale interface.

In Section 3 (behind the Larimer County Landfill), the contact is gradational (a slow, gradual color change) except in an area which is hummocky cross-stratified (Figure 21). Near the base of this section, a 1.2 foot (36.6 cm) thick hummocky cross-stratified, very fine-grained sandstone interval truncates the upper portion of the Blue Hill Shale. Laterally, this cross-stratified interval lenses out rapidly and the contact once again is gradational. Because of the difficulty in picking the Carlile/Codell contact, all sections were measured from the overlying Fort Hays/Codell contact.

The Rhoades #1 core which comprises Section 4 also contains a gradational lower contact with the underlying Carlile Shale. Figure 22 depicts a schematic representation of the gradational relationship between lowermost Codell and uppermost Carlile strata. Photographs of the lower portions of the Rhoades #1 core (Figures 23 & 24) indicate that the degree of bioturbation and frequency of siltstone partings slowly decrease as the Codell Sandstone grades into the Blue Hill Shale Member of the Carlile Shale Formation. Tan to brown bioturbated siltstone grades downward into gray to black fissile shale which contains very fine, 1/4 inch (.7 cm) thick carbonate partings. It should be noted that unlike the outcrop sections, the color change in the core between the two members is much more subtle. It is likely that surface weathering phenomena enhance the contact distinction. Lowman (1977) also encountered problems in picking the contact in her study of the Codell Sandstone near Boulder, Colorado and hung her outcrop sections from the overlying Fort Hays/Codell contact. Regional correlations

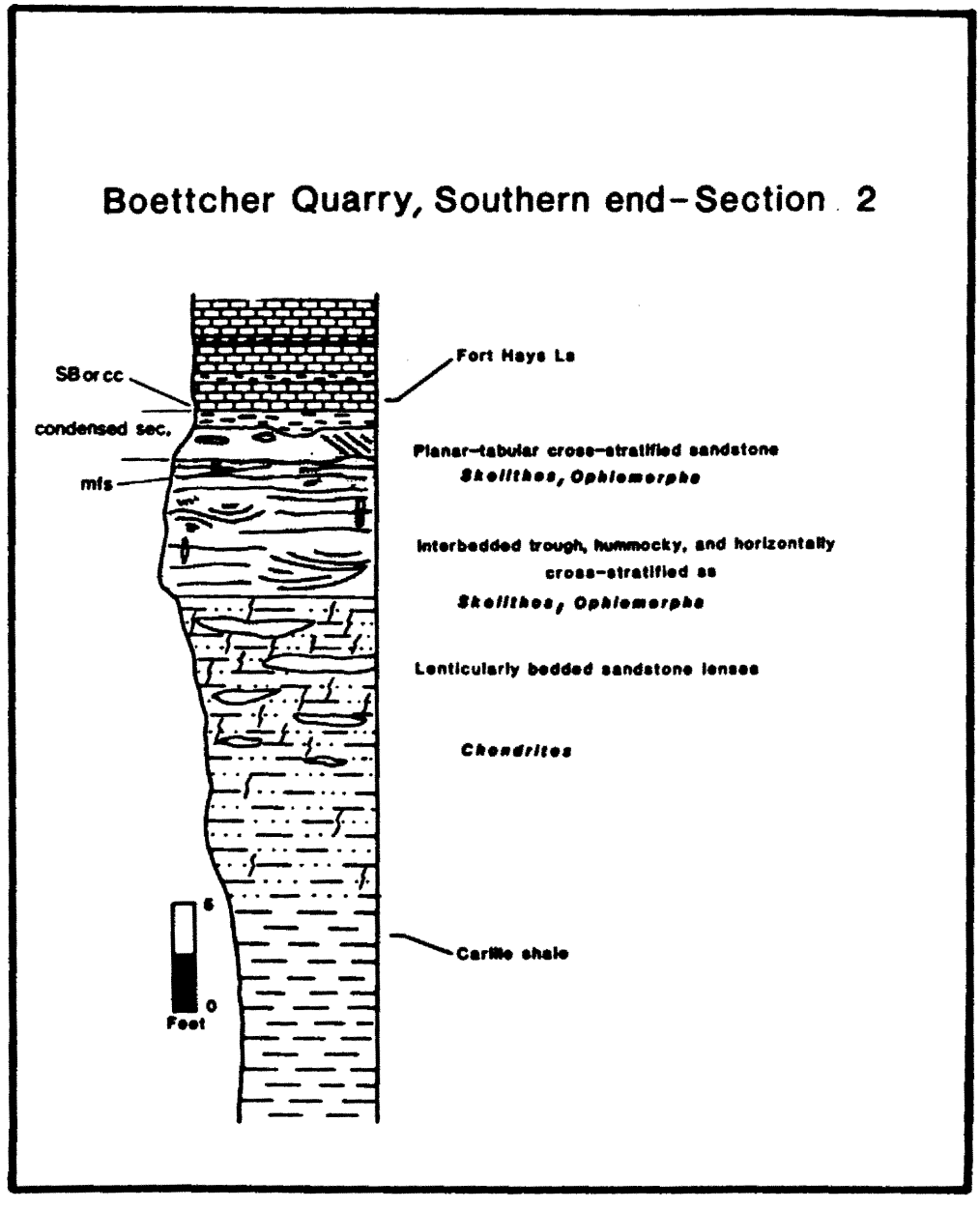

Figure 20. Section 2 - Measured outcrop at southern end of Boettcher Quarry. mfs - marine flooding surface, SB - sequence boundary, and cc - correlative conformity.

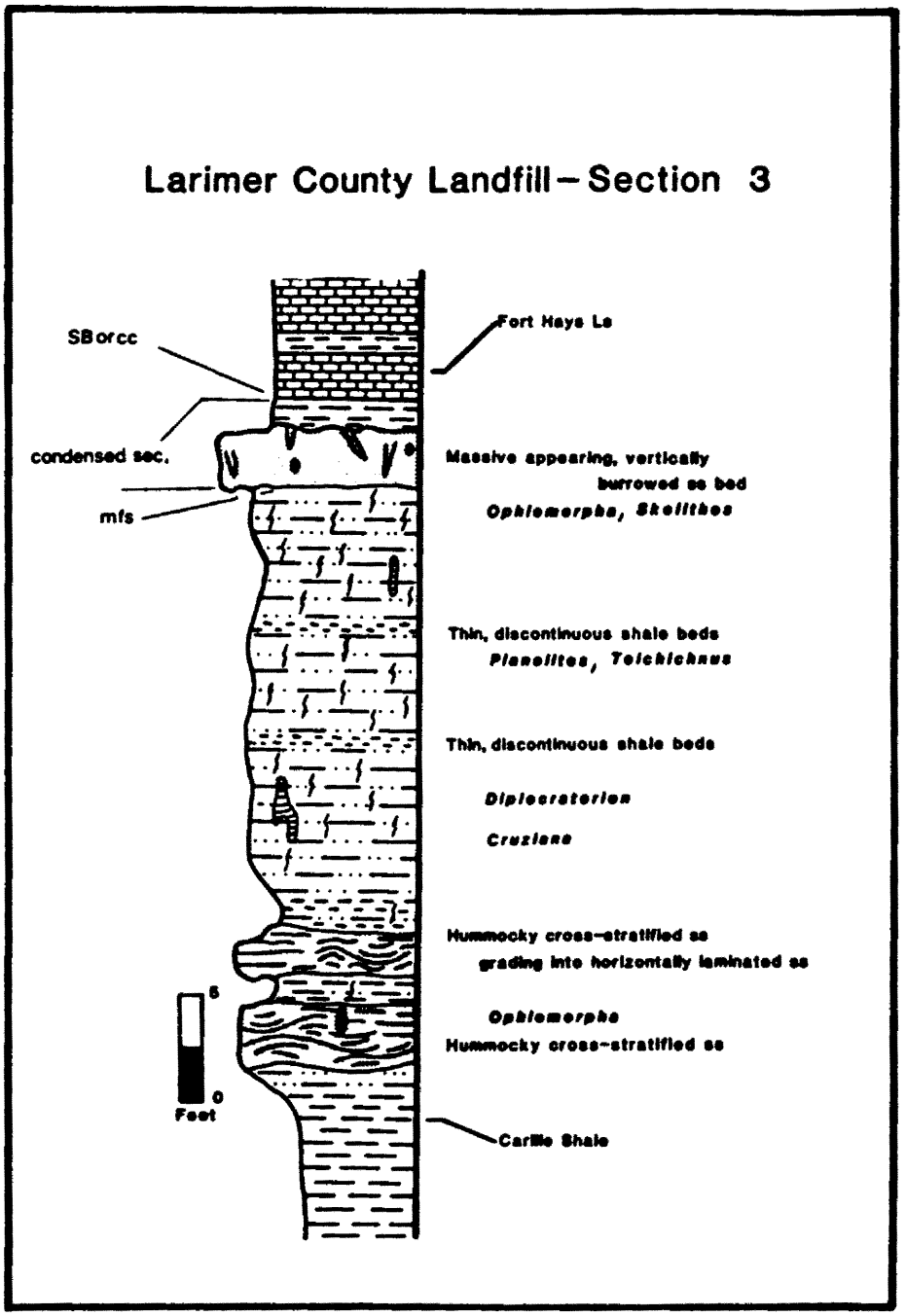

Figure 21. Section 3 - Measured outcrop at Larimer County Landfill. mfs - marine flooding surface, SB - sequence boundary, and cc - correlative conformity.

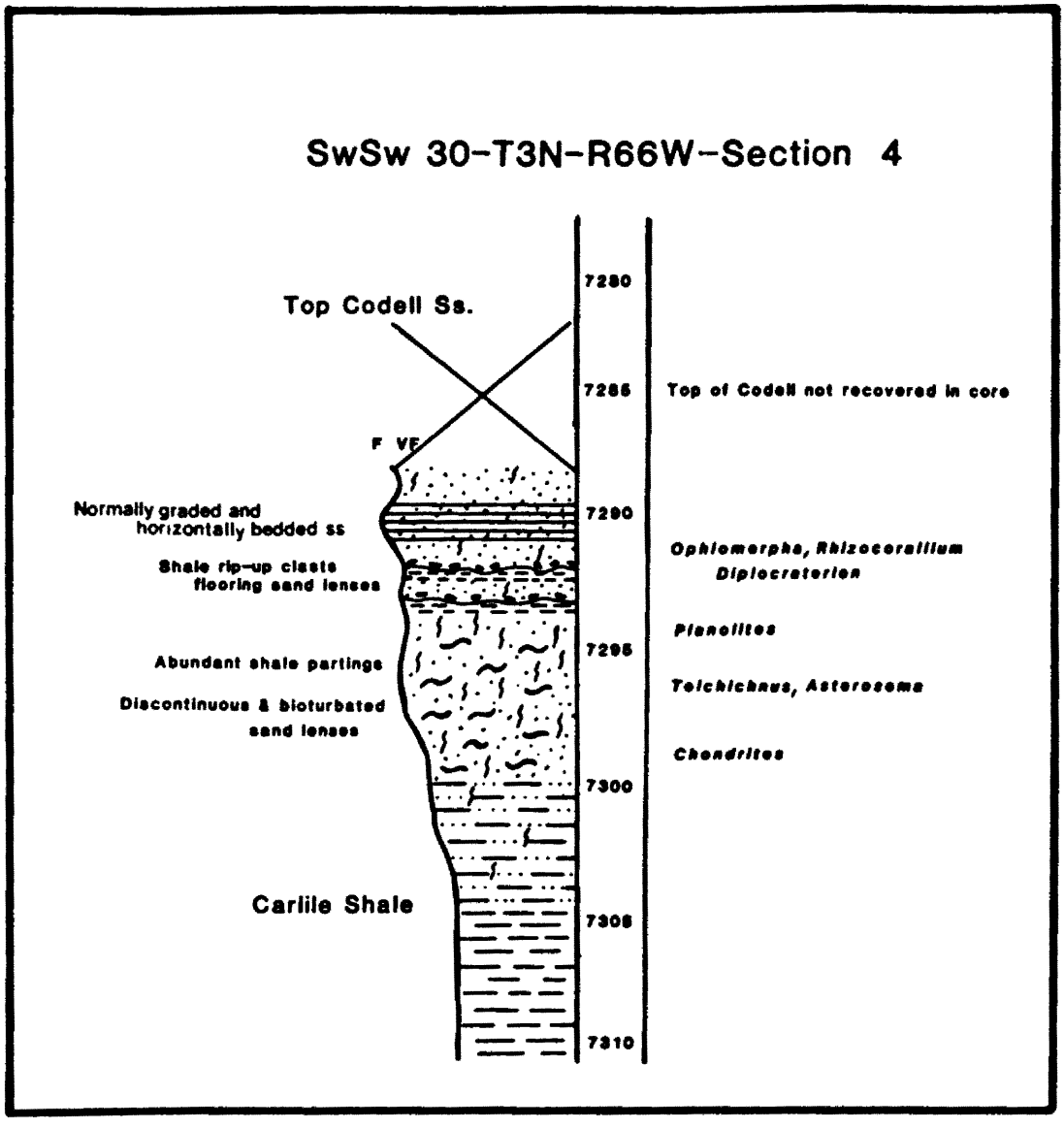

Figure 22. Section 4 - Measured core from Rhoades #1, SwSw 30-T3N-R66W.

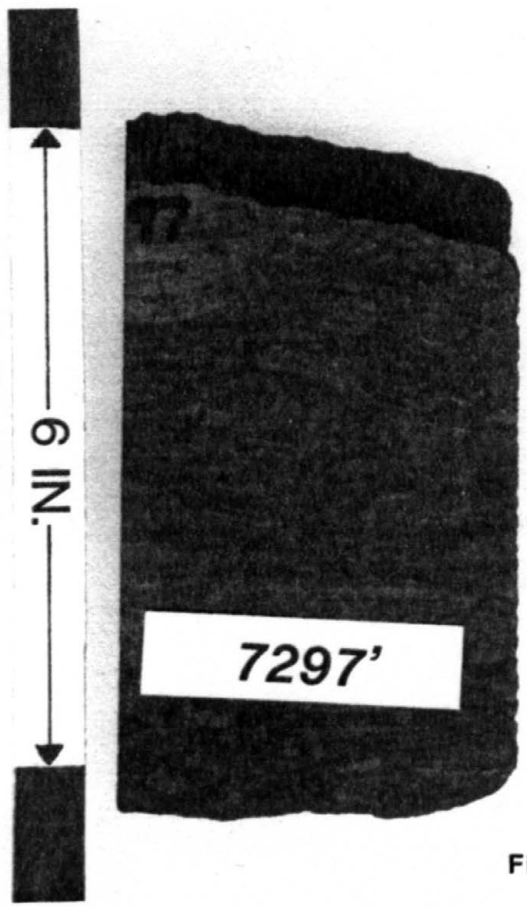

Figure 23. Extensively bioturbated section of the Codell Sandstone in Rhoades #1 core.

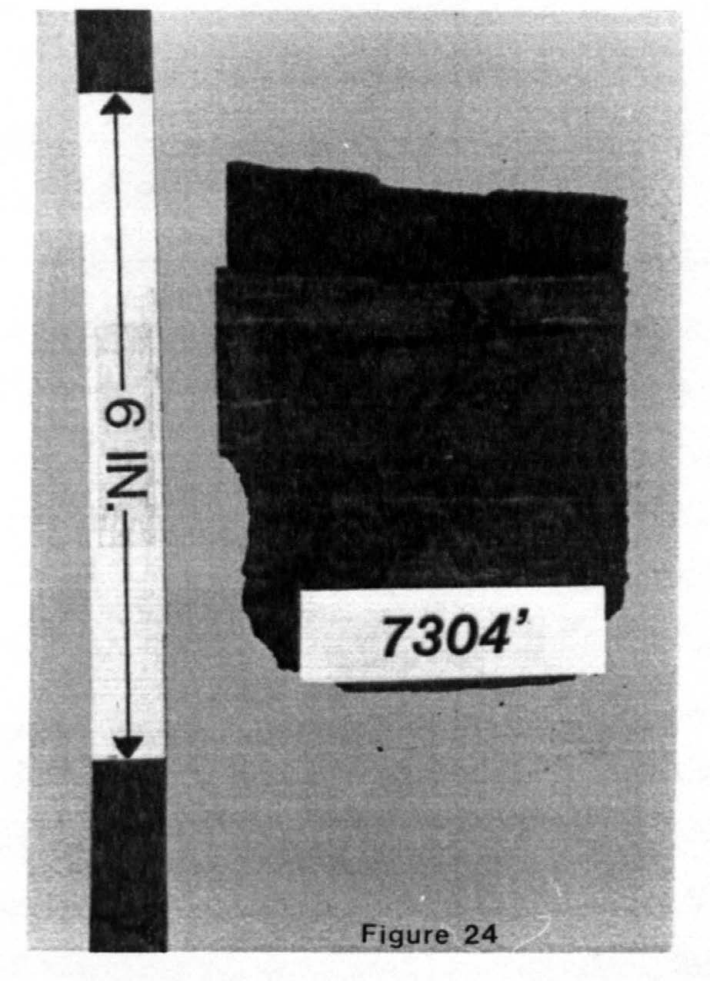

Figure 24. Typical section of the Carlile Shale from the Rhoades #1 core. Light colored lenses are siltstone partings.

completed by Merewether and Cobban, of the U.S. Geological Survey (1983) indicate that the Carlile Shale is roughly time correlative to the lower Mancos Shale of north central New Mexico and east central Utah, the upper part of the Frontier Formation in central Wyoming, and the Carlile Shale in northeastern Wyoming. These regionally extensive marine shale sequences were deposited in portions of the Western Interior Cretaceous Seaway.

Codell Stratigraphy

Boettcher Quarry (northern part), Section 1

Interbedded layers of sandstone, siltstone, and shale comprise the Codell interval in this area (Figure 19). Recalculated composition values from hand specimens show the Codell to be a quartz arenite according to the standard ternary diagrams. However, the framework constituents comprise: 88% quartz, 3% mica flakes and feldspar grains, 3% rock fragments, 4% heavy minerals, and 2% chert grains. The quartz grains range from subangular to subrounded and are equant to spherical. In the sandstone lenses, the grains are moderately to well sorted. In zones affected by bioturbation, the range is from moderately to poorly sorted. Specific petrologic aspects of the Codell Sandstone will be treated in a later chapter. In the lower portions of the formation, the sandstone is friable and clay-cemented. Near the top of the interval (the upper 1-2 feet, 30.5 - 61 cm), the sandstone is well indurated and cemented by calcite. (This unit has been referred to as the 'calcarenite unit' or the Juana Lopez member). Individual sandstone lenses are fairly 'clean', less than 10% clay matrix. However, the overall formation has a visual estimate of matrix as high as 30%. This is due to intense burrowing activity which mixed silt, clay, and sand-sized sediment with organic matter during the deposition of the Codell Sandstone. Total thickness of the interval as measured from the Fort Hays/Codell contact is 24 feet (7.3 meters).

Physical Structures Most of the interval consists of hummocky cross-stratified to horizontally stratified, very fine-grained sandstone lenses interbedded with zones of intensely bioturbated siltstone and silty shale (Figure 19). Near the base of the formation, thin (< 2-3 in., 5-7.6 cm) lenticularly bedded sandstone and sandy siltstone lenses are common. They are overlain by massively bedded(?) to hummocky cross-stratified sandstone lenses. These lenses range from 3-6 feet (85 cm to 1.8 meters) in length and pinch-out rapidly in a lateral direction (Figure 25). Typically, these units have an erosional to sharp contact with an underlying, bioturbated shale interval (Figure 26). Generally, the lenticular sandstone beds are capped by thinly interlaminated shale and horizontally stratified, very fine-grained sandstone layers (Figure 26). The thinly laminated shale layers are less than 1/2 inch (1.5 cm) in thickness. Total thickness of the sandstone packages range from 9-30.7 inches (23-78 cm). At first glance, some of the lenses appear massively bedded with no obvious stratification apparent. On closer inspection, gently inclined foreset laminae truncate each other at low angles, portray a convex or concave upward form, are subparallel to parallel in arrangement, and subtly pinch and swell in thickness. This internal configuration of foreset laminae is typical of hummocky cross-stratification.

Each of these stratified intervals are overlain by intensely bioturbated siltstone and shale zones ranging from 1.5-2.5 ft (43-76 cm) in thickness. Approximately 1 foot (30.5 cm) from the top of the Codell Sandstone, a 2.5-3 foot (70-91.5 cm) thick, horizontally laminated sandstone grades laterally into planar-tabular angle-of-repose cross-bedding (Figure 27). Bedding thicknesses for the planar cross-stratified intervals range from 6-10 inches (15-25 cm) and typically pinch-out in a lateral direction over a distance of 5-8 feet (1.5-2.5 m). The uppermost portion of the Codell Sandstone contains massively bedded and planar-tabular cross-stratified, very fine-grained sandstone. A discontinuous, lenticular scour surface is present at the top of the Codell. The scour surface is devoid of any discernible lag deposits.

Figure 25. Isolated swaly sandstone lenses near the base of Section 1, Boettcher Quarry.

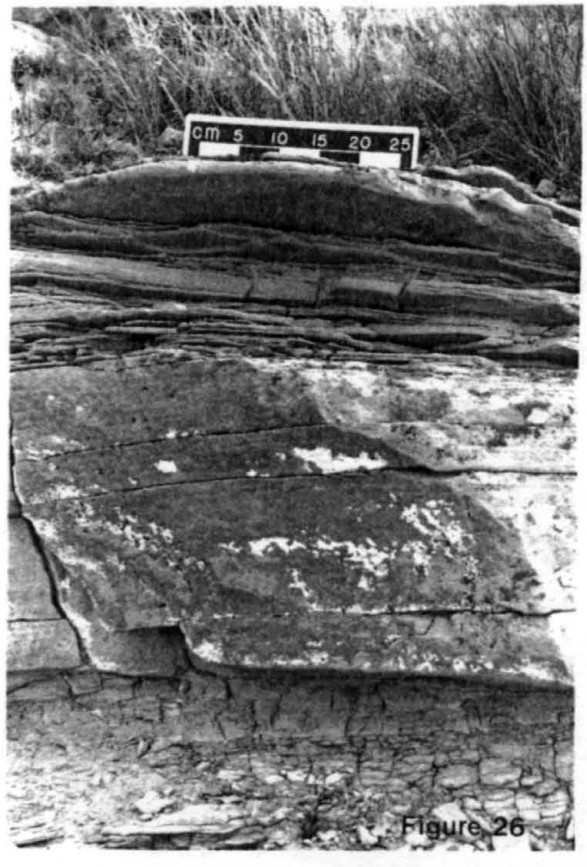

Figure 26. Sharp based hummocky cross-stratified sandstone lens grading upward into thinly interlaminated sandstone/shale layers. Thin sandstone layers show parting lineations - Section 1.

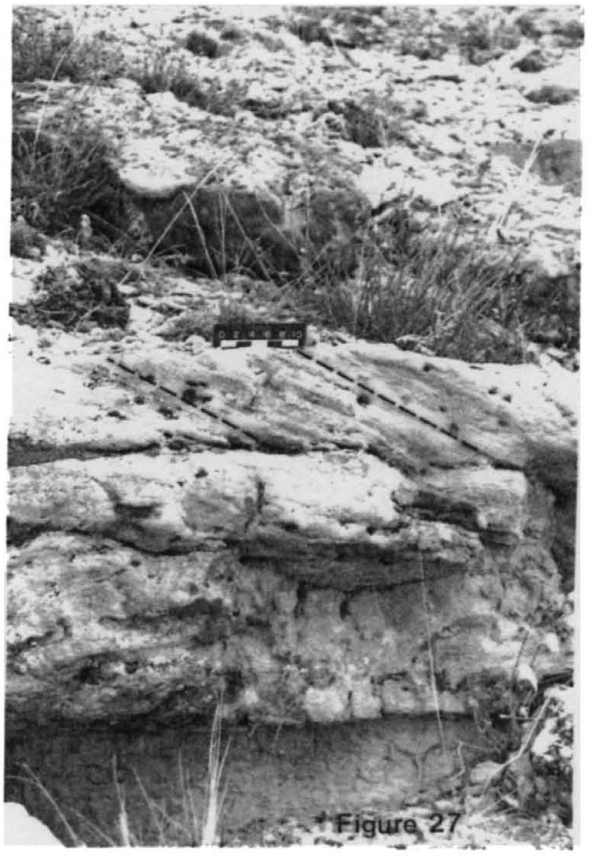

Figure 27. Angle-of-repose planar cross-stratified sandstone lens near the top of Section 1.

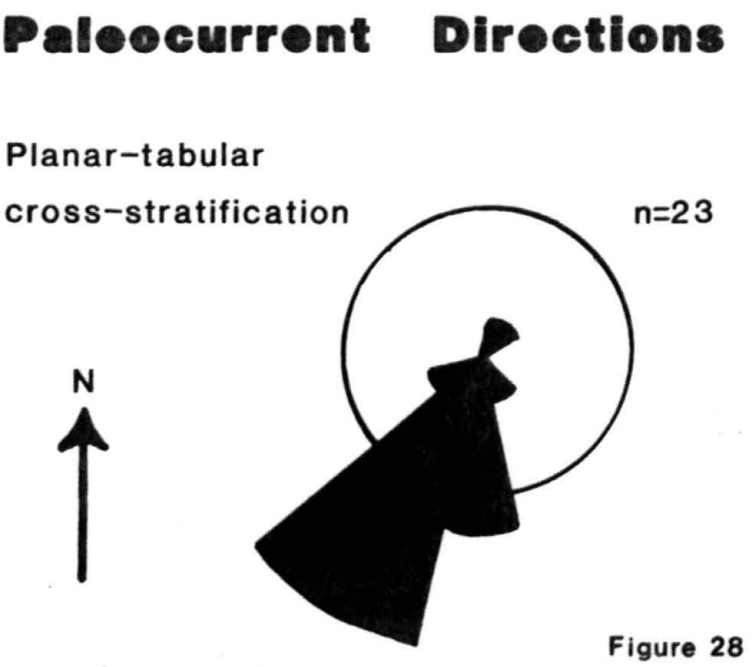

Figure 28. Rose diagram depicting apparent paleocurrent directions. Measurements taken from planar cross-stratified sandstone lenses.

Apparent paleocurrent directions were derived from the planar-tabular cross-bedded sandstone lenses. Because all foreset laminations are exposed in cross-section and only in two-dimensions, true foreset orientations may not have been measured. All measurements grouped in the south to southwest direction (Figure 28).

Biogenic Structures In the bioturbated silty sandstone, siltstone, and shale intervals, the abundant trace fossils are largely of the *Cruziana* ichnofacies. Calcite cored burrows of *Chondrites* and *Planolites* cause the complex mottling pattern which totally obscures any discernible stratification in these zones. Vertically stacked spreite of *Teichichnus* are less common. Polyphase burrowing activity is documented by the near vertical burrows of Rhizocorallium and smooth-walled vertical burrows (*Skolithos* ?) depicted in Figure 29. In the hummocky and horizontally cross-stratified sandstone lenses, trace fossils of the *Skolithos* ichnofacies occur. Near vertical burrows of *Ophiomorpha* occasionally disrupt the stratified bedding (Figure 30). These burrows range in size from 2-5 inches (5-12 cm). Along bedding planes in the sandstone, branching patterns of *Thalassinoides* and *Planolites* are common and typically obscure the bedding surface (Figure 31). Sandstone beds commonly truncate burrows in the underlying bioturbated siltstone and shale intervals.

Textural Trends and Contacts An overall coarsening upward trend in grain size is not evident in this section. The sandstone lenses range in grain size from upper very fine-grained to lower fine-grained. The top portion of the Codell is no coarser than the bottom-most hummocky cross-stratified interval. Internally, the sandstone lenses are massive or normally graded. All contact relationships between sandstone, siltstone, and shale are either sharp or erosional. However, no major truncation surfaces are apparent except for the scour surface which caps the Codell interval. The contact relationship between the Codell and the overlying Fort Hays limestone is sharp and is marked by a 4-7 inch (10-18 cm) thick calcareous, black fissile shale (Figure 19). No discernible lag deposits are contained in the shale. However, the base of the first limestone bed in the Fort Hays is paved with *Inoceramus* prisms, quartz grains, and mud clasts.

Figure 29. Smooth-walled vertically oriented *Skolithos* burrow - Section 1.

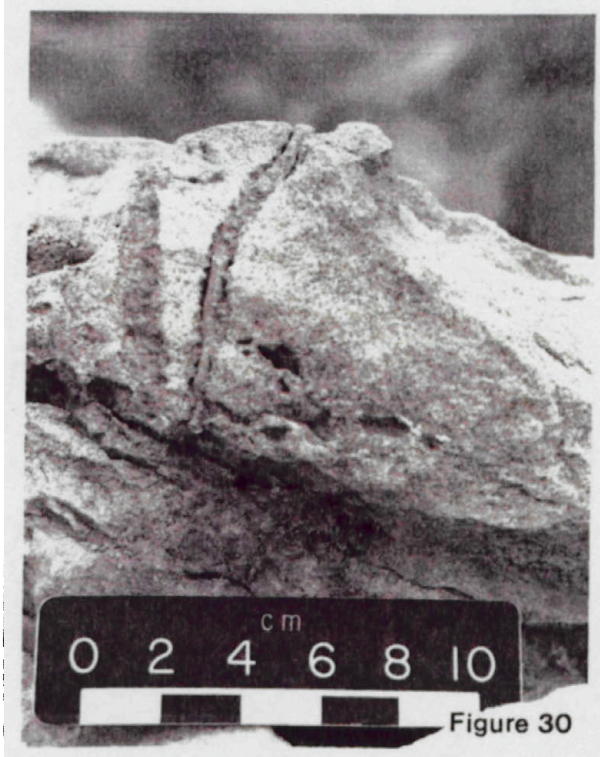

Figure 30. Near vertical, knobby-walled *Ophiomorpha* burrow located in top of horizontally cross-stratified sandstone - Section 1.

Figure 31. Branching patterns of *Thalassinoids* and *Planolites* along bedding plane of a horizontally cross-stratified sandstone bed - Section 1.

Boettcher Quarry (southern part), Section 2

Twelve hundred and fifty feet (382 m) south of Section 1, a complete portion of the Codell Sandstone exhibits a completely different arrangement of physical structures (Figure 20). As before, the Codell interval is composed of sandstone, siltstone, and shale interbeds. The sandstone ranges from light tan to brown in color. A quartz arenite in recalculated composition, the grain size ranges from lower fine-grained to upper very fine-grained. The framework constituent breakdown is very similar to that described for Section 1. The sandstone is composed of 88% quartz, 3% rock fragments, 5% heavy minerals, 1% chert, and 3% mica flakes and feldspar grains. Quartz grains in the Codell interval range from subangular to subrounded and are equant, blocky, and spherical in form. The sandstone beds tend to be generally well sorted. Unlike the outcrop in Section 1, the top seven feet (2 meters) is calcite-cemented and only the thin, lenticularly bedded sandstone lenses at the base are clay cemented (Figure 20). In bioturbated zones, the visual estimate of matrix is very high (25-35%). In zones which are cross-stratified, the sandstone is 'cleaner', with a matrix estimate ranging from 8-10%. Total thickness of the interval as measured from the Codell/Fort Hays contact is 23.8 feet (7.3 meters).

Physical Structures At the base of the formation, lenticularly bedded sandstone lenses are totally encased in a tan to gray colored siltstone. Internally the lenses are massively bedded and range in thickness from 2-7 inches (5-18 cm). Typically, they pinch-out in a lateral direction over a distance of only 5-18 inches (13-46 cm). The thickness and length of these discontinuous sandstone beds slowly increase upward with a coincident increase in bioturbation intensity (Figure 20). Lower fine-grained, cross-stratified sandstone compose the top 7-8 feet (2-2.5 m) of the formation. In the lower portion of this unit, 5-6 inch (12-15 cm) thick trough cross-stratified sandstone beds occur. These bi-polar (but not necessarily bi-modal) cosets truncate each other in a tangential manner (Figure 32). These beds lense out rapidly and grade into horizontally

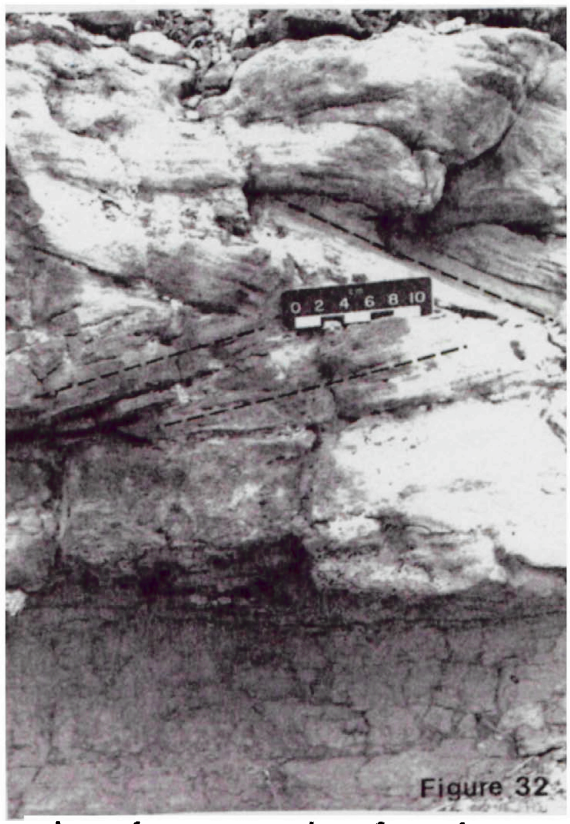

Figure 32. Apparent ninety degree truncation of trough cross-stratified sandstone beds in the lower portion of Section 2.

Figure 33. Immediately adjacent to the sandstone beds pictured in figure 32 the cross-stratified interval grades into horizontally stratified sandstone - Section 2.

cross-stratified sandstone beds (Figure 33). Occasional, thin shale interbeds drape some of the horizontally cross-stratified sandstone beds (Figure 33). Zones of planar angle-of-repose, ripple cross-stratification are arranged immediately adjacent to horizontally bedded intervals (Figure 34). They are small-scale features and lense out rapidly over a distance of 16-30 inches (40-75 cm). The top 1.3 feet (34 cm) of the Codell Sandstone is composed of massively bedded sandstone which is occasionally modified by angle-of-repose cross-stratification. Also present are intervals which are horizontally cross-stratified. The planar-tabular cross-beds pinch out rapidly (Figure 20), as do zones which are horizontally cross-stratified. A discontinuous scour surface is present at the Fort Hays/Codell contact. It undulates gently and locally scours only a few inches into the underlying massive to horizontally cross-stratified sandstone bed.

Biogenic Structures Distinct trace fossil assemblages are rare in the siltstone intervals of Section 2 because the intense bioturbation has obscured most of the patterns. However, a few calcite-cored *Chondrites* burrows are apparent. In the cross-bedded sandstone zones, near vertical burrows of *Skolithos* and *Ophiomorpha* are common. These stratified beds typically truncate bioturbated shale and siltstone intervals. Occasionally, the tops of the stratified sandstone beds are burrowed and mottled. These trace fossil assemblages are similar to those described in Section 1. Biogenic structures of the *Cruziana* ichnofacies dominate the bioturbated siltstone and shale zones while structures of the *Skolithos* ichnofacies are confined to the cross-stratified sandstone beds. The intensity of bioturbation gradually increases from the base of the Codell upward through the siltstone and lenticularly bedded sandstone interval (Figure 20).

Textural Trends and Contacts The section is gradually upward coarsening and upward thickening. No major truncation surfaces are present except for the scour surface at the Codell/Fort Hays contact. The surface is fairly discontinuous, and is capped by a thin, 4-7 inch (10-18 cm) shale layer. Contacts between the stratified sandstone beds are sharp to erosional but grade laterally into conformably arranged, horizontally stratified beds.

Figure 34. Isolated, planar angle-of-repose, ripple cross-stratified sandstone lens abruptly overlying low-angle foreset laminations (hummocky cross-stratification). Section 2.

Larimer County Landfill, Section 3

Approximately six miles south of the Boettcher Quarry, a large gully behind the Larimer County Landfill has exposed a complete section of the Codell Sandstone and an incomplete portion of the overlying Fort Hays Limestone (Figure 21). As in Sections 1 & 2, the Codell is composed of interbedded sandstone, siltstone, and shale. The sandstone ranges in size from lower-upper fine-grained and is a quartz arenite in composition. In this outcrop section, lithic rock fragments comprise a slightly larger percentage of the framework constituents when compared to the sections in the north. The breakdown of the framework grains is as follows: 86% quartz, 5% lithic rock fragments, 4% heavy minerals, 3% chert grains, and 2% mica flakes and feldspar grains. Quartz grains in the sandstone range from subangular to subrounded and are equant, blocky, and spherical in form. In stratified intervals, the grains are well sorted whereas in bioturbated zones are generally poorly sorted. Unlike Sections 1 & 2, most of the Codell interval is clay-cemented and friable. A 1.3 foot thick, well-indurated sandstone bed caps the Codell and marks the contact with the overlying Fort Hays Member of the Niobrara Formation (Figure 21). This top unit is silica-cemented rather than calcite-cemented as was the case in Sections 1 & 2. Visual estimates of matrix content are quite high for most of the interval, ranging from 25-35%. However, as was the case in the other outcrops, cross-stratified lenses are much 'cleaner'. Total thickness of the formation as measured from the Codell/Fort Hays contact is 24.5 feet (6.9 m).

Physical Structures A dominant aspect of Section 3 is the presence of a thick interval (15.5 feet, 4.7 m) of structureless, sandy siltstone (Figure 35). Light gray in color, the siltstone is mottled and devoid of discrete sandstone lenses due to intense bioturbation (Figure 36). Occurring at the base of the Codell, three discrete cross-stratified, light brown-tan sandstone beds are lateral to and underlie the bioturbated

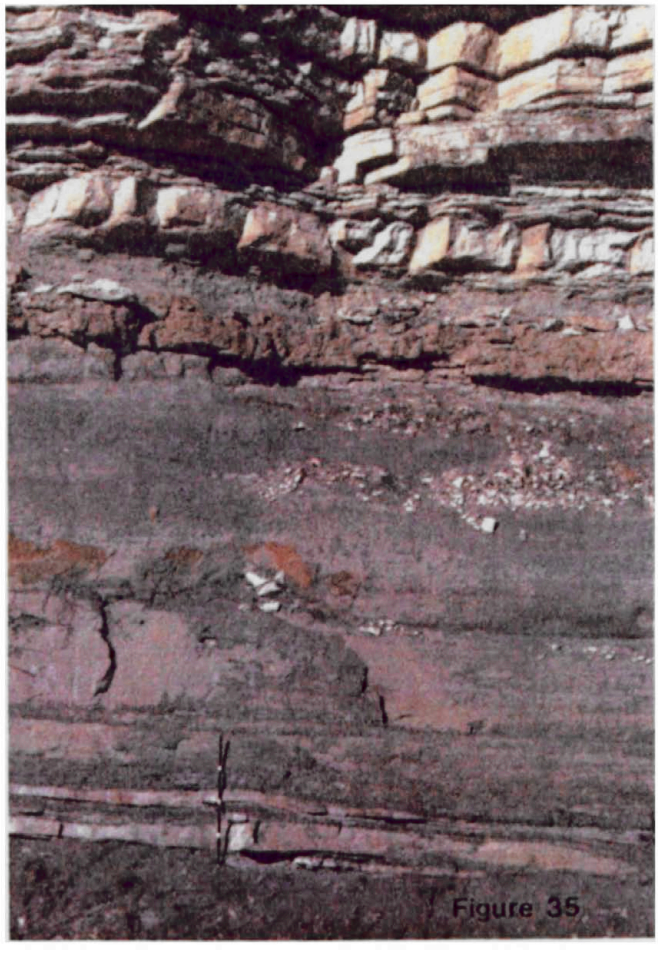

Figure 35. Overview of Section 3, showing hummocky cross stratified lenses near the base, an extensively bioturbated middle portion and the tan sandstone bed which caps the Carlile interval.

Figure 36. Close-up view of the mottled, bioturbated portion of Section 3. Scattered vertical burrows are apparent.

siltstone interval. They range in thickness from 4.5-7 inches (11.4-18 cm) and lens out rapidly over a distance to 45-62 feet (14-19 m) into non-calcareous silty shale (Figure 37). Internally, the sandstone beds contain gently inclined foreset laminae which are distinguished by low-angle truncations (Figure 38). The beds are marked by a sharp, gently undulating basal surface and grade upward into lenticularly bedded, rippled, and bioturbated silty shale and siltstone (Figure 38). In places, the inclined foreset laminae grade laterally into horizontally stratified intervals.

Small, (<1 inch) elongate to striated, randomly arranged tool marks are present on basal surfaces of siltstone and stratified sand sequences (Figure 39). Capping the bioturbated siltstone interval is a 2-2.5 foot thick (61-76 cm), silica-cemented, light brown sandstone bed (Figure 40). It is massive in appearance and contains abundant vertical to near vertical *Skolithos* and *Ophiomorpha* burrows. The sandstone ranges in grain size from lower to upper fine-grained. It is laterally continuous across the 154 feet (50 m) of surface exposure. A discontinuous scour surface is present at the top of the sandstone bed and randomly incises only 3-4 inches (7.6-10 cm) into the underlying bed (Figure 40). The surface is capped by a 2.5-3 foot (76-90 cm) thick gray, calcareous shale which contains no discernible lag deposits. This shale interval is overlain by the first gray limestone bed of the Fort Hays Member of the Niobrara Formation.

Biogenic Structures Burrowing is rare in the hummocky and horizontally cross-stratified sandstone lenses; only a few vertical to nearly vertical *Ophiomorpha* are present. In the intensely bioturbated siltstone and silty sandstone intervals, a mixture of *Skolithos* and *Cruziana* ichnofacies are present. Vertically oriented *Diplocraterion* obscure *Planolites* and horizontally oriented clay-lined, smooth-walled burrows. This may be an indication of polyphase burrowing activity. Oblique views of *Teichichnus* are also apparent. All physical structures in the 15.5 feet (5 m) thick siltstone interval have been totally obliterated by bioturbation. Along bedding planes, crawling traces

Figure 37. Lateral pinch-out of hummocky cross-stratified sandstone bed located near base of Section 3. Staff is divided into 1 foot increments.

Figure 38. Close-up view of internal stratification of the hummocky cross-stratified bed pictured in figure 37. Note low-angle truncation surfaces, sub-parallel and hummocky to swaly laminae arrangement. Hammer is approx. 1 foot long.

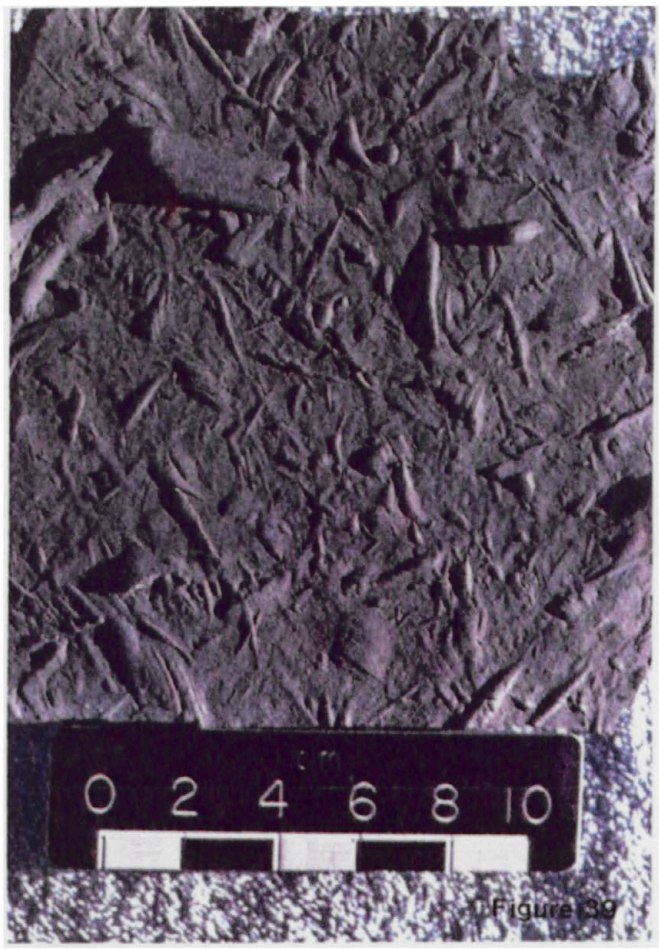

Figure 39. Randomly oriented, striated tool marks on basal surface of bioturbated silty shale bed.

Figure 40. Sandstone bed at top of Codell interval. Note small scour surfaces in and on top of the silica-cemented interval. Rock hammer for scale.

such as *Cruiziana* are common. Diversity of trace fossils in this interval is high. Diversity is low in the uppermost sandstone bed of the Codell as the only two burrow types present are vertically oriented *Ophiomorpha* and *Skolithos*. However, the bed is mottled with these structures so the abundance is high of the two burrow types.

Textural Trends and Contacts All stratified sandstone beds in this section have sharp, basal contacts and sharp to gradational upper contacts. Except for the top of the interval, all sandstone units lens out rapidly and are highly discontinuous. A coarsening and thickening upward trend is not evident in this exposure. The sandstone beds at the base of the Codell interval are only slightly finer-grained (< one ø unit) than the continuous sandstone bed at the Fort Hays/Codell contact. As was present in Sections 1 & 2, a major truncation surface is present at the top of the interval. The scour surface in this exposure undulates gently in places, but generally is expressed as a sharp contact between the beds above and below.

Rhoades #1 - - - SwSw 30-T3N-R66W, Section 4

Approximately 18 miles southeast of the outcrop belt along the western edge of the D-J basin, a core was taken through the Codell interval from a well whose location is depicted in Figure 4. The top five feet of the Codell Sandstone was not cored because of an incorrect core point estimate (Figure 22). However, the contact between the Codell and the underlying Carlile Shale was recovered. Most of the interval is light gray in color and intensely bioturbated. A few discrete gray sandstone lenses and non-calcareous, black shale drapes are present (Figure 41). The Codell Sandstone in this portion of the basin is composed of bioturbated siltstone, thin sandstone lenses, and shale partings. After recalculation, the Codell is a quartz arenite in composition. Breakdown of the framework constituents in hand sample is as follows: 92% quartz, 2% lithic rock fragments, 2% heavy minerals, 3% chert grains, and 1% mica flakes and feldspar grains. Thin sections taken from this core will be examined in detail in a

Figure 41. Overview of the top portion of the Rhoades #1 core - Section 4. The whole interval looks extremely 'shale-rich'.

following chapter. As depicted in Figure 22, the major portion of the Codell section contains bioturbated siltstone and thin intervals of normally graded and/or horizontally laminated sandstone. Total thickness of the Codell interval recovered in the core is 18.5 feet (5.6 m). Subsurface log information shows the total interval thickness to be 23.5 feet (7 m).

Physical Structures At the very top of the Rhoades #1 core is a interval of bioturbated to non-bioturbated couplets (Figure 42). Two inch thick (5 cm) siltstone layers are separated by a 1.5 inch thick (3.8 cm) shale interval. This interval at 7289' has been partially mixed by burrowing activity. A similar shale unit at 7290' exhibits structures associated with an increased degree of burrowing activity. These thin, bioturbated zones grade upward into massive appearing siltstone which have only been slightly affected by burrowing activity. Directly underneath the couplets, a normally graded, very fine-grained sandstone bed is present at 7291' (Figure 43). An escape structure interrupts the bedding of this 5 inch thick (12.7 cm) thick sandstone interval. Each lamination is internally normally graded with very fine-grained sandstone grading upward into coarse (and darker colored) siltstone. Whether these laminations are part of a normally graded sandstone interval or the low-angle part of a hummocky cross-stratified bed cannot be ascertained. It is also possible that the core could have intersected a small portion of a large-scale trough cross-stratified sandstone bed. However, due to the subtle grading of individual laminations and the near vertical orientation of the escape structure, the bedding is most likely a result of sediment fall-out processes.

At 7292', an erosional scour surface is present at the base of a horizontally laminated sandstone sequence (Figure 44). The top portion of the laminated interval is partially obscured by burrowing structures. Floored by shale rip-up clasts, the scour surface gently undulates and marks the contact. The overlying 3 inch (7.6 cm) horizontally laminated interval is capped by a thin zone of bioturbation which is in turn

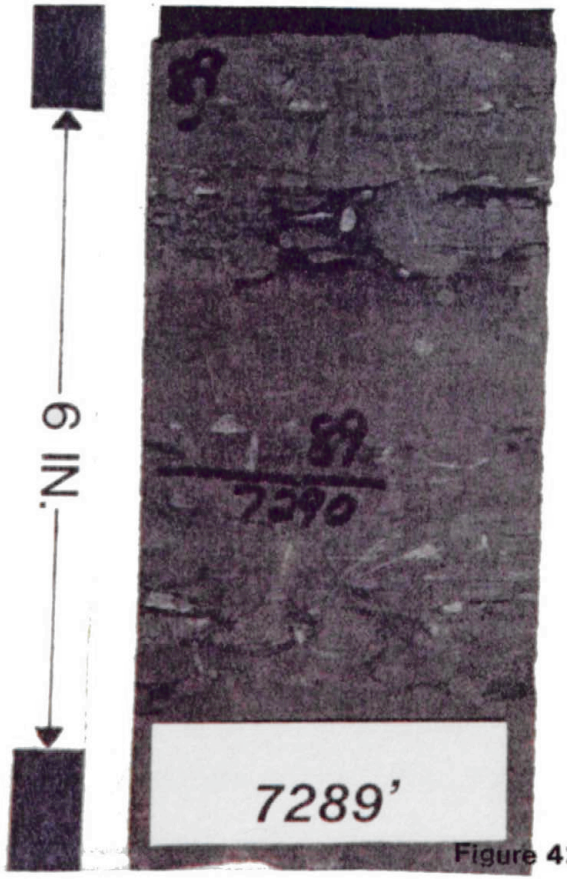

Figure 42. Close-up view of bioturbated to non-bioturbated couplets in sandstone/shale sequences a 7289'.

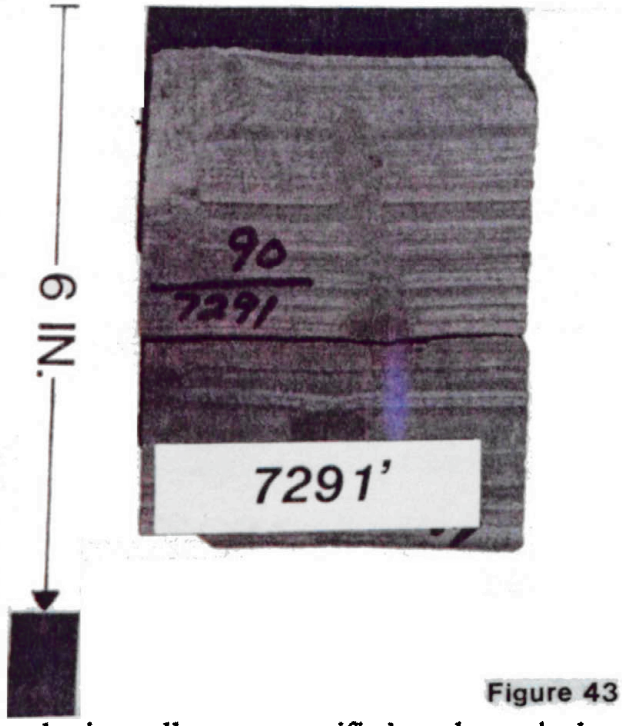

Figure 43. Apparent horizontally cross-stratified sandstone bed at 7291'. Note normal grading of laminations and escape structure in middle of the interval.

capped by another shale layer (Figure 44). This is an example of a classic laminated to burrowed sequence frequently described in literature as an indicator of lower shoreface, nearshore to offshore marine environments. The rest of the core contains intensely bioturbated siltstone (Figure 45) in which the degree of bioturbation slowly diminishes downward until it grades into black, silty shale (Figure 24). This contact is very gradational and totally dependent upon the degree of bioturbation in the sequence. As a consequence, the contact between the Codell and the Carlile Shale was picked at the last siltstone/shale interface in which no bioturbation was present.

Biogenic Structures Due to the intense mottling of most of the cored sequence, discrete traces are difficult to find. However, Figure 45 exhibits a burrowing pattern typical of *Planolites, Teichichnus*, and *Asterosoma.* Small (< 2 cm), light-colored, spherical to elongate traces in Figure 23 are probably *Chondrites.* The concave-upward feeding pattern of *Rhizocorallium* (or *Diplocraterion*) is present near the top of the core interval presented in Figure 42. An escape structure pictured in Figure 43 may be an indistinct *Ophiomorpha* burrow. The Codell interval preserved in the Rhoades #1 core contains a diverse assemblage of trace fossils in which bioturbation intensity is high.

Textural Trends and Contacts Because of the missed core point, a definitive measurement of textural trends through the Codell is not possible. However, throughout the rest of the cored interval, the horizontally laminated or normally graded sandstone beds (lower fine-grained) are only slightly coarser than the bioturbated siltstone. Because of the interlaminated nature of the sandstone and siltstone beds, it is likely that a clearly defined coarsening upward trend may be present. Evidence for this supposition is strengthened by the gamma ray log signature taken from the wire-line logs run through this interval. Figure 46 shows a portion of the log suite run over the Codell and Carlile Shale sequence. The gamma-ray curve is serrated with the API units decreasing to the left upward through the Codell interval. At 7283.5' the curve jogs abruptly to the left and marks the contact with the overlying Fort Hays Limestone Figure

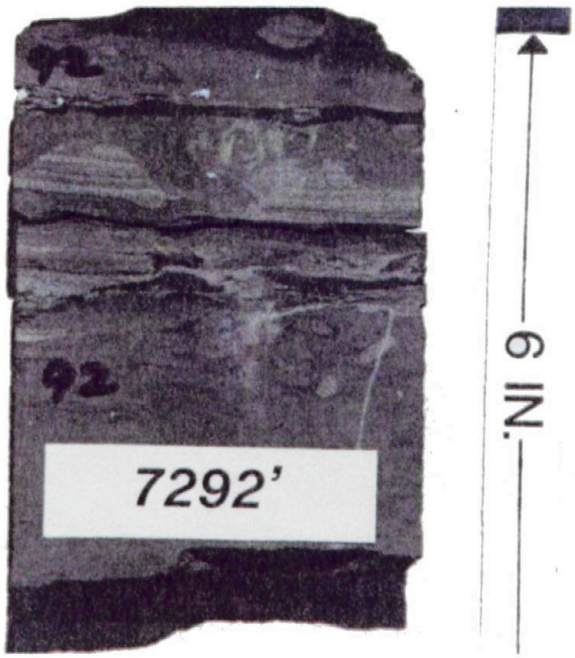

Figure 44

Figure 44. Laminated to burrowed sandstone/shale sequence at 7292'. Note shale rip-up clasts at base of horizontally cross-stratified interval. Burrowing obscures top of sandstone bed which is then draped by another shale interval.

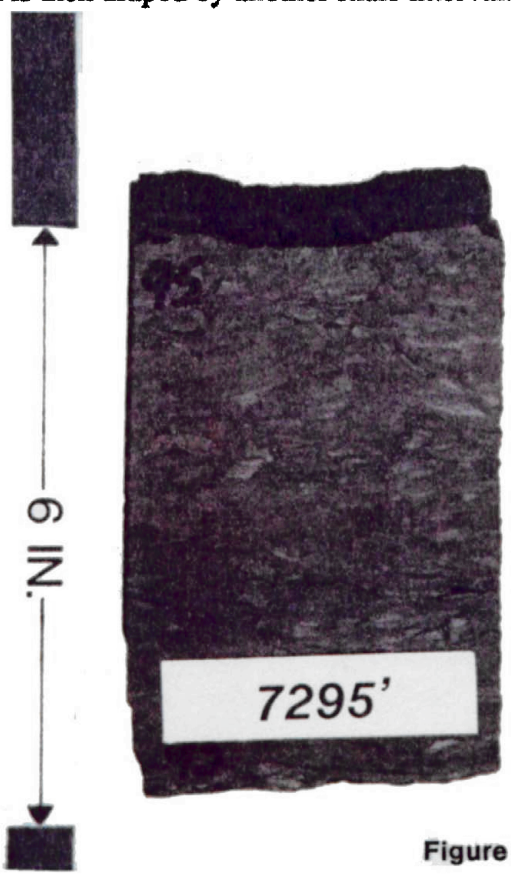

Figure 45

Figure 45. Intensely bioturbated siltstone interval at 7295'. Note complex mottling patterns.

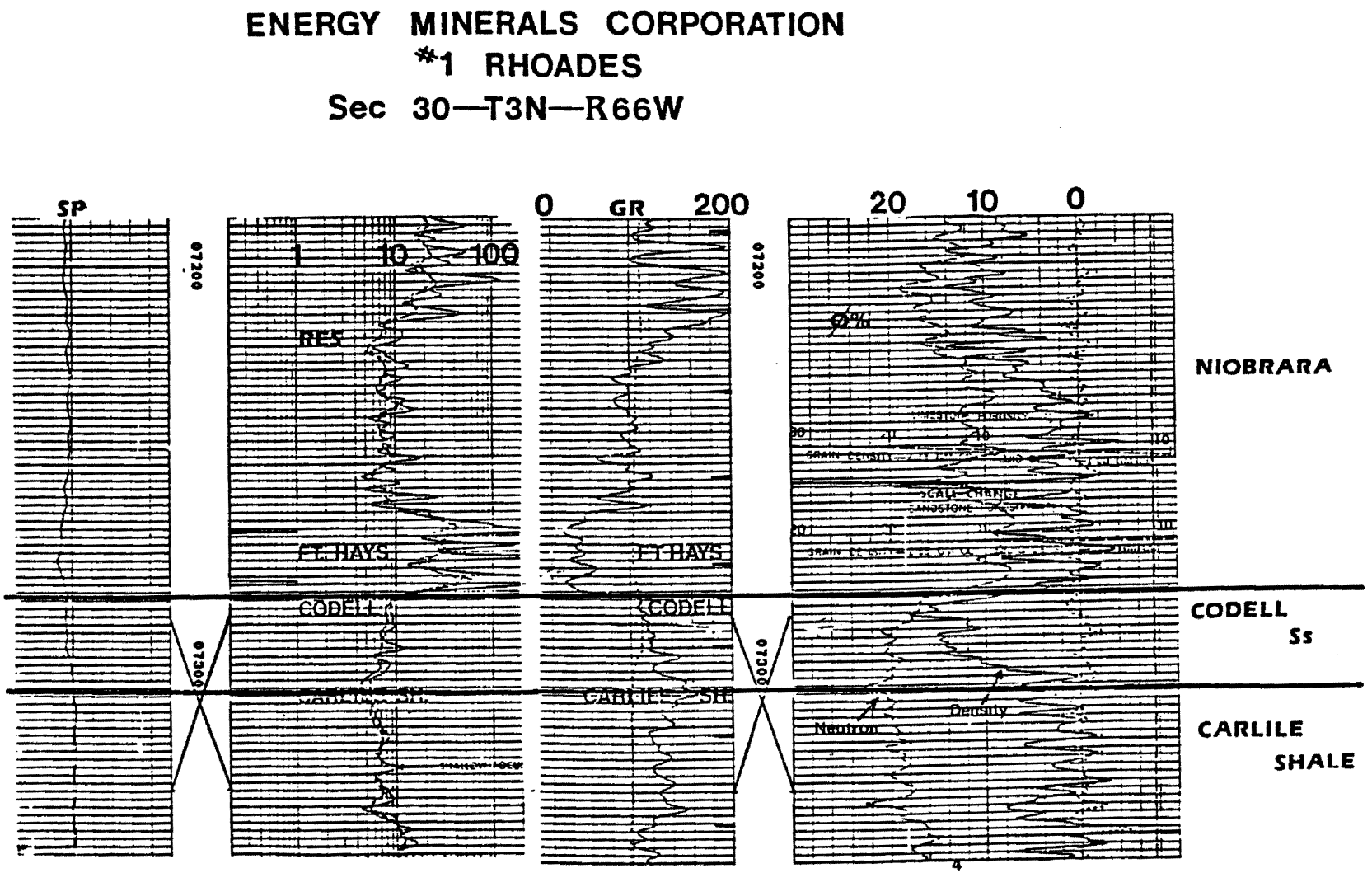

Figure 46. Wire-line log patterns from Rhoades #1 - Section 4.

(Figure 46). The serrated nature of the curve probably reflects the interbedded distribution of the sandstone/bioturbated siltstone beds previously described in core. However, the thin-bedded nature of the individual units are beyond the resolution of the logging tool. An overall coarsening upward textural trend is recorded by the API units which also confirm the existence of a sharp contact separating the Codell and overlying Fort Hays.

Discussion

The irregular nature and arrangement of bedding styles in the Codell Sandstone make grouping of similar lithology, sedimentary structures and trace fossils difficult. However, several lithofacies seem to be common to both outcrop and core.

Lithofacies (LF)

I. Medium to large-scale, discontinuous sandstone lenses which are horizontally to hummocky cross-stratified are common to outcrop and core. These lenses have sharp to erosional contacts into underlying shale layers. Internally, some appear massive or normally-graded. The upper contact into overlying shale zones may be gradational or sharp. Sporadic, vertical burrows are concentrated in the uppermost portion of some sandstone lenses.

II. Numerous, extensively bioturbated siltstone and sandstone intervals occur in outcrop and core. Most of the complex mottling patterns are produced by burrowing types typical of the *Cruziana* ichnofacies. Polyphase burrowing activity is indicated by distinct, vertically-oriented burrows in some sections of extensively bioturbated zones.

III. Lenticular, angle-of-repose cross-bedded sandstone occurs in two outcrop sections. Small-scale planar-abrupt to ripple cross-stratified sandstone are infrequently found. These zones rapidly pinch-out into horizontally bedded sandstone or shale.

IV. Bioturbated to non-bioturbated sandstone shale couplets are obvious in the Rhoades #1 core, but less obvious in outcrop.

Some generalizations can be made about the arrangement of lithofacies. LF I & II can be distributed from the basal portion through the top of the Codell Sandstone. LF III is normally found only near to or in the uppermost portion of the Codell interval. LF IV is usually found in the middle or basal portion, and because of oxidized and weathered outcrop, it is difficult in some sections to pick discrete couplets.

Several distinctive aspects of the Codell Sandstone warrant further discussion. All physical structures preserved in the outcrop sequences lens out rapidly. Correlation of specific bedding styles over distances more than a few feet is not possible. These structures are highly discontinuous and frequently grade into other bedding styles. In Section 1, horizontally laminated sandstone grades laterally into small-scale, tabular-planar, angle-of-repose cross-bedded sandstone (Figure 27). The inclined foreset cross-stratification lenses out over a very short distance of less than 3 feet (approx. 1 m). Section 2 also exhibits this kind of discontinuous bedding arrangement. Medium-scale trough cross-stratification grades laterally into horizontally laminated sandstone (Figure 33). In addition, immediately lateral to and vertically above the trough cross-bedded units, small tabular-planar, ripple-scale cross-stratification interrupts an otherwise horizontally cross-stratified sequence (Figure 34). This rapid change in bedding style indicates frequently fluctuating hydrodynamic energy levels. Comparisons of Sections 1, 2, & 3 reveal bedding patterns which are randomly distributed throughout the exposure in both lateral and vertical directions. Correlations between even thicker stratigraphic 'sequences' is at best highly speculative. Further discussion and interpretation of bedding styles, stability fields of physical structures, and trace fossil assemblages are presented in the last chapter.

Fluctuating hydrodynamic conditions are also indicated by the horizontally laminated laminated sandstone and shale couplets (Figure 33). The sandstone laminations are generally less than 9 cm in thickness and are abruptly overlain by thin shale layers (usually less than 3 cm). This frequent change in bedding style is indicative of episodic flow conditions. In this case, the change reflects juxtaposition of high energy levels generally associated with traction currents with deposition of silt and clay-size particles by suspension processes (very low energy levels).

Preserved hummocky cross-stratified sandstone beds in the Codell sequence indicate that episodic flow conditions existed during Codell deposition. The hummocky cross-stratified sandstone lenses are fairly small in cross-section and pinch-out rapidly into shale and siltstone beds. They are individually arranged and not amalgamated (Figure 25). General consensus among most workers suggest that hummocky bed forms are produced under flow conditions in which strong, unidirectional current flow is modified by a oscillatory component caused by shear stresses induced by wave orbitals. In addition, the bedform cannot be produced unless the overlying water column is saturated with abundant amounts of entrained sediment. According to Nottvedt & Kreisa (1987), hydrodynamic energy levels needed for the formation of this bedform range from moderate-high, and require that the sediment in suspension be fine-grained or smaller. The hummocky cross-stratified sandstone lenses documented in this study are totally encased in shale and siltstone suggesting that episodic, high energy flow conditions produced the arrangement. Subsequent quiescence allowed deposition of silt and clay-size particles which totally encased and ultimately preserved the sandstone beds.

Another distinguishing characteristic of the Codell interval is the relatively thin-bedded nature of most sandstone sequences. The thickest sandstone interval contained in Sections 1, 2, 3, &4 is less than 3 feet (.9 m), generally most sandstone lenses are < 1.5 feet in thickness. Similar bedding styles are also present in portions of the Tocito sandstone in the San Juan basin (Nummedal, *et al.*, 1989). Bedding styles preserved in

the Rhoades #1 core are typical of the thin-bedded nature of the sandstone intervals. Reasons for this arrangement might be 1) the duration of flow conditions needed to entrain and subsequently deposit sediment occurred over (geologically) short time spans (frequently fluctuating hydrodynamic conditions) 2) the supply of sediment into the receiving basin or hydrodynamic setting was restricted, and 3) the fine-grained nature of the sediment facilitated sediment by-pass into areas more conducive to deposition and accumulation. It is likely that all the reasons listed above may have contributed to the morphology of the Codell Sandstone in the study area.

It is immediately apparent upon inspection that the Codell Sandstone is highly bioturbated. In Section 1, fully 50% of the formation is intensely bioturbated (Figure 19). Tops of cross-stratified sandstone beds are typically burrowed while thick siltstone and silty shale intervals are totally re-worked by burrowing organisms. Bioturbated to non-bioturbated sandstone/shale couplets are common and reflect the nature of feeding organisms in episodic flow regimes. Burrowing activity is highest when hydrodynamic energy levels and sediment deposition are low. During these quiescent periods, burrowing organisms occupy and re-work the sediment in their attempts to feed. A high energy event coupled with increased sedimentation restricts their movement and buries needed organic food supplies. Cessation of the event allows the organisms to re-establish their dwelling and food supply network in the sediment/water interface. In some instances, the organisms may not be able to totally re-work the sediment before the next high energy event, ultimately giving rise to the preserved stratified to burrowed couplets we see today. Alternatively, if the time interval between high energy events is large, the organisms can totally re-work the sediment obscuring all physical structures. The thick, intensely bioturbated siltstone and shale intervals preserved in the Codell sequence probably reflect this scenario.

Finally, the top of the Codell interval is marked by a lenticular, cross-stratified sandstone bed which <u>can</u> be correlated over distances greater than several feet. In

Section 3, it is continuous along the outcrop exposure while in the northern sections (1 & 2) it tends to be more discontinuous. Because the sandstone bed can be correlated to sections measured by Lowman (1977) 12-18 miles (7-11 km) to the south and is roughly synchronous; a unique set of sediment and hydrodynamic conditions must have existed to account for its deposition. Possible explanations for the presence of this unit and its relationship to the overlying unconformity surface is best investigated by surface and subsurface log correlations which are treated in a subsequent chapter. As previously discussed, some workers refer to this interval as the Juana Lopez Member of the Carlile Formation and according to their studies in the southern portion of the basin, it contains abundant lag deposits. These lag deposits are composed of sharks teeth, phosphate nodules, mud clasts, and coarse quartz grains and have been typically referred to as a winnowed, transgressive interval. In the northern portion of the basin, the unit is almost exclusively composed of silica to calcite-cemented sand grains.

CHAPTER IV

Subsurface Investigations

Integration of surface information from the Codell Sandstone with available subsurface data located immediately adjacent in the Denver-Julesburg basin is the purpose of this portion of the study. Analysis of wire-line log patterns and well production characteristics allows delineation of reservoir geometry and production trends. Stratigraphic relationships between the Codell, Carlile, and Niobrara Formations can also be studied on a larger scale using subsurface information throughout the basin. Because of their position straddling the basin axis and prolific production histories in the Codell Sandstone, townships T5N-67W &T5N-66W were studied in detail (Figure 4). Their link to surface sections is through township T6N-67W. In addition, representative wells in T-4N through T12N, and R66W through R59W are used in cross-sections which span the north-central portion of the D-J basin.

Reservoir Geometry

Standard isopach maps across T5N R67-66W show sheet-like to broadly lobate geometries. Figures 47 & 48 are isopach maps contoured on 2 ft. intervals with thicknesses derived from gamma-ray log picks (see Figure 46 for typical example). Both figures exhibit sheet-like geometries oriented in a southern or southeast-northwest direction. It is important to note that thicknesses do not vary more than 10 feet across the 72 sq. mile area. The thickest portions of the townships are covered by a stippled pattern and exhibit elongate (low width to length ratios) geometries broken by narrow embayments of thinner Codell section (e.g. 23-5N-66W & 15-5N-67W).

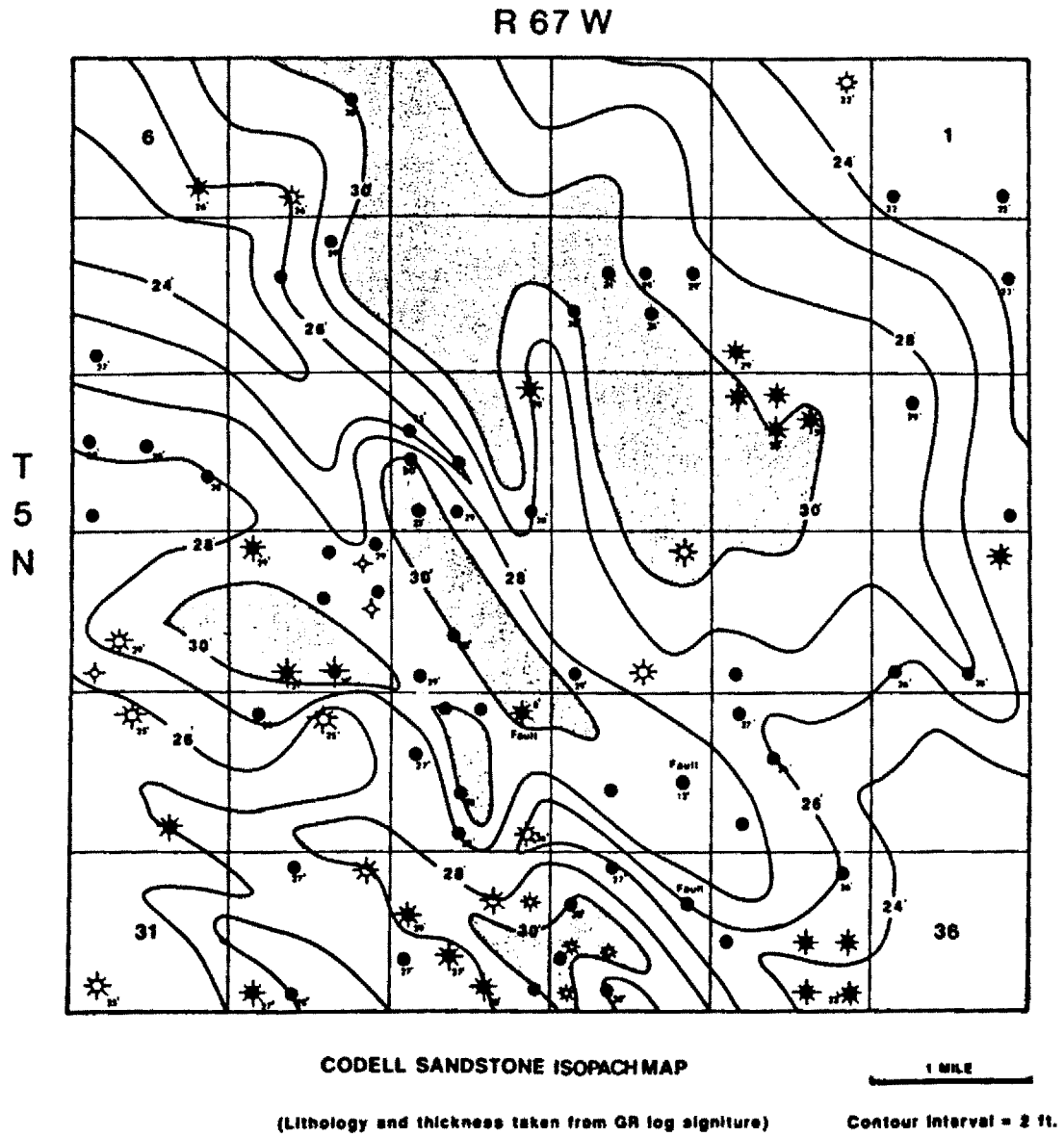

Figure 47. Codell Sandstone isolith map across T5N-R67W. Stippled pattern indicates thicker sandstone intervals (>30 feet thick).

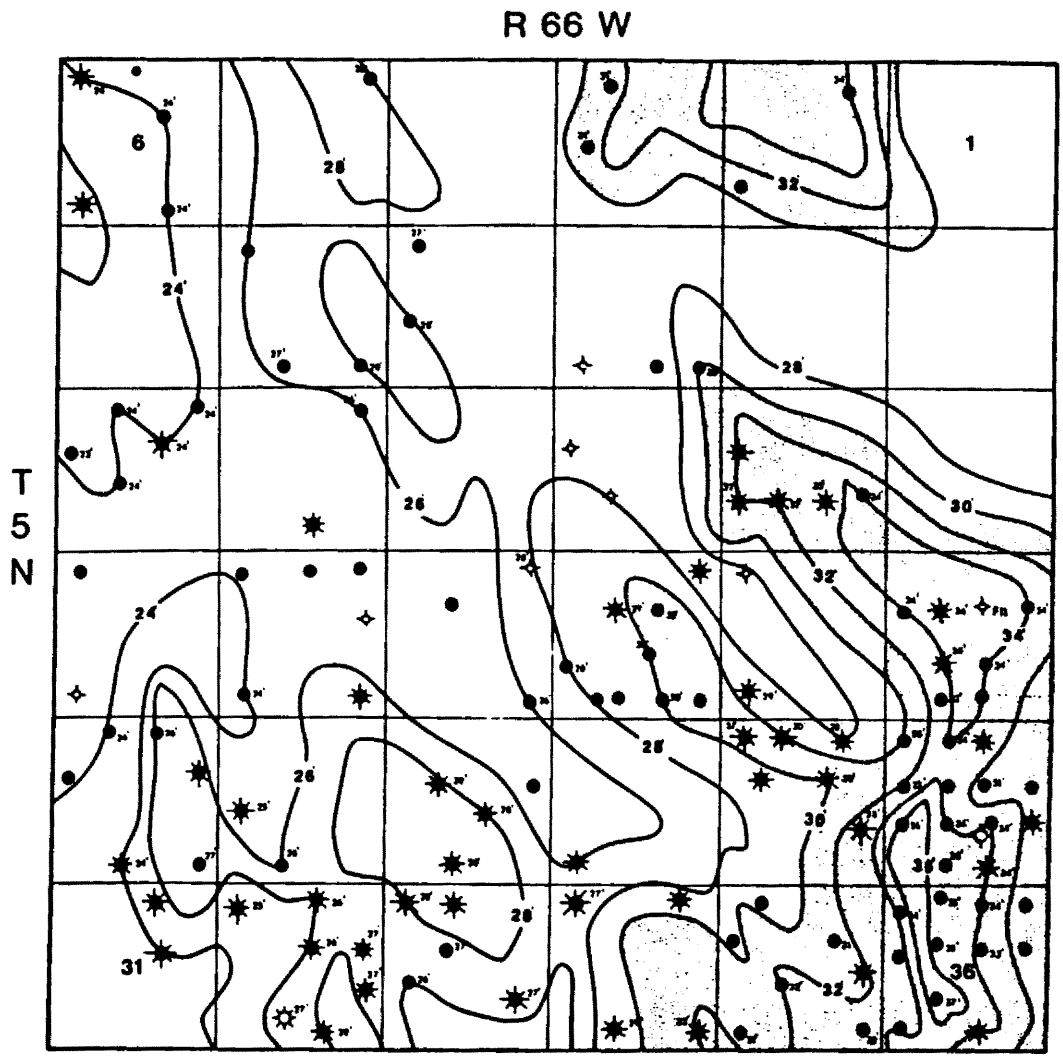

Figure 48. Codell Sandstone isolith map across T5N-R66W. Stippled pattern indicates thicker sandstone intervals (>30 feet thick).

Isopach coverage shown in Figure 49 of T6N-67W also portrays similar patterns. Even though data control is non-existent in the southern portion of the township, it was included to provide a control link to outcrop located in the eastern part of T6N-R69W. Sandstone porosity-percent maps shown in Figures 50 & 51 exhibit a more patchy distribution of sandstone thicks when compared to the isopach maps. Thicknesses were determined from a net 12% porosity cutoff, sandstone which contained 12% or greater porosity values were counted as potential reservoir. Also included on the maps are maximum porosity values recorded for each well. An important observation to note is the high porosity values (18-22%) encountered in a sandstone which has a very 'dirty' (high API units) gamma ray signature. In addition, the zones of high porosity values don't always correspond to the isopach thicks pictured in Figures 47 & 48. For example, the stippled patterns in the lower 1/3 of Figure 50 do not correspond one to one with isopach thicks pictured in Figure 47. The same sort of relationship exists between the isopach and sandstone porosity-percent maps of T5N-R66W. The high porosity values, patchy distribution, and irregular correspondence between gross and net sandstone thickness patterns indicate that secondary diagenesis plays a major role in the development of reservoir quality intervals.

Lithology relationships and geometries across the basin axis are portrayed in Plate I. The vertical black lines represent approximate position of wells from which the lithology picks and ties were made. Thin sandstone/shale beds of the Codell Sandstone are capped by the Fort Hays member of the Niobrara Formation. It is important to note the continuity of the thicker sandstone and shale intervals of the Codell across approximately 230 sq. miles of northern Colorado. The top sandstone or shale bed pinches out occasionally which probably reflects the erosional surface present at the Codell/Fort Hays contact. There is no distinct change in bedding architecture across the basin axis which suggests that what is now synclinal trough was not a structural element (either positive or negative) during time of deposition. It is also apparent that while the

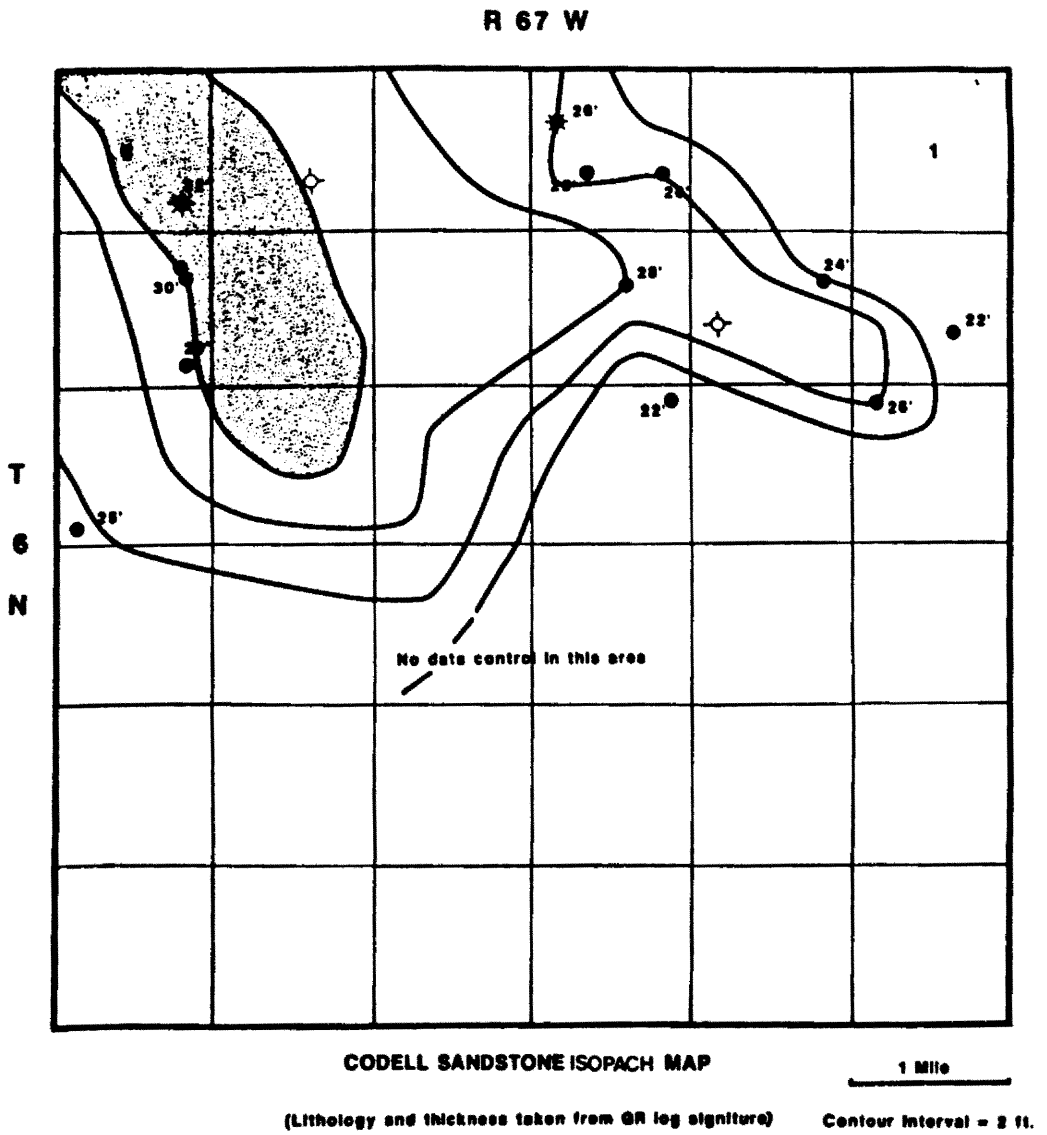

Figure 49. Codell Sandstone isolith map across T6N-R67W. Stippled pattern indicates sandstone intervals >30 feet thick. Note the position of this township is adjacent to outcrop sections located in T6N-R69W.

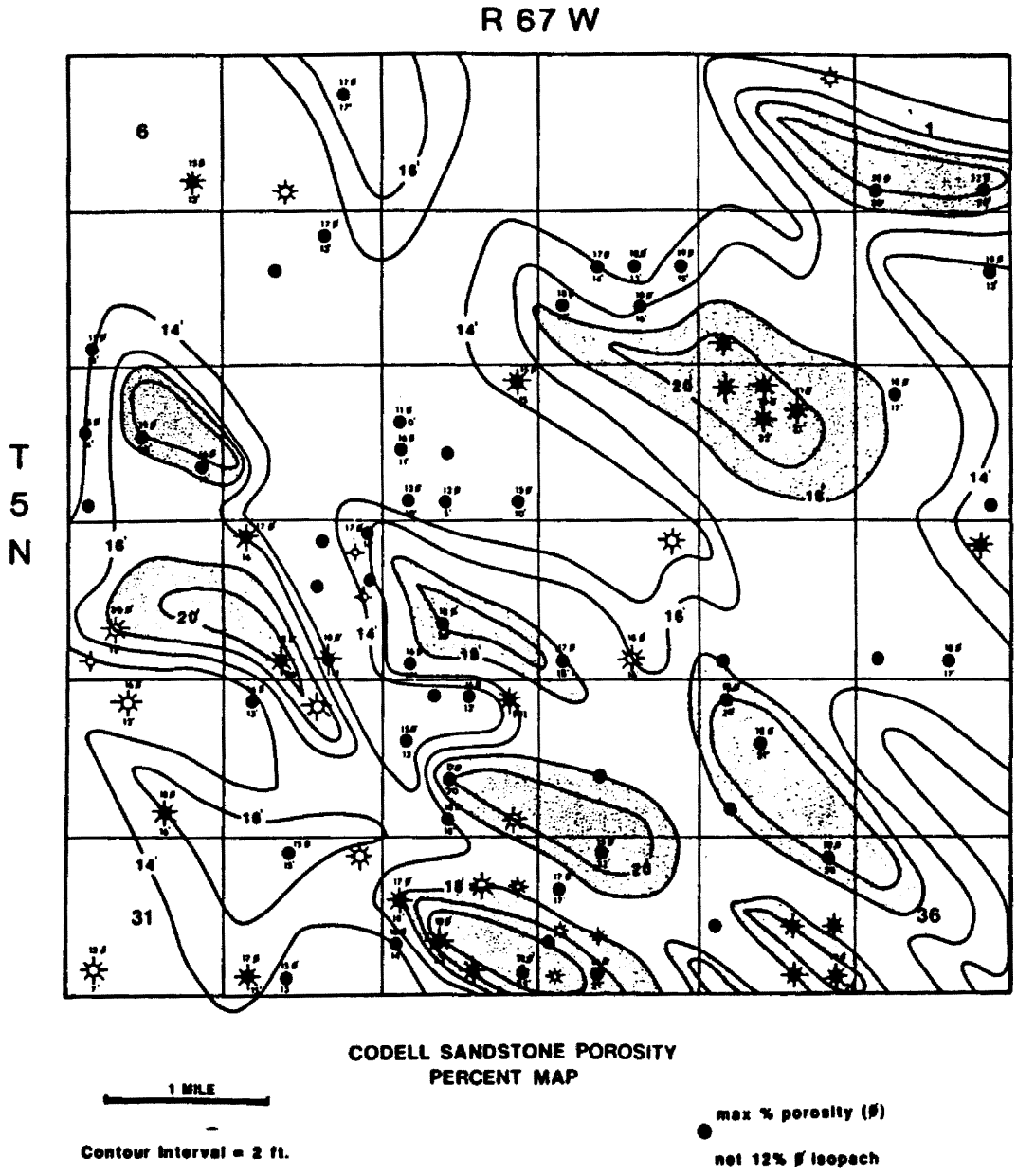

Figure 50. Codell Sandstone isopach map across T5N-R67W. Stippled pattern indicates sandstone intervals thicker than 12% ø.

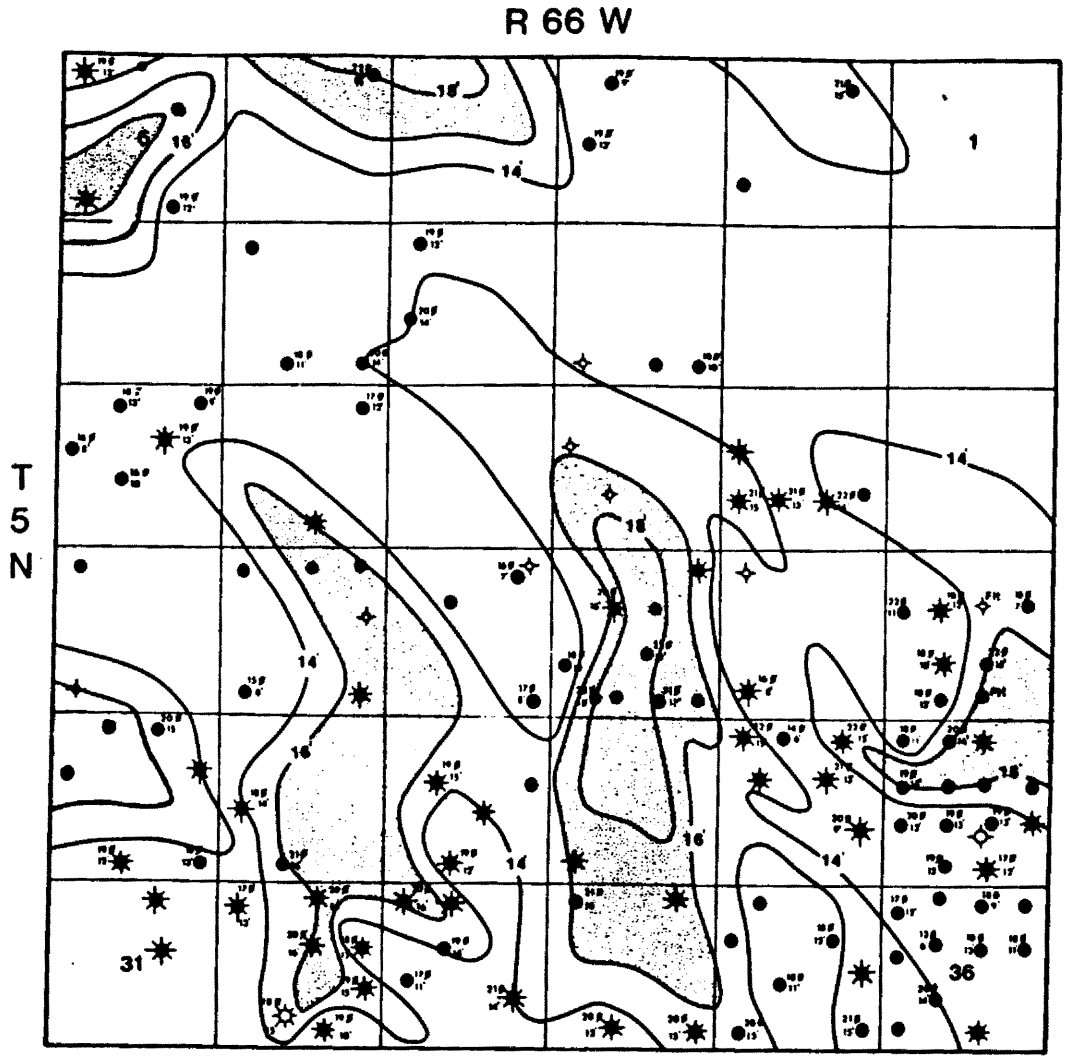

Figure 51. Codell Sandstone isopach map across T5N-R66W. Stippled pattern indicates sandstone intervals thicker than 12% ø.

gamma-ray log signature portrayed in the western portion of Plate I shows a distinct coarsening-upward trend, the other two have more rounded or sharp-based profiles. The thin-bedded nature of the Codell Sandstone in outcrop and core suggest that these correlatable sandstone intervals are really composed of a complex assemblage of sandstone/shale lenses. The Fort Hays limestone varies only slightly in thickness across the basin axis and is a consistent log marker throughout the northern portion of the D-J basin.

Structural Relationships

Mapping of structural elements on a large, regional scale produce an asymmetric, north-south directed profile of the D-J basin (Figure 3). Upon closer inspection, portions of the basin, especially that area across the basin axis, show a more complex arrangement. Figures 52 and 53 are structure contour maps picked on the top of the Codell Sandstone. An intricately folded and faulted region is present in the upper portion of Figure 52 with anticlinal/synclinal couplets oriented in a north-south direction. Structural dip is generally to the northeast except in the southeast corner of the township, in which dip is directed almost due east. Immediately apparent in the figure are a series of northeast oriented normal fault systems. The smaller fault systems abruptly cut anticlinal noses and one synclinal trough. Little or no roll-over into the faults indicate that these are not growth features. The major fault located in the southeast corner of the township has over 200' of throw and divides the region into two distinct structural regimes based upon direction of structural dip. Distribution of producing wells do not correspond in a systematic way with the arrangement of faults, or for that matter, most of the anticlinal features. An exception is present in Section 14 where five wells are grouped in a faulted anticlinal structure with 2-way closure.

Figure 53 contains broader anticlinal/synclinal features but generally shows many of the same structural elements depicted in Figure 52. A series of en-echelon faults are

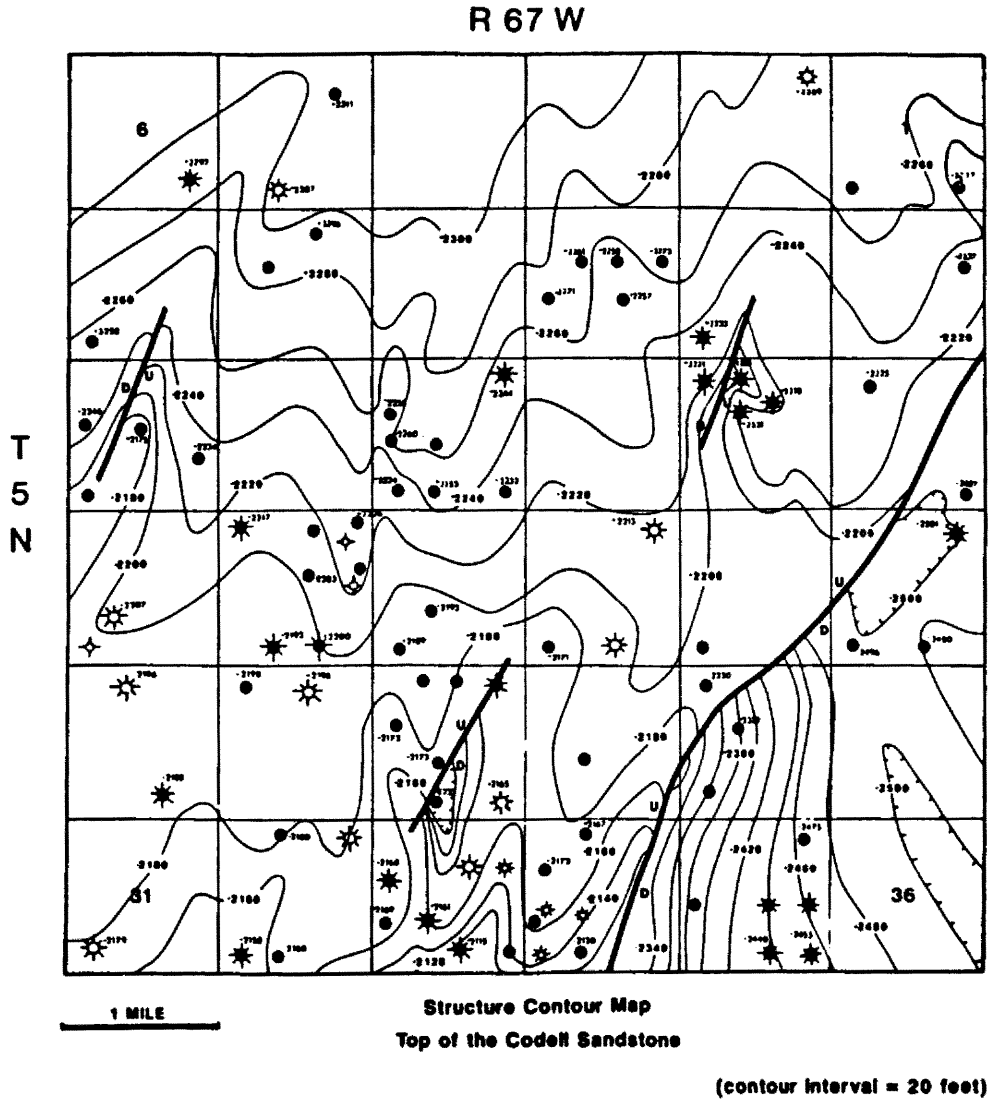

Figure 52. Structure contour map of the Codell Sandstone in T5N-R67W. Hachured marks indicate structural low areas.

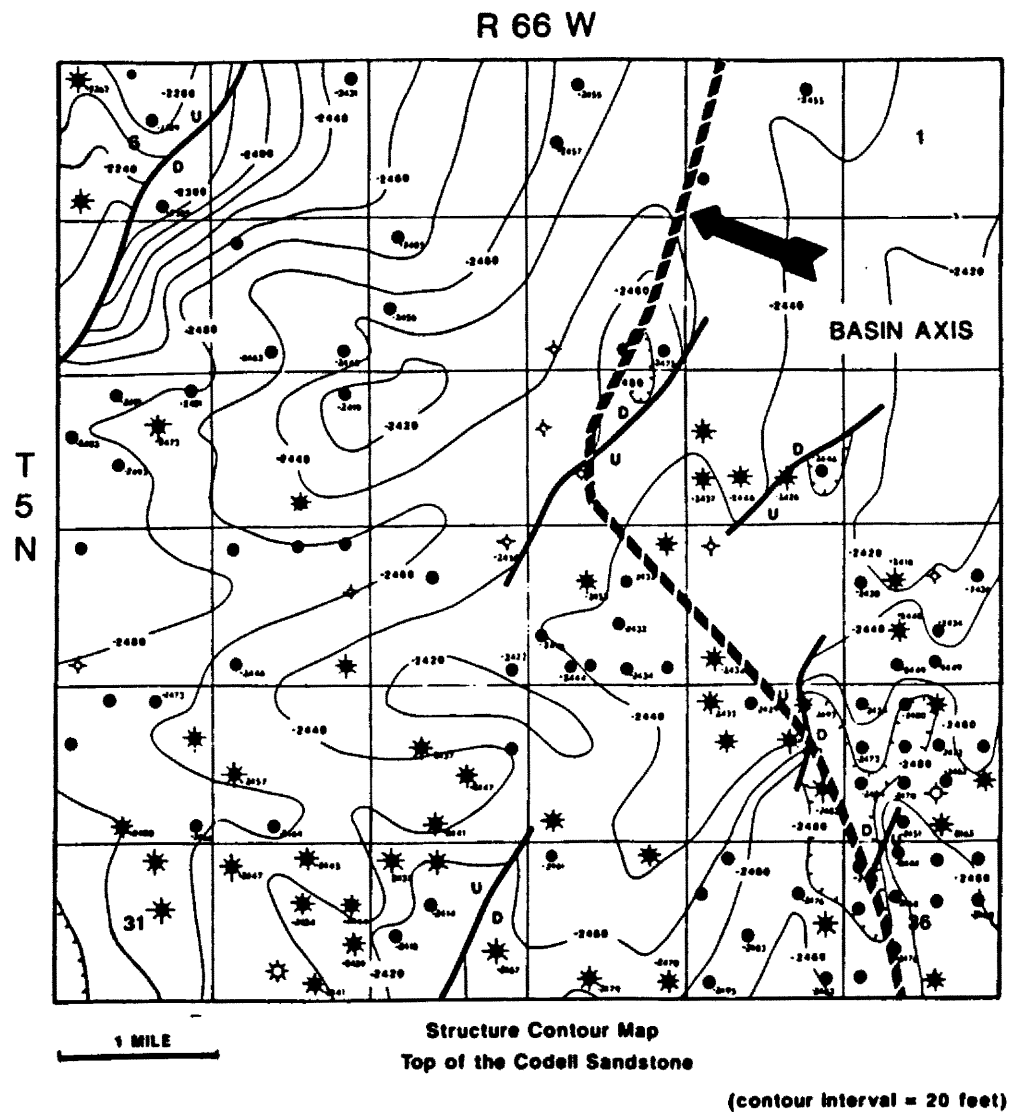

Figure 53. Structure contour map of the Codell Sandstone in T5N-R66W. Hachured marks indicate structural low areas. Approximate position of basin axis is also depicted.

grouped around the basin axis depicted in the eastern portion of the township. Most of the faults are segmented and fairly small in plan view (2640'-6000' in length) with less than 40 feet of throw. However, continuation of a major fault system in T5N-R67W cuts through the extreme northwestern corner of T5N-R66W. Throw on this fault is diminishing to the north. It is important to note that most of the producing wells are located near the faulted basin axis.

Normal faulting in this region is presumably related to the Laramide deformation of the Front Range uplift in northern Colorado and southern Wyoming. Fault systems preferentially cut into upper Carlile and Niobrara strata. It is common to encounter missing intervals of Niobrara and upper Carlile sequences in this portion of the basin. However, it is difficult to project the trace of most fault systems more than 1.5 miles in plan view. This constraint is consistent with the hypothesis that these features are essentially accommodation structures. Dips across the basin axis are steep, at times greater than 20' per 2000'. To allow for compression adjustment related to the adjacent foreland deformation, en-echelon arranged normal faults provide opportunity for slip. The Owl Creek uplift (foreland) located adjacent to the Wind River basin produces similarly arranged normal fault systems in older, basinal stratigraphic sequences (Lowell, 1983). Figure 53 depicts the approximate position of the basin axis, where east-directed dip changes permanently to west-directed. It is important to note that the area bracketed between the basin axis and the major fault in the northwest corner is complexly folded and warped. This may represent the broad, segmented hinge area of the basin synclinal trough.

Production Trends

Initial production figures from were collected for T5N-R67-66W and are depicted on Figures 54 and 55. Because of rapid initial decline rates, variable completion techniques, and differing company policies, cumulative production figures are

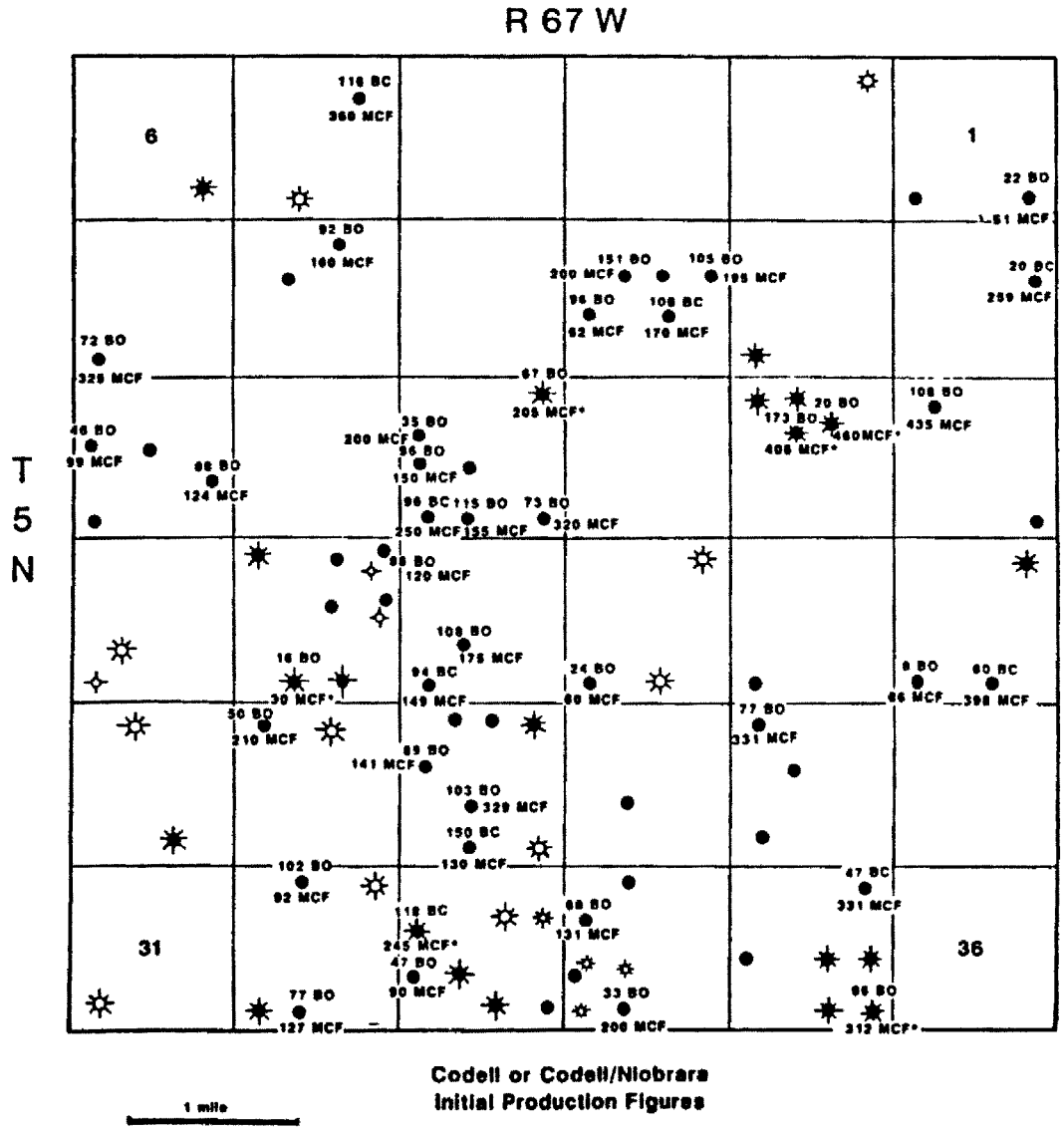

Figure 54. Initial production figures from the Codell Sandstone for T5N-R67W. All rates listed in BOPD & MCFPD.

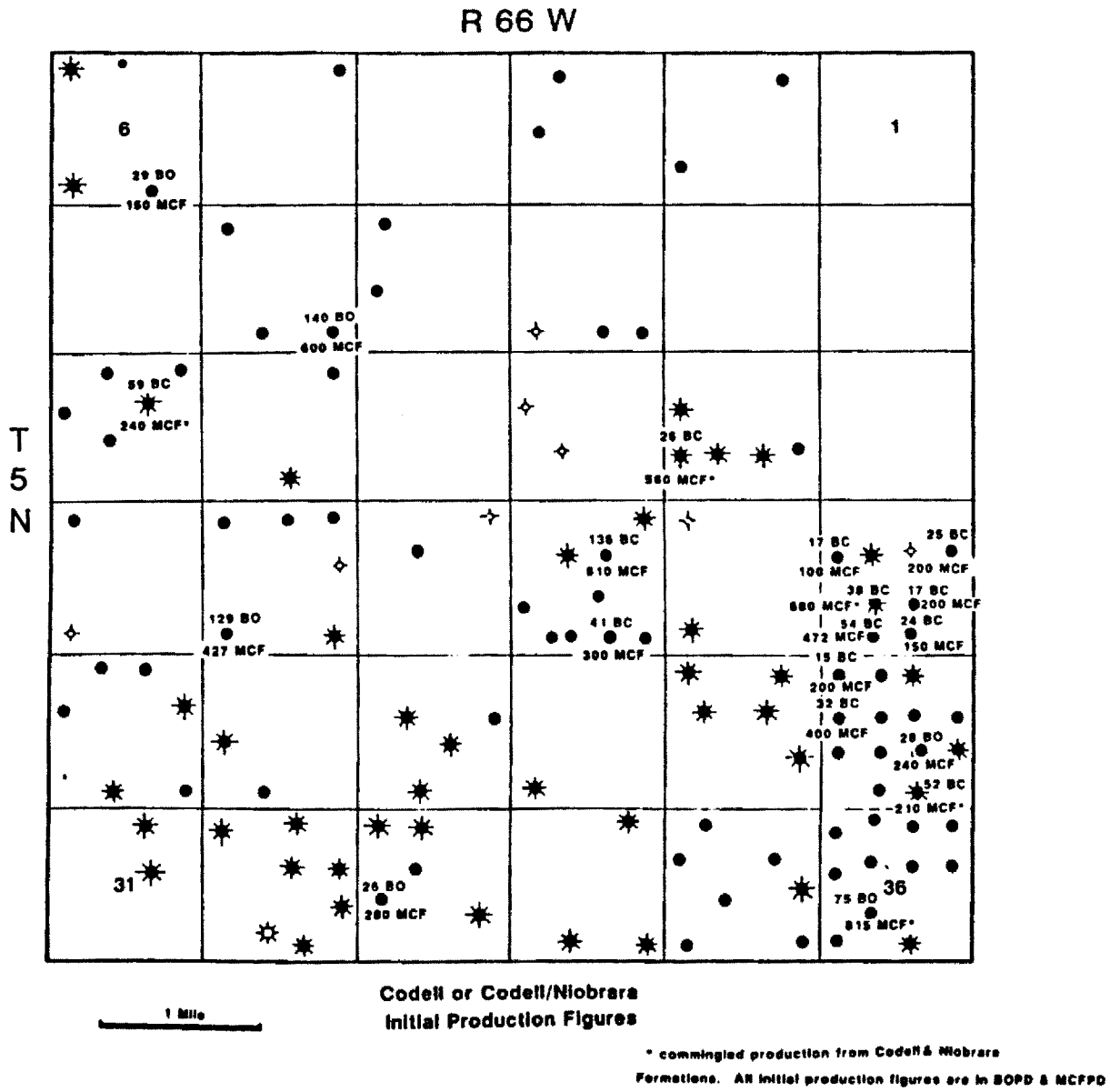

Figure 55. Initial production figures from the Codell Sandstone for T5N-R66W. All rates listed in BOPD & MCFPD.

somewhat misleading unless continuously plotted over a 24 month period (Wright & Fields Jr., 1988). Even though initial production can produce highly erratic daily rates, wells which produced at high initial rates (over 70 BOE per day equivalent) correlated best with geologic information. It should be noted that wells which were tested as commingled Codell/Niobrara produce essentially identical production profiles when compared to wells completed only in the Codell Sandstone (Wright & Fields Jr., 1988). Gas to Oil ratios (GOR) were calculated from the initial production data to properly classify the type of reservoir(s) contained in the Codell (Figures 56 & 57). Empirical criteria may be used to define the reservoir type. The generally accepted format is as follows: initial GOR's < 1000SCF/STBO with API stock tank liquid gravities below 45 API indicate a Black Oil reservoir; initial GOR's between 5,000-100,000SCF/STBO with stock tank liquids above 45 API indicate a Retrograde Gas-Condensate reservoir. Those reservoirs whose GOR's plot between the two, exhibit Volatile Oil reservoir behavior. Finally, wells which calculate GOR's greater than 100,000SCF/STBO and produce little associated liquids, are termed Dry Gas reservoirs (Ferderer, 1987, per. comm.).

GOR's from Figures 56 and 57 were plotted on Figure 58 to ascertain reservoir type. Two distinct domains representing well distribution are apparent on the diagram. Most wells in T5N-R67W plot in the Volatile Oil region, while Retrograde-Gas Condensate characteristics are more typical in T5N-R67W. Approximate positions of fault systems and basin axis are plotted along with GOR information on Figures 56 & 57. Volatile Oil reservoir behavior is exhibited in a large portion of Figure 56. However, a sharp increase in the GOR is apparent near the major fault system in the southeast corner. Moving eastward to that area covered by figure 57, Retrograde-Gas Condensate reservoir behavior is typical of the whole township. It is critical to note the dramatic increase in GOR near the position of the faulted basin axis. Retrograde-Gas Condensate is a term used to describe the condensation effects of reduced reservoir

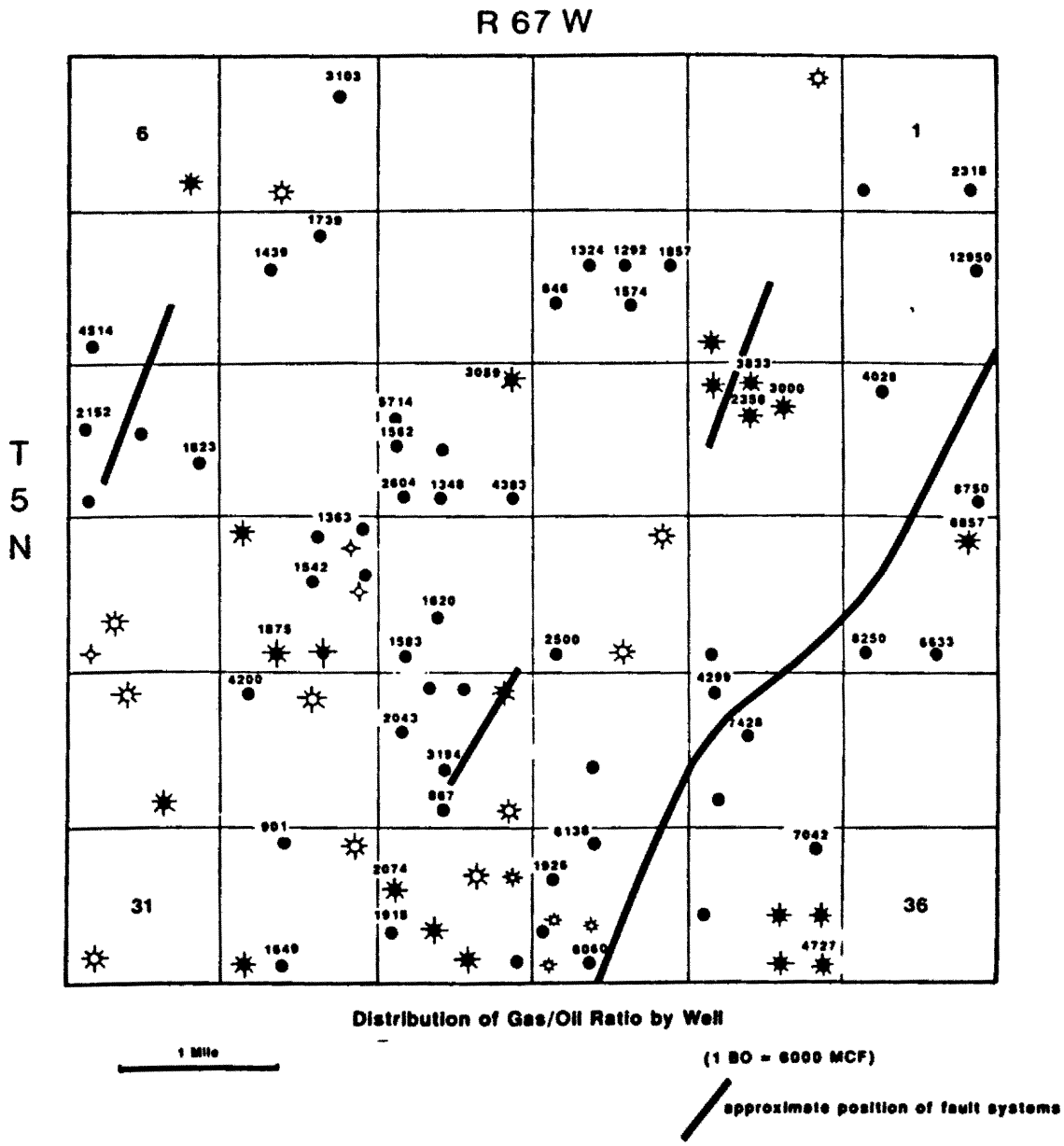

Figure 56. Distribution of Gas/Oil ratios (GOR) in T5N-R67W. 1 BOE = 6000 MCF. Approximate position of fault systems depicted.

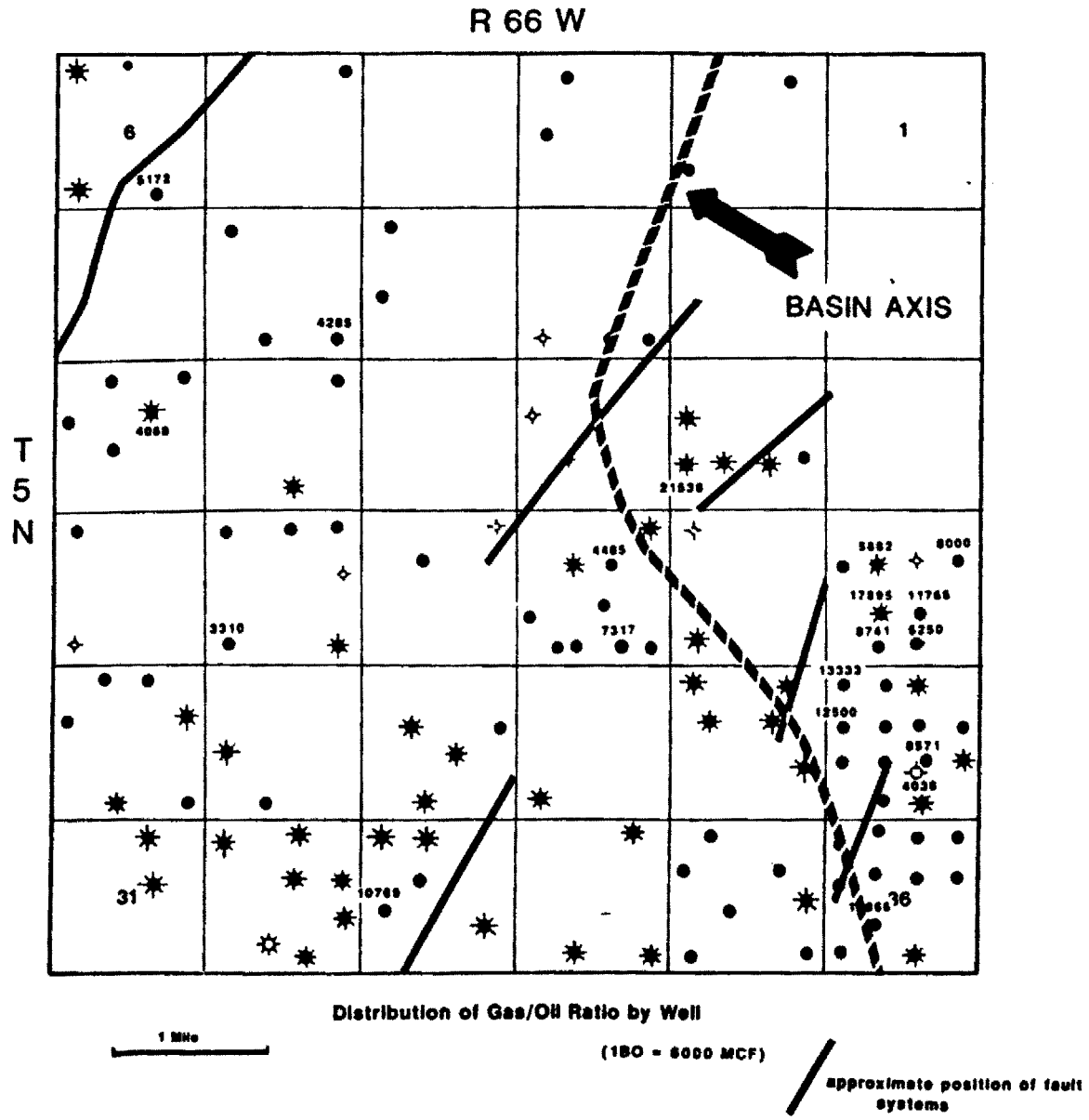

Figure 57. Distribution of Gas/Oil ratios (GOR) in T5N-R66W. 1 BOE = 6000 MCF. Approximate position of fault systems depicted as well as basin axis.

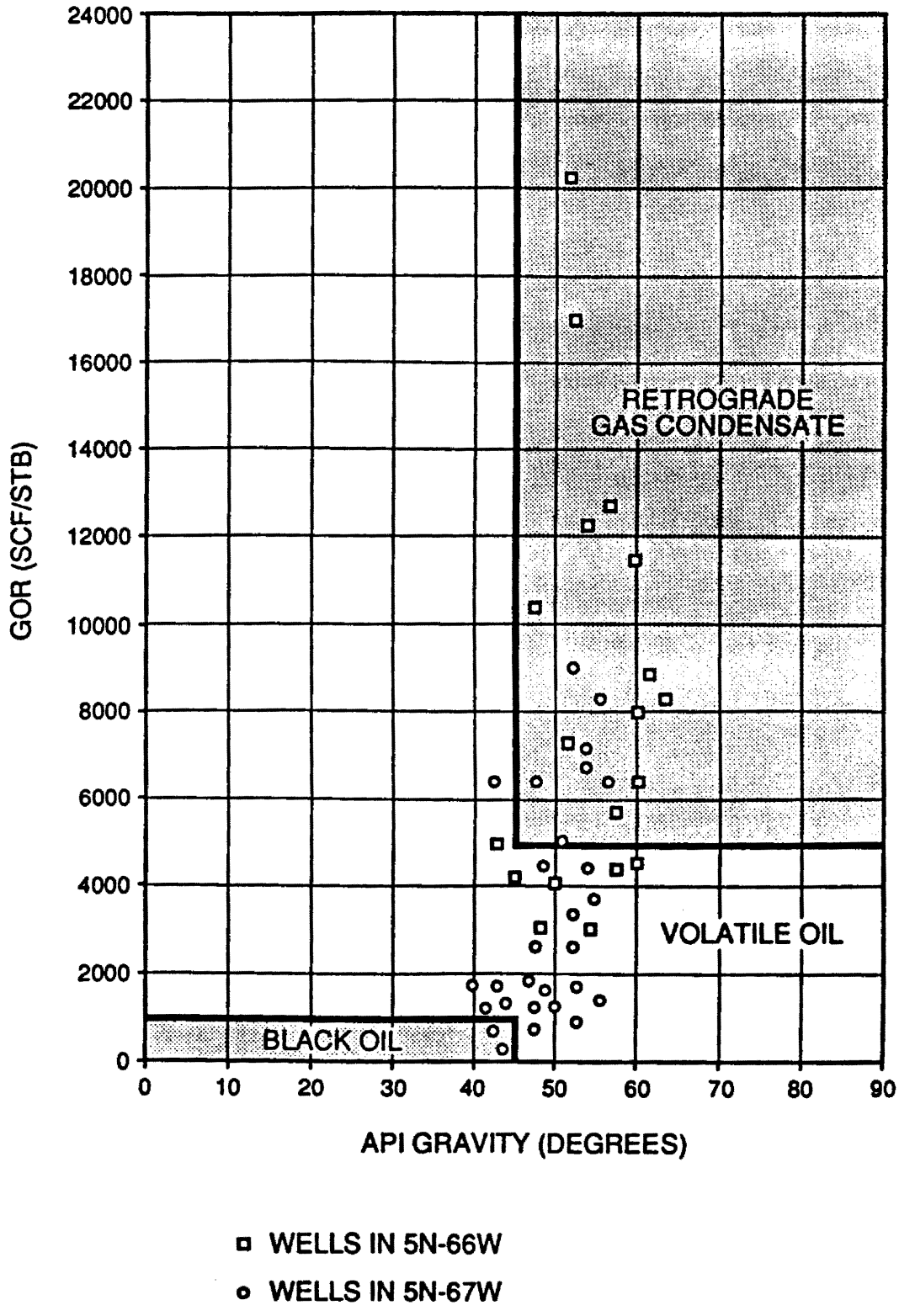

Figure 58. Reservoir classification chart based on GOR & API gravity data. Squares indicate wells in T5N-R66W and circles indicate wells located in T5N-R66W.

pressure. At depth, the condensate is in a gaseous state, perforating and producing the reservoir reduces the overburden pressure which normally keeps the gas from condensating in the pore throats. As the gas travels up the well bore, it reaches the dew point condensation level. Because of this problem, oil recovery will be enhanced by keeping the reservoir pressure at a maximum for the longest possible time. Volatile Oil reservoir characteristics include fairly high API gravities due to the high percentage of dissolved gas in the liquid. Solution gas drive is the mechanism for the hydrocarbon charging system in these reservoirs. Little to no water is produced with the hydrocarbons in this area suggesting there is no attendant water contact in the reservoir interval.

Initial production rates in T5N-R67W were superimposed upon isopach, sandstone porosity-percent and structure contour maps with varying results. Figure 59 depicts the strong correspondence between isopach thicks and high initial production rates (> 70 BOE per day). Almost every well in this range falls in or between the 28-30' thick isopach interval. The same distribution of wells were superimposed on the sandstone porosity-percent map with similar results. However, when the same pattern was overlaid on the structure contour map in Figure 60, it was unclear whether the structural component played a significant role in pooling hydrocarbons. The best production is scattered across synclinal troughs as wells as faulted anticlines. To further investigate this problem, a graphical 3-D representation of the top surface of the Codell was constructed (Figure 61). Viewing angle of the township is from the southeast looking northwest. A limited number of bivariate smoothing algorithms were used to interpolate between values so that strict adherence to the raw data values was attained. The downthrown portion of the block in the southeast corner corresponds to the major fault system in this area (see Figure 60). It becomes clear that hydrocarbon migration occurred in stepped intervals updip of the downthrown side of the fault. Local dip reversals, permeability barriers, or small fault networks enhance the probability of

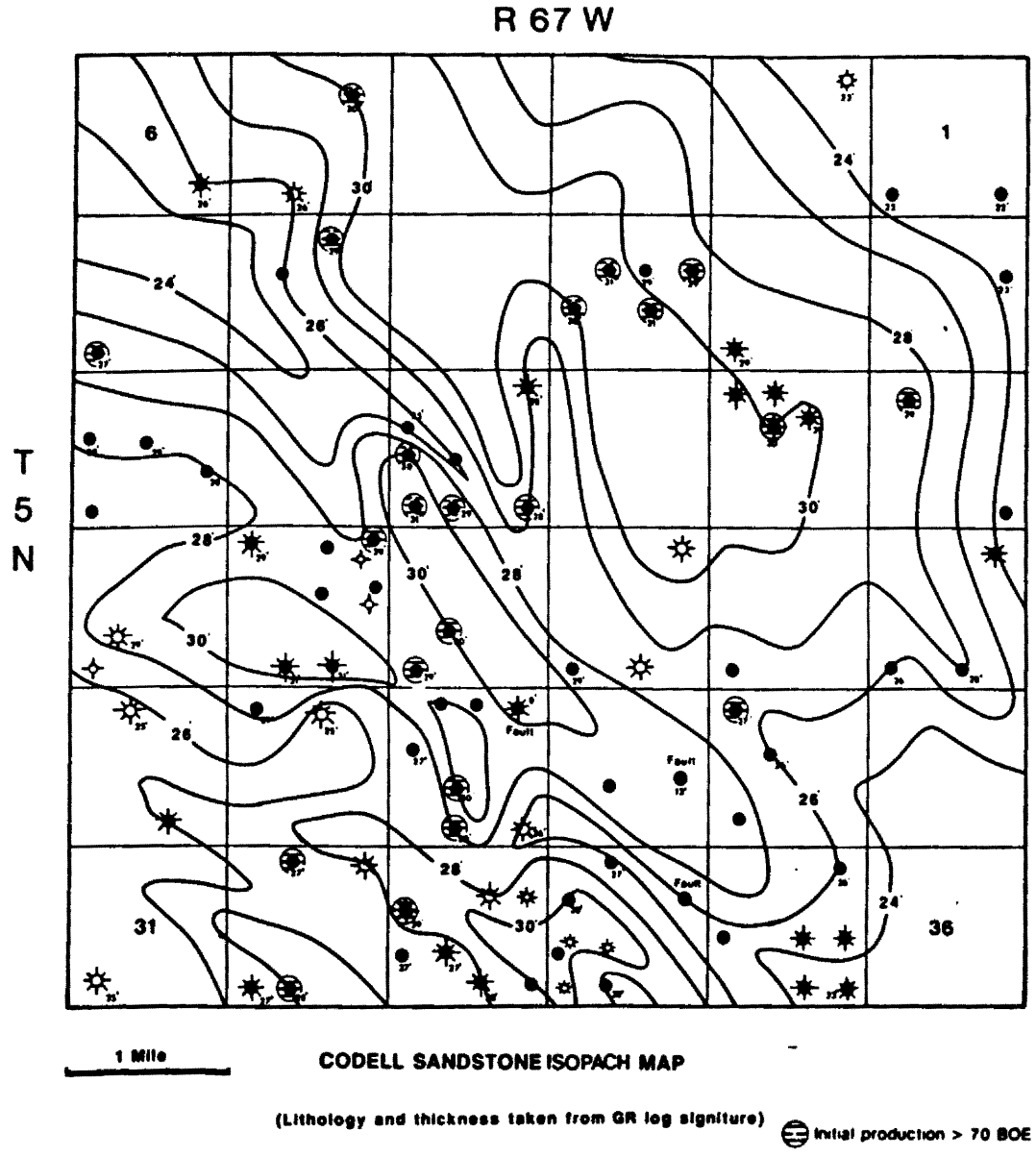

Figure 59. Diagram depicting correspondance between isolith thicks in T5N-R67W and high initial production rates. Striped pattern indicates IP's >70 BOEPD.

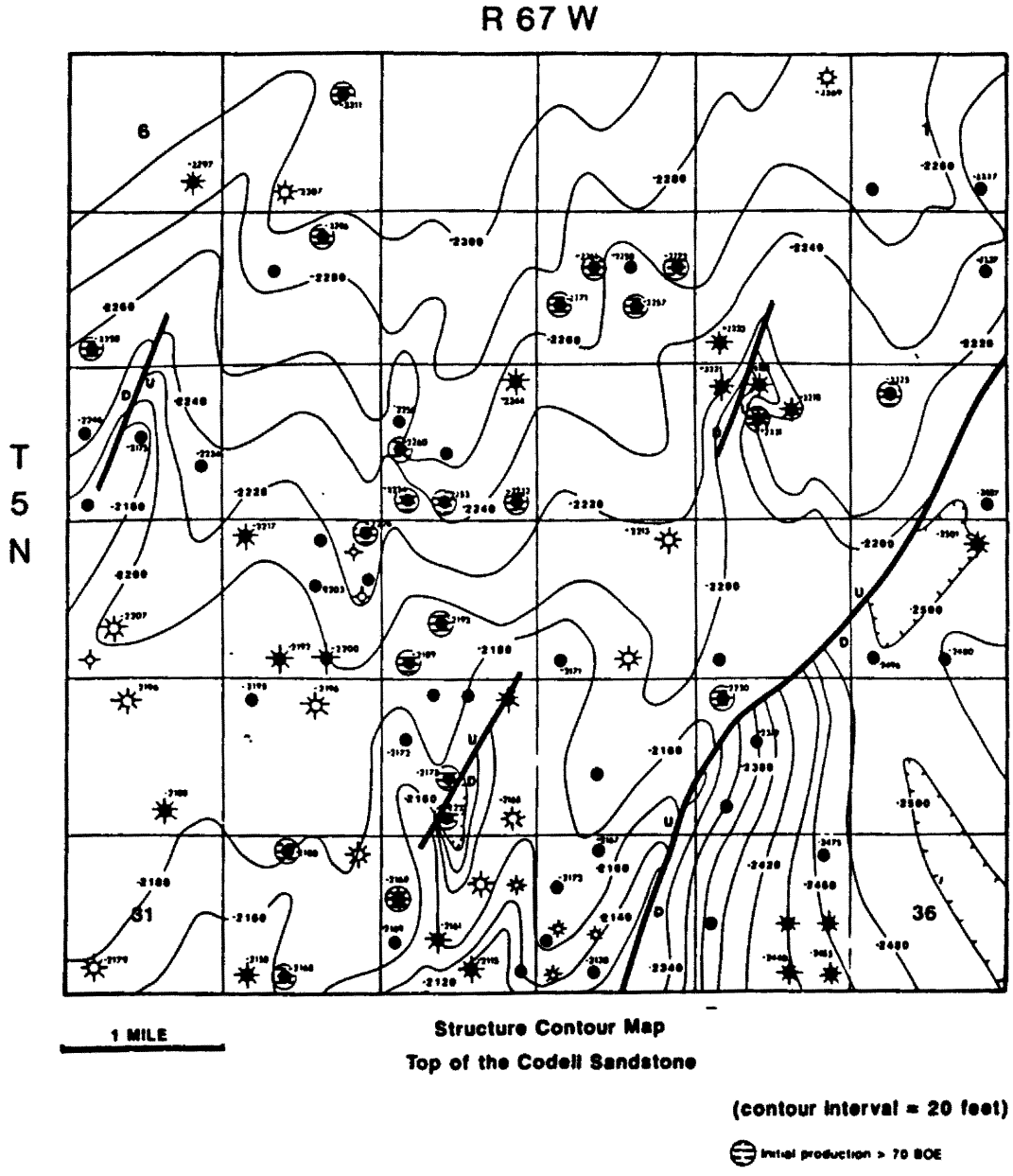

Figure 60. Diagram depicting high initial production rates (>70 BOEPD) superimposed on the structural elements in T5N-R67W.

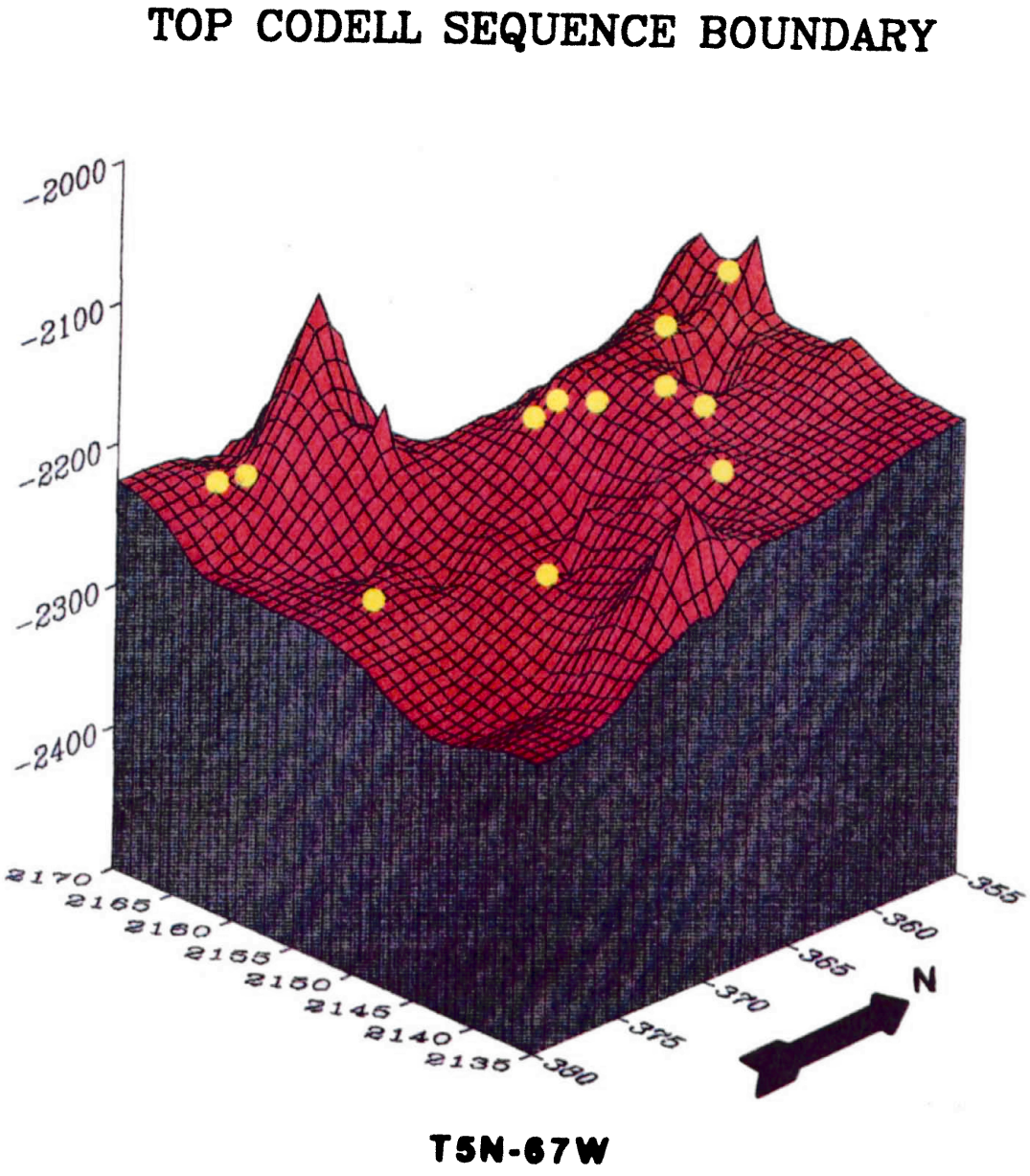

Figure 61. 3-D trend surface diagram depicting surface elevation topology of the Codell sequence boundary. Vertical (z axis) is measured in feet. The x & y directions are in xy digitizer units. Azimuth=135 & Z factor=70. Yellow dots indicate approximate position of better producing wells completed in the Codell sandstone in T5N-67W.

hydrocarbon entrapment. Comparison between Figure 59 and Figure 61 illustrates the almost one to one correspondence between best productive intervals and the steep, updip portions of the diagram. Apparently, because of the low permeability of the formation, three or four-way structural closure is not absolutely needed for accumulation to occur. Notice that there are poor production rates in the northeast corner of the township. The structure map over the same area depicts a flat zone with a gentle reversal of dip to the east in the same area.

Keeping in mind the GOR data from Figure 56, it is easy to envision a scenario in which high GOR's created from increased thermal gradients and fluid conductivity across major basinal bounding faults, charge the system with solution driven gas. This produces an extremely mobile hydrocarbon environment. Because the formation is porous, but fairly impermeable, any slight reversal in dip direction trap the hydrocarbons along the updip flank of the township forming a classic combination structural/stratigraphic trap. Areas in or immediately adjacent to fault systems in the basin axis should be avoided as potential drilling sites. These areas have been flushed to a greater degree because of the high mobility of gaseous fluids. Understanding the migration pathways away from the basin axis seems to be the key in predicting the best reservoir quality distribution. A similar series of steps were complete for T5N-R66W with almost identical results. The best production was found in thicker Codell intervals along steep flanks updip from major fault systems. In the interest of manuscript space, only T5N-R67W has been presented.

An attempt was made to also correlate lower water saturation percentages with higher production rates. Calculation of correct water saturation values was in and of itself a problem due to the high shale content in the Codell Sandstone. Shaly sandstones which contain abundant effective shales affect log analysis calculations dramatically. Water saturation (Sw) values can be anomalously high, between 80-100%. Effective shales are the multilayer clays such as the smectites (montmorillonite and bentonite) and

illite. These clays have high CEC values (cation exchange capacitance), this is a measure of the ease in which clays exchange cations in their crystal lattice sites. Noneffective shales usually contain near zero CEC values, and are almost always kaolinite and chlorite. Chlorite can have high CEC values if it is iron bearing. See Table 1 for the effects of both kinds of shales on log responses.

Algorithms based on the Archie Equation where Sw = Fr Rw//Rt (Fr = formation factor, Rw true resistivity of formation water, and Rt = true resistivity of the formation) were used to calculate apparent water saturation values in T5N-R67W. Typical Sw values ranged between 80-100%, the standard industry cutoff of 60% would indicate that this formation should not be productive. Obviously, since this area contains prolific production, a shaly sand correction factor must be applied to account for the matrix density differences and bound water effects associated with shaly sandstone reservoirs. In this case, the shaly intervals in the Codell Sandstone are almost exclusively composed of effective shales with high CEC values (see following section for bulk composition values). By applying the correction factors, water saturation values in T5N-R67W range between 35-70% (Figure 62). These figures are probably more accurate but still surprisingly inconsistent when compared to initial production values (Figure 54). Wells which exhibit better production rates don't necessarily correspond to the lower Sw values. In fact, the wells located in Section 16 which have anomalously higher Sw values, are some of the more prolific producers. Perhaps design differences in logging tools, differing mud systems between contractors, or tool malfunctions account for part of this problem.

Sequence Stratigraphy

This relatively new sub-discipline is proving to be a useful tool in exploring for and developing hydrocarbon reservoirs. Working with regional seismic lines, interpreters 'break out' a stratigraphic section into succeeding geologic units, each of which is

Table 1. Shale Effects on Log - Responses

	Effective Shales	Noneffective Shales
Resistivity (R_t)	lowers	no effect except Fe-bearing chlorite will lower R_t
water saturation (Sw)	increases	little to no effect
Spontaneous Potential (SP)	Amplitude reduced	no effect
resistivity of formationwater (Rw)	increases	no effect
Gamma Ray (GR)	API units increase (appears dirtier)	API units decrease slightly (appears a little cleaner)
Density Log (ø) porosity	Montmorillonite - matrix ρ is 2.33 gm/cc sandstone appears to have higher ø Illite - matrix ρ is 2.76 gm/cc sandstone appears to have lower ø	Kaolinite - ρ is 2.69 gm/cc negligible change Chlorite - ρ is s.77 gm/cc sandstone appears to have lower ø significant when reservoir ø are low (< 9%)
Neutron Log (ø) porosity	increases Montmorillonite - show up as ø > 40% Illite - shows up as ø > 30%	increases Kaolinite - shows up as ø > 40% Chlorite - shows up as ø > 40%

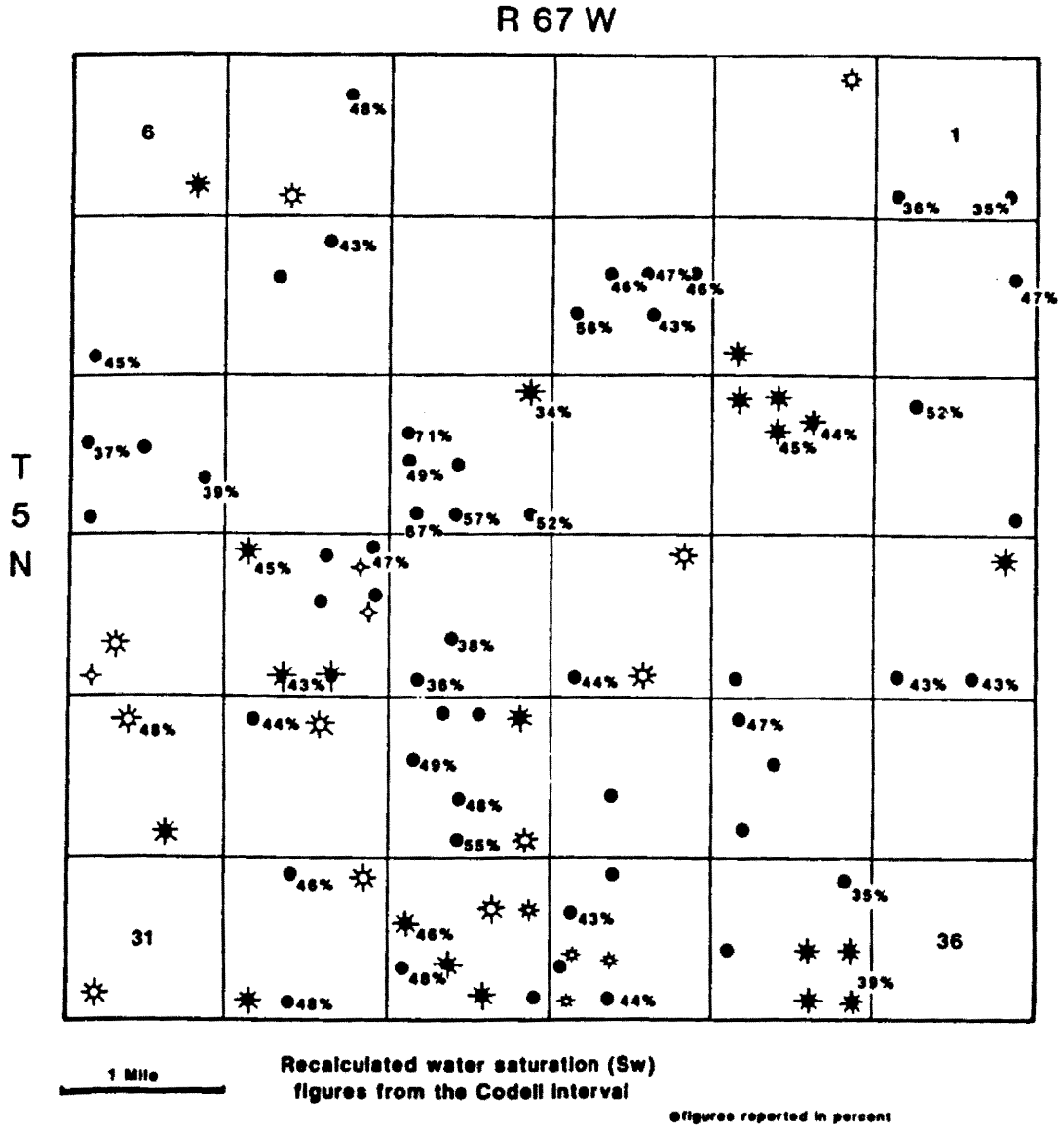

Figure 62. Recalculated water saturation values (SW) in percentages in T5N-R67W.

separated by a major unconformity or depositional discontinuity. Using the character and geometry of the seismic reflections, an interpreter can attempt to describe the geologic history of an area including information on direction of sediment sources, inferred paleoenvironments, and an inferred relative sea-level history for the area. Considerable debate surrounded the methodology when it was first introduced by Vail, P.R. *et al.* (1977) and Payton, C.E., (1977). Much of this criticism has been directed towards the insistence of honoring global sea-level curves and onlap charts when the methods used to derive it may be flawed (Miall, 1986). More recently, renewed attention is being given to separating the tectonic vs. eustatic mechanisms for creating sequence boundaries (Hubbard, 1988; Gallagher and Tauvers, 1988). It is now generally accepted that correlation of sequence boundaries between basins is at best speculative except when constrained with biostratigraphic age dates. Other workers have attempted to integrate seismic stratigraphy fundamentals into a genetic sequence approach of rock stratigraphy by identifying depositional process with accumulation patterns.

Without the aid of seismic over the study area, basin wide correlations of genetic sequence packages is not possible. It is my intent, however, to answer a couple of fundamental questions regarding the relationship of the Codell with overlying and underlying units. A sequence boundary is defined as either a distinct lithologic break, an erosional unconformity, or hiatal disconformable surface. However, sequence boundaries imply that landward of basin deposition, subaerial erosion of older strata produces a seaward displacement of depocenters which produce a "downward shift in coastal onlap" (Nummedal *et al.*, 1989). This term was introduced to explain the position of deposits representing a given water depth directly superposed on facies representing deposition in much deeper basinal settings. In other words, Walther's Law of Facies was violated and this anomalous contact relationship was referred to as a sequence boundary.

This arrangement does not necessarily occur in all instances where significant erosion takes place. Marine erosion surfaces sometimes produce facies architecture characterized by abrupt deepening. For example, fine-grained inner shelf deposits may be overlain by transgressive deposits and/or much deeper basinal mudstones or limestones (Nummedal *et al.*, 1989). A hiatal surface is present but whether it is a major sequence boundary in the strict sense of the word or a marine flooding surface is subject to interpretation.

To account for this problem, the term parasequence has been introduced into the literature as a way of describing higher-frequency oscillations in sea level and shoreline position (Van Wagoner *et al.*, 1988). These sequences should be separated by flooding surfaces so that individual sequence tracts contain a series of stacked parasequence tracts in which multiple flooding surfaces are present (Nummedal *et al.*, 1989). However, this term and concept is still a subject of much controversy. At any rate, by any of the above criteria, a major hiatal surface separates uppermost Codell deposits from the overlying Fort Hays member of the Niobrara Formation. Weimer (1983) suggests, however, that another surface or sequence boundary is present at the base of the Codell sequence. This hypothesis is based on 2-3 missing faunal zones in the top of the Carlile Formation in central Wyoming (Merewether, *et al.*, 1979).

In both outcrop and core (see Chpt. III), the Codell contact into the underlying Carlile deposits appears gradational. A distinct hiatal break is not readily apparent, no lithologic breaks or lag deposits (phosphate nodules, shark teeth, etc.) seem to exist near the base of the Codell sequence in the study area. In an unusual circumstance, the Codell surface is exposed in the Boettcher Quarry (Sections 1 & 2) giving an unparalleled view of a major sequence boundary or hiatal surface. The surface is extremely planar and consistently devoid of major truncation surfaces. If a sequence boundary is present at the base of the Codell, arrangement of this surface should be similar to the one above, assuming that the erosional processes are similar. This

assumption would prove correct if erosional processes occurred under subaqueous conditions. To investigate this problem, 3-D diagrams were created using both surfaces, top of the Codell (Figure 61) and base of the Codell (Figure 63). Because these sections had to be condensed to fit the manuscript format, some of the resolution has been sacrificed. Still, a few observations can be made.

The perspective of the diagram in figure 63 is from the southeast looking northwest. The high peaks and steep one-point lows correspond to fault systems previously described. Comparison of the two figures show little difference except in the extreme northeast corner of the diagrams. Figure 61 has a more jagged appearance because of a sharp low which does not correspond to a fault. In contrast, Figure 63 has a more gentle, rolling profile. This difference was investigated further with an expanded, higher resolution 3-D diagram. Upon closer inspection, Figure 61 had a much higher degree of angularity over this area when compared to Figure 63. One interpretation for this difference may be that since the boundary at the top of the Codell is essentially flat except when broken by faults or an occasionally deep erosional scour, the resultant topology would have an angular appearance. The more rounded profile of Figure 63 suggests that indeed the two surfaces are somewhat dissimilar and the base of the Codell Sandstone may not represent a sequence boundary. Further modeling is needed to conclusively investigate this hypothesis. One option would be to take away the effects of the faults (subtract throw from the surface elevation) and see what topology differences would be apparent. It is possible by using this technique to eventually model the surface on which the Codell rests if the resolution of the software package will allow it.

To further investigate the relationship between the Carlile and Niobrara strata, two schematic cross-sections were constructed using wire-line log picks for correlation purposes. Gross stratigraphic intervals were selected for correlation purposes; Greenhorn, Carlile, and Niobrara intervals represent genetic depositional packages. It

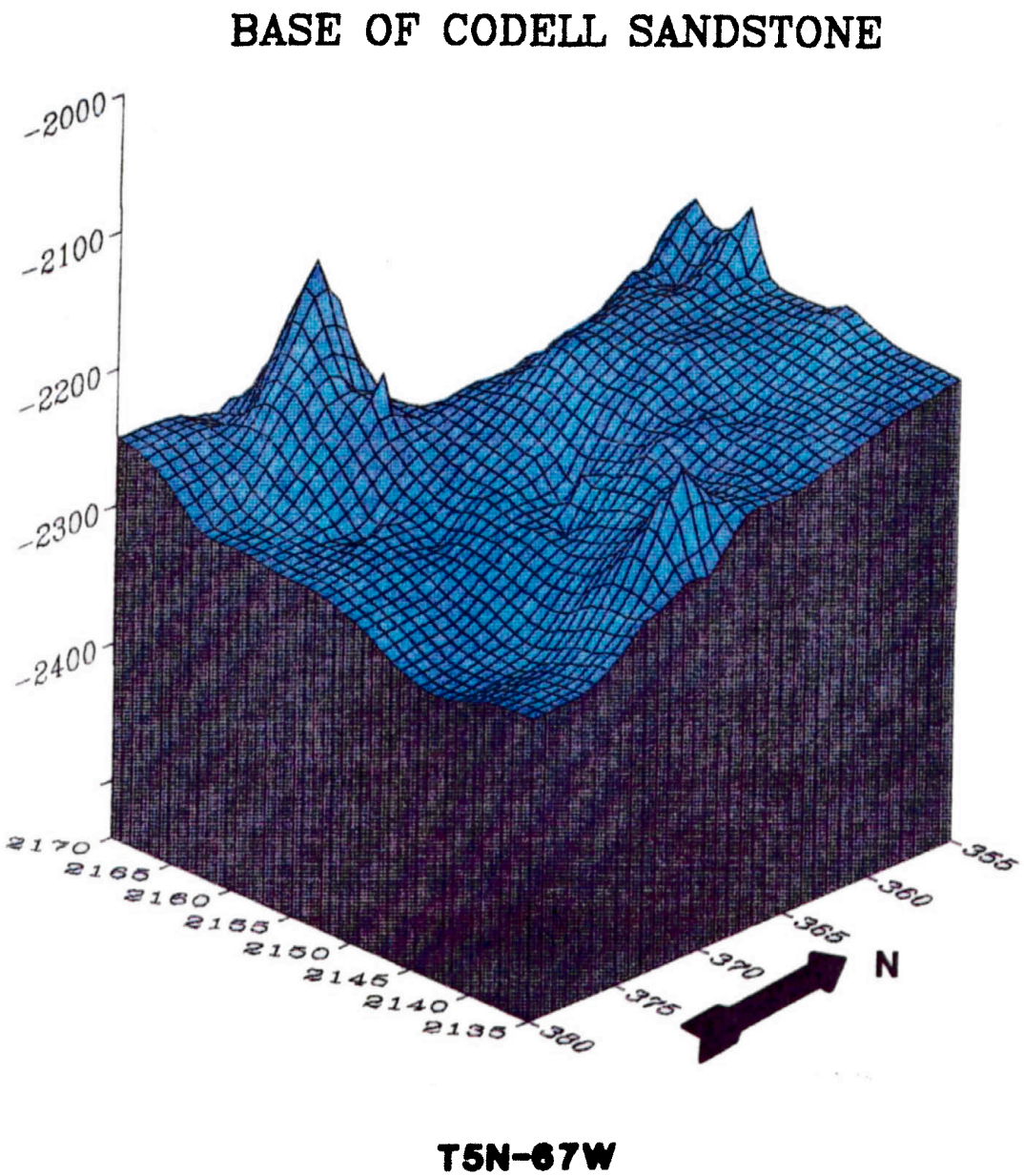

Figure 63. 3-D trend surface diagram depicting surface elevation topology of basal Codell sequence. Vertical (z axis) is measured in feet. The x & y directions are in xy digitizer units. Azimuth=135 & Z factor=70.

was not possible to definitively break-out the Codell Sandstone because of the lack of porosity and GR log data. Only resistivity electric logs were consistently run over the interval, and at times, SP shifts suggest sandstone development at the base of the Fort Hays limestone. Cross-section A-A' (Plate 2) is oriented southwest-northeast across north-central Colorado. Cross-section B-B' (Plate 3) is oriented in a due east-west direction across Weld & Morgan counties of Colorado (Figure 64). A bentonite marker used as a log pick for the top of the Graneros shale, was picked as a datum point from which the sections were hung. The Greenhorn interval is remarkably consistent in thickness across both sections. This is not the case of the overlying Carlile interval. In cross-section A-A', the Carlile interval thickens, thins, and then thickens again toward the northeast. The upper Carlile/Fort Hays contact shows evidence of erosional scour while the lower Carlile/Greenhorn contact is fairly regular and flat in form. It is interesting to note that the Carlile thickens to the northeast at the expense of the Niobrara interval. SP characteristics on the electric log suggest that the Codell also thickens to the northeast. Faults through the Niobrara in wells #2 and #16 account for the stepped pattern across portions of the cross-section.

Cross-section B-B' (Plate 3) depicts a gradual thickening of Carlile strata to the east with a coincident thickening of Niobrara deposits. The erosional nature of the upper Carlile/Niobrara contact is still apparent. Apparently, this surface truncates the Codell sandstone to the east as the SP log trace is flat beneath the Fort Hays limestone. The SP response could be misleading if the Codell is more porous to the east and filled with fairly fresh water.

These cross-sections agree in a general way with studies by Weimer and Sonnenberg (1983). The Carlile interval thickens both to the north and east and a major unconformity at the upper Carlile/Niobrara contact apparently truncates Codell strata to the east. It is also plausible that the Codell simply pinches out to the east. Weimer suggested that a basement bulge called the Transcontinental arch warped the basin,

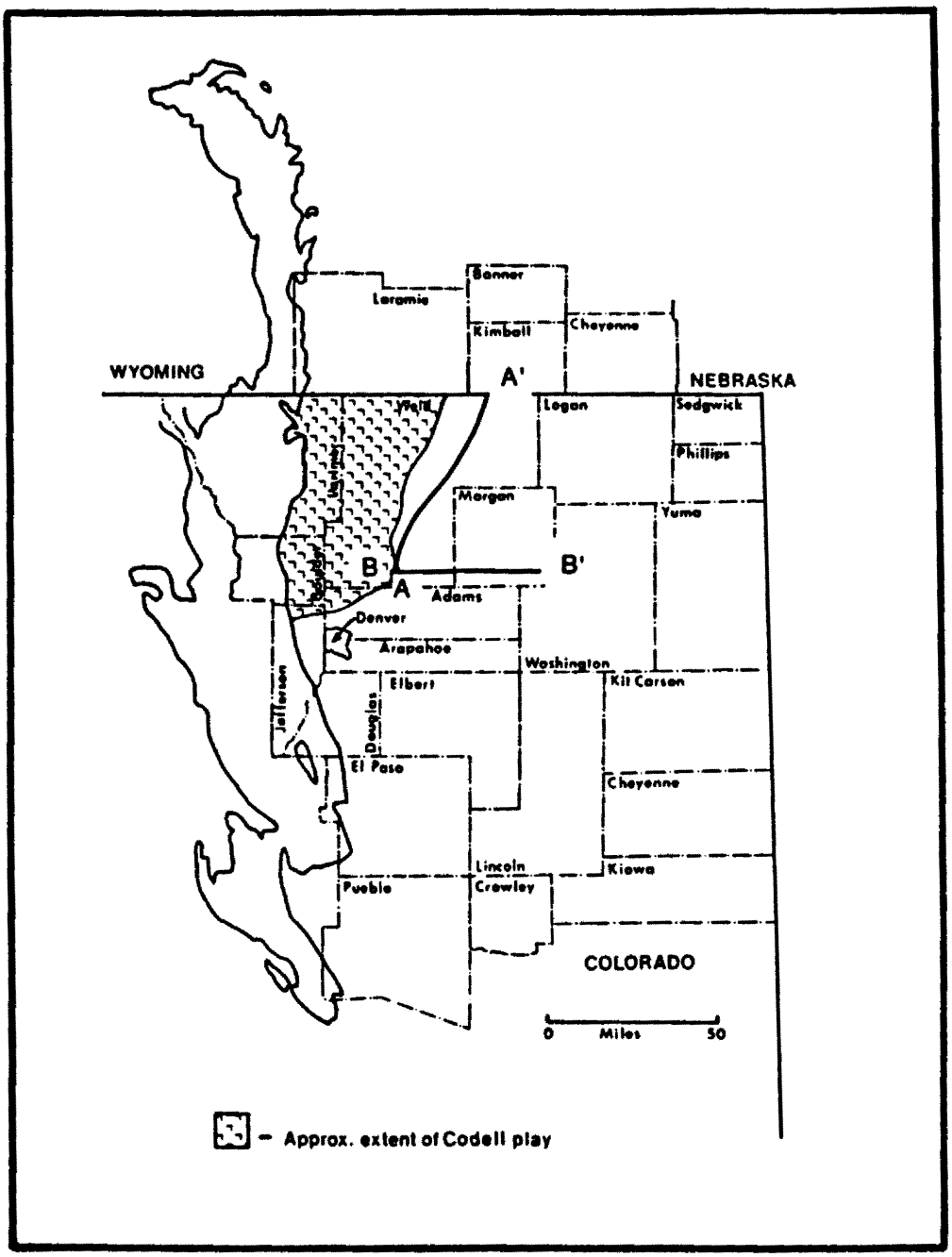

Figure 64. Approximate geographic location of cross-sections A-A' & B-B' across north central Colorado.

which resulted in a complex arrangement of erosion surfaces that lingered on into the Upper Cretaceous (Figure 10). Even though Plate 3 does not extend as far east as Kansas, it is apparent that the thickness of the Greenhorn interval is remaining constant while the Niobrara interval is gradually thickening. In fact, on Plate 2 the Greenhorn interval is actually thickening to the northeast (in the same general position where the arch should be). This suggests that the structural influence of the arch was waning during upper Cenomanian and lower Turonian time. The arrangement of unconformity surfaces may be more directly related to base level changes.

Composition and Hydrocarbon Recovery Techniques

X-ray diffraction analyses of the bulk and clay size fractions were performed on plugs from the Rhoades #1 core (Section 4). Using acetone, the samples were pulverized then were dried and pressure-packed onto aluminum powder mount holders to measure whole-rock characteristics. A separate portion of each sample was suspended in deionized water using a sonic probe and centrifugally size-fractionated to isolate the clay-size (<4 micron) materials. The oriented clay mounts were analyzed in both the air-dried and glycol-solvated states over an angular range of 2-31 degrees 2-theta at a scan rate of 2 degrees/minute.

Three samples at depths of 7289', 7291', and 7296' were chosen to represent typical Codell composition. Results of the whole-rock and clay-fraction XRD analyses are summarized in Table 2. According to the Folk classification, this sandstone is a subarkosic arenite in composition. This differs from the composition determined in outcrop hand specimens, this difference may be due in part to surface weathering phenomena. Whole rock XRD analysis indicates that the samples are composed primarily of quartz with subsidiary amounts of plagioclase feldspar and clay minerals. Minor amounts of pyrite were detected in all three samples. It is the fairly high total layer silicate (clay minerals) percentages which are of interest in this interval. Analysis

TABLE 2

X-Ray Diffraction Data

SAMPLE DEPTH (FEET)	7289	7291	7296
QUARTZ	67.8%	66.5%	61.7%
K-FELDSPAR	0.0%	0.0%	0.0%
PLAGIOCLASE	12.6%	12.8%	15.4%
PYRITE	1.0%	0.9%	0.9%
TOTAL LAYER SILICATES	18.6%	19.8%	22.0%
TOTAL	100.0%	100.0%	100.0%
ILLITE	32.5%	30.9%	31.0%
ILLITE/SMECTITE	58.8%	59.7%	60.8%
KAOLINITE	0.0%	0.0%	0.0%
CHLORITE	8.6%	9.4%	8.2%
TOTAL	100.0%	100.0%	100.0%

of the oriented clay mounts reveal that the three samples have nearly identical compositions. Mixed-layer illite/smectite is the dominant layer silicate, followed by illite and chlorite. No kaolinite was detected in the samples. The interstratified illite/smectite present in all three samples is ordered and contains approximately 20% smectite(montmorillonite) layers.

SEM (Scanning Electron Microscope) analyses were run over the same three samples from Rhoades #1. The samples were broken to expose fresh surfaces and placed on aluminum stubs for mounting. Samples were heat dried to drive off any hydrocarbons still present. Following the heat treatment, the samples were gold spatter-coated. The samples were then examined with secondary electron imaging at 30kV using an ISI WB-6 SEM.

Figure 65 at 7289' shows a smooth quartz overgrowth surface fringed by layered illite/montmorillonite particles. Fibrous illite structures are also apparent. Figure 66 from the same interval, shows pore throats fringed by smectite particles and quartz overgrowths. The pores show moldic configuration, i.e. pores opened after dissolution of a framework constituent. In the 7291' interval, Figure 67 depicts a heavily altered feldspar grain in the central portion of the photograph. Bundles of smectite particles fringe the grain in addition to covering the middle portion of it. Discrete chlorite rims around pore throats were not found during the SEM examination.

Figure 68 is a photomicrograph of a typical framework grain, cement, and clay configuration from the Codell Sandstone. Isolated moldic porosity is surrounded by quartz grains with extensive overgrowths (center) and a clay matrix composed of illite and smectite layers (low, straw-colored birefringence). This photograph also illustrates part of the dissolution mechanism for the feldspar grains. Calcite cement is present (in red) coating a feldspar grain, subsequent dissolution of this cement would create an isolated pore throat similar to that pictured in the upper left corner. Also depicted are rounded and compressed sedimentary rock fragments (brown colored, shale fragments)

Figure 65. SEM photograph at 1700x of the 7289' interval of the Rhoades #1 core showing quartz overgrowths and fringing smectite/illite clay arrangement.

Q - quartz overgrowths
sm - layered illite/montmorillonite
il - illite structures

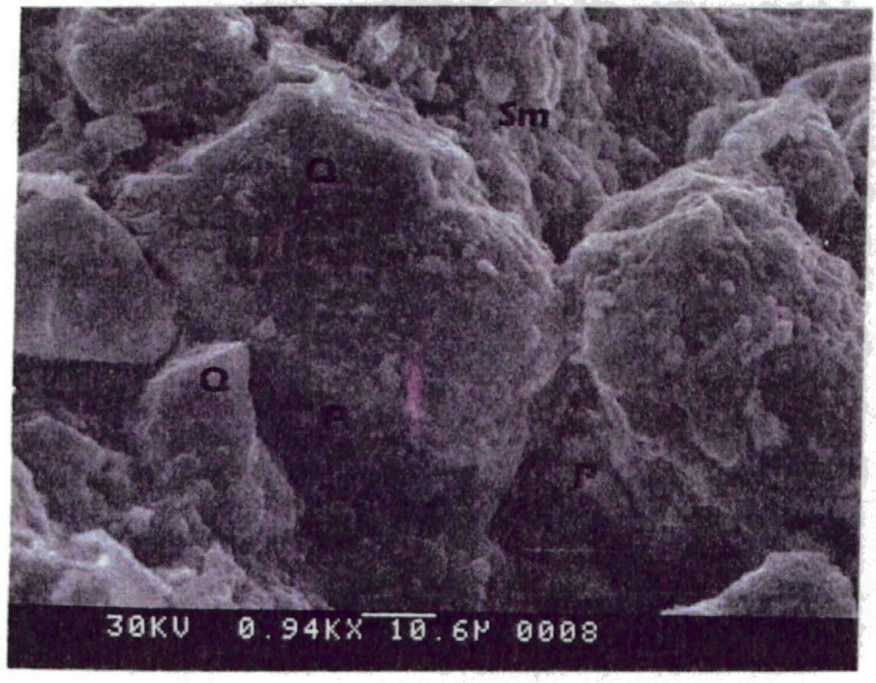

Figure 66. SEM photograph at 940x of the 7289' interval of the Roades #1 core showing moldic porosity quartz overgrowths and fringing smectite/illite clays are present.

Q - quartz overgrowths
sm - layered illite/montmorillonite
P - pores

Figure 67. SEM photograph at 1700x of the 7291' interval of the Rhoades #1 core showing a highly altered plagioclase feldspar. Fringing clays are present.

F - altered and etched feldspar grain
sm - layered illite/montmorillonite

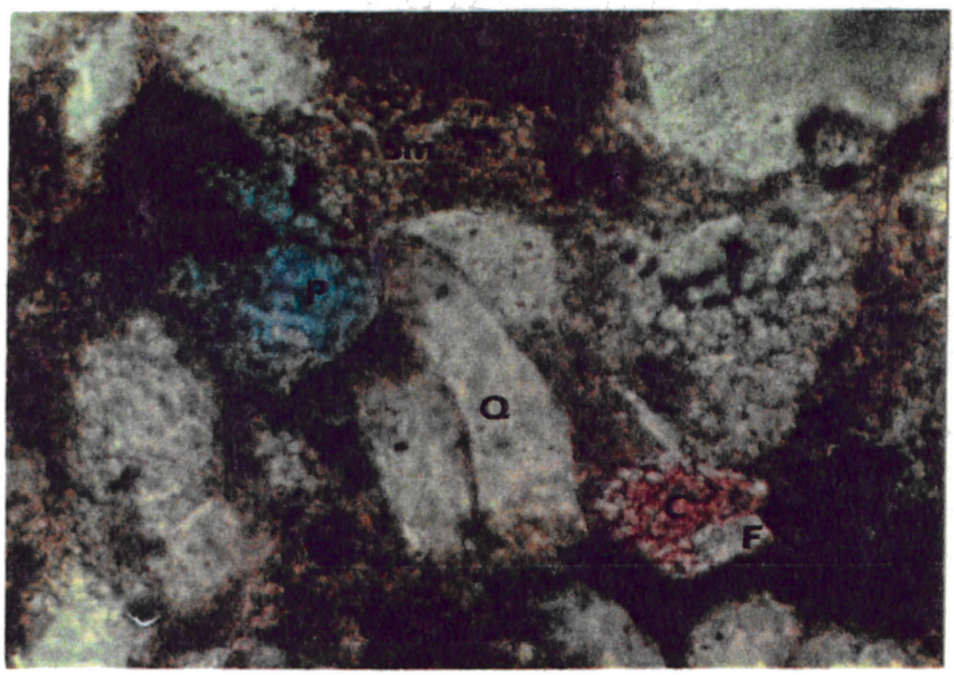

Figure 68. Photomicrograph of 7289' interval of the Rhoades #1 core. Shows typical arrangement of framework constituents, quartz, altered feldspar and clay matrix. Porosity shows up as blue and calcite cement as red.

sm - sillite/montmorillonite layers
Q - quartz overgrowths
P - pore throat
C - calcite cement
F - partilally dissolved feldspar grain

filling some of the interstices between framework constituents. Rounded chert fragments are also common in thin section, but are not pictured here.

The high clay content throughout this whole interval is directly related to the intense bioturbation in most portions of the core. Mixing of mud and organic material by organisms facilitated the distribution of clay and occluded almost all of the original porosity. Subsequent dissolution of unstable framework grains during diagenesis created the secondary porosity. If this diagenetic mechanism had not occurred, there would be no production from the Codell Sandstone. The Rhoades #1 core (Section 4) is fairly typical of the Codell sequence throughout the play area.

A preliminary overview of thin sections from the Rhoades #1 indicate that the diagenetic history and resultant paragenetic sequence show a complex series of relationships. However, a general model of diagenesis can be inferred from the XRD, SEM and photomicrograph data.

1. Initial deposition of framework constituents, rock fragments, and detrital clays.
2. Extensive bioturbation and deposition of organic material.
3. Formation of quartz overgrowths and initial sericitization of feldspars.
4. Calcite invasion and further dissolution of unstable feldspar grains.
5. Dissolution of calcite cement and formation of isolated, moldic secondary porosity.
6. Minor amounts of authigenic clay development around pore throats.

This sequence differs from some diagenetic models in which carbonate cementation occurs early and pre-dates quartz overgrowth development (Hart *et al.*, 1989). However, most diagenetic models involving clay-rich marine sandstones invoke a major episode of carbonate dissolution subsequent to cementation that accounts for secondary porosity development. This interpretation also supports these generalizations.

Principal production problems associated with Codell development are associated with the abundant effective shale fractions in the interval. High smectite/illite contents

enhance absorption of water from both drilling and fracturing fluids and consequent swelling of the layered clays results. Those clays which may coat pore spaces or partially bridge pore throats may expand considerably, effectively sealing off the natural porosity and greatly reduce already low permeabilities. It has been reported by the Western Company, that only between 15 and 30% of load fluids are recovered after fracturing the Codell (Kennedy, 1983). In addition, clays such as illite and chlorite may be dislodged during the injection and withdrawal of fracturing fluids and eventually clog pore spaces. The hyperbolic decline rates associated with first-year production from the interval may be the result of cumulative clogging problems. Initially, large acid treatments were used as the standard method for opening pore throats. However, this practice aggravated the already complex problem of swelling and dislodged clay fractions. Effects of dissolution of the remaining calcite cement, are offset by the flocculation of clays in high pH fracturing fluids. Irreversible formation damage results.

Hydraulic fracturing of the interval is critical to effective completion since the reservoir is so 'tight'. The usual proppant is sand and fracturing is done through tubing. The introduction of sand into the formation may be facilitated by high or low pH, cross-linked gels. The more acidic water-gels remain stable under higher temperatures. Generally, the main advantage to high pH delivery systems is their low cost and ability to distribute a greater concentration of sand per square foot. However, the resultant formation damage may shorten dramatically the life expectancy of the well (Kennedy, 1983). The more weakly acidic fluids distribute less sand but may actually increase permeability by partial disintegration of the clay matrix. However, the resultant introduction of fines into the system may eventually cake around the fractures. Some fairly exotic treatments have been tried in order to reduce the amount of reservoir damage. Methanol/CO_2, polymer emulsions, and foam fracs using methanol/KCl blends have met with limited success. Their application is expensive and therefore impractical in today's economic climate.

CHAPTER V

Summary

Discussion

Recent sedimentological studies of depositional systems are giving more emphasis to genetic depositional architecture and the bounding surfaces that define them. Major bounding surfaces are generally defined by unconformable relationships. These sequence boundaries bracket genetically related strata and typically grade basinward (seaward) into correlative conformable surfaces (Van Wagoner *et al.*, 1988). Studies of the Codell Sandstone to the southwest of the study area suggest depositional environments ranging from shoreface to nearshore/offshore marine bar deposits (see Chpt. II). However, all interpretations contain one similar observation, a major lithologic and /or unconformable boundary caps the Codell interval.

This boundary is marked by the abrupt lithology change from sandstone to marine limestone and in places, the contact is paved with transgressive lag deposits (phosphate pebbles, sharks teeth, abraded bivalve fragments, etc.). A gently undulating scour surface is sporadically present at this boundary in outcrop showing a typical maximum relief of only 1 foot (34 cm). In southern Colorado, this bioclastic calcarenite unit is called the Juana Lopez member of the Carlile Shale while in northern Colorado, the contact is marked by the uppermost unit of the Codell Sandstone (Lowman, 1977; Weimer & Sonnenberg, 1983). This distinction is based on the absence of typical transgressive lag deposits at the top of the Codell Sandstone in the study area, the silica or calcite-cemented sub-arkosic arenite composition of the uppermost unit, and the sharp to very erratic, low-amplitude erosional surface at the Codell/Niobrara contact (Fig. 40). While the uppermost portion of the Carlile shale interval represents deposition in the

expanding seaway, most workers consider basal Codell Sandstone deposits to represent a minor regressive (90 m.y.) pulse sandwiched between the Greenhorn and Niobrara transgressive cyclothem (Weimer & Sonnenberg, 1983; Glenister, 1985). However, recent sequence stratigraphy models pose the possibility for different methods of emplacement.

Because of the strandline depositional origin to the south, there has been some speculation that the Codell in northern Colorado could represent re-worked transgressive systems tract deposits (barrier, estuarine and strandline depositional environments) in which some, if not all of the parental strandline facies associations have been erased. Recent work in the Cardium Formation, Alberta suggest that previously interpreted shelf systems could represent truncated and re-worked narrow shoreface deposits (Walker & Eyles, 1988). These systems although geographically distant from the Codell Sandstone, were deposited along the same western margin of the Interior Cretaceous Seaway. Several relationships of both meso and macro-scale in the Codell interval help resolve the question of depositional origin.

Lithofacies relationships suggest that the Codell was originally emplaced as a nearshore inner shelf deposit and not as part of a strandline system. Regressive barrier and shoreface systems exhibit a regular arrangement of lithofacies starting from transitional (shale and lenticular sandstone beds), lower shoreface (laminated to burrowed, sandstone/shale sequences), upper shoreface (trough to planar cross-stratified sandstone), to foreshore (planar to low-angle swash laminated sandstone) deposits. Because of the hydrodynamic processes operating at the strandline (swash, backwash, & storm currents), these systems coarsen upward and are typically capped by either finer-grained lagoonal or delta plain deposits. These sequences are broken in a strike direction, by dip-oriented distributary or tidal inlet channels (Barwis & Hubbard, 1976). The frequency of tidal inlet fills is directly proportional to the increase in tidal range, the highest frequency being around the mesotidal range. Transgressive barrier

systems tracts produce abbreviated shoreface facies relationships which still exhibit regular grouping of bedding structures. Internally, these major systems tracts are composed of facies which contain abundant flaser bedding, erosional scour and fill structures, and cross-bed sets called tidal bundles. Tidal bundles consist of small-scale, low-angle, sigmoidal cross-beds which truncate each other near 180°. Elliott (1987) suggested that the presence of these bundles may be more common than previously recognized in Cretaceous sandstones. He concluded that storm-dominated interpretation of shelf environments may be incorrect in some Cretaceous sequences.

The Codell Sandstone lithofacies relationships are much more erratically arranged than what would be typical of strandline systems. Horizontally stratified intervals grade into angle-of-repose bedding over a distance of a few feet (Figure 34). The juxtaposition of this kind of stratification suggests a very erratic current regime. Immediately adjacent to these sandstone beds, shale intervals are common and indicate deposition under suspension processes. Comparison of Figures 19, 20 and 21 show that none of the sandstone beds in the Codell (except the uppermost bed), are correlatable for more than 4-5 feet.

Randomly arranged between the lenticular sandstone beds are thick intervals of bioturbated siltstone and silty sandstone (LF 2). No primary depositional sedimentary structures are preserved in these zones (Figure 36). Because of the marine affinity of the trace fossil assemblage (*Cruziana* ichnofacies), there is no evidence to suggest that these intervals could represent fine-grained, bioturbated lagoonal or inlet fill deposits. In the subsurface, laminated to burrowed couplets are common (Figure 44). These features are common in storm-generated inner shelf sequences (Walker, 1985). No major erosional scour surfaces exist internally within the Codell interval unlike shoreface sequences which commonly contain erosional surfaces associated with the migration of tidal inlet channels (Barwis & Hayes, 1979).

Hummocky-bedded sandstone (LF 1) is present throughout the sections but is typically more common in the lower portion of the Codell interval (Figures 25 & 26). Typically the hummocky stratified lenses are either capped by horizontally stratified laminations or planar-tabular ripple cross-stratified sandstone (Figure 34). This arrangement indicates rapidly waning flow conditions (Clifton, 1986). Horizontally stratified and planar-cross stratified sandstone beds become more common at or near the top of the interval (Figure 27). The presence of small-scale planar angle-of repose bedding only in the "winnowed" top of the Codell is important and will be discussed later. Together these relationships indicate that deposition occurred under rapidly fluctuating hydrodynamic conditions. Bedding arrangement indicates that current regimes fluctuated erratically. Current regimes set up from episodic storm-generated processes provide the best hydrodynamical interpretation of bedding structure associations.

Figure 69 graphically illustrates the sequence stratigraphic relationships interpreted to be present in the Codell sandstone. Wiemer (person. comm. 1987) suggests that a major sequence boundary exists at the base of the Codell based on pebble lags found in subsurface cores. This surface supposably represents the parental strandline barrier sequence from which the Codell Sandstone was formed. However, no discernible pebble lag deposits were found in either outcrop or core in this study (see the first part of Chpt. III). It is possible that lag concentrations are associated with the basal surfaces of hummocky cross-stratified sequences and therefore, are lensy and sporadically arranged and do not represent a basin-wide correlative surface. If the Codell interval was derived from a totally obliterated shoreface sequence, why are roughly coeval barrier sequences preserved just 45 miles to the southwest (McClane 1983) in the Codell Sandstone? Depositional processes operating during transgression of a shoreface should not differ so dramatically in such a short geographical distance. It is more reasonable to interpret that the Codell sequence in the study area represents nearshore marine deposition (inner shelf) basinward of coeval barrier systems to the southwest.

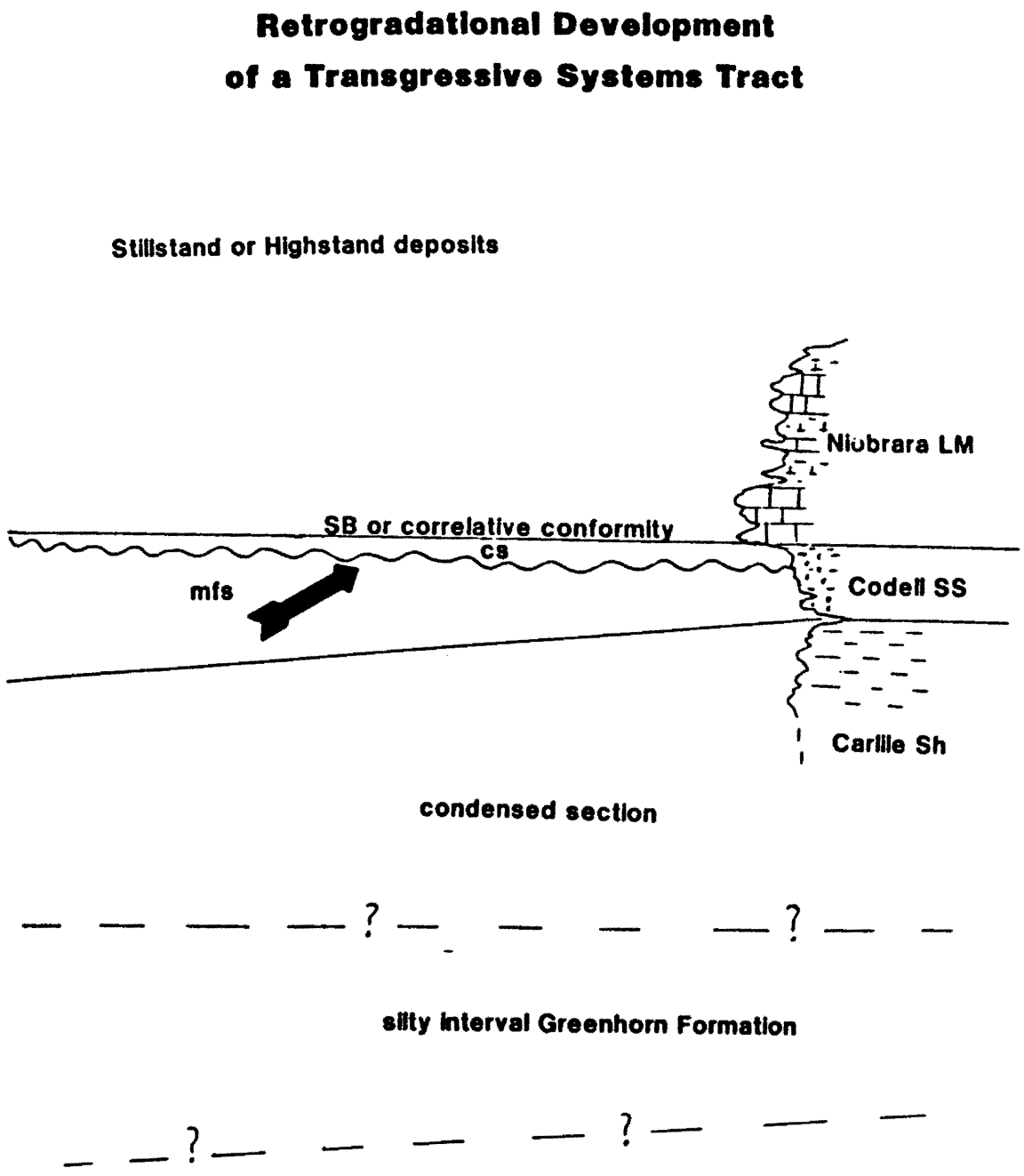

Figure 69. Schematic representation of sequence stratigraphic development of the Codell sandstone. SB - Sequence boundary, mfs - marine flooding surface, and cs - condensed section. Greenhorn internal, indicated by the dashed lines, may represent an earlier pulse of transgressive systems tract development.

It is assumed from data supplied by previous workers and paleocurrent indicators that range from southwest to southeast that sediment from Frontier age delta systems located in northwestern Wyoming were redistributed by storms and shelf currents into inner shelf deposits to the southeast and into strandline deposits to the south and southwest. during the 90 m.y. lowstand. A slight deepening of sea-level occurred as evidenced by the marine flooding surface which separates Codell deposits into normal inner shelf deposits in the lower portion and a condensed section at the top. As this sea-level adjustment occurred sediment influx into this portion of the seaway diminished and a starved basin condition existed (a condensed section). As long as the shelf floor remained within storm wave-base, this area was repeatedly affected by episodic storm currents and therefore "winnowed". Further deepening placed the shelf floor beyond the reach of storm wave base and the Codell sandstone was abruptly overlain by the Fort Hays member of the Niobrara formation. In sequence stratigraphic terms the whole package of regressive or "lowstand" deposits capped by a marine-flooding surface and condensed section is referred to as retrogradational development of a transgressive systems tract. The Codell sandstone represents the basinal equivalent of this transgressive systems tract while the Niobrara represents the overlying still-stand or high-stand systems tract that is the result of further deepening of the Western Interior Cretaceous Seaway (figure 69).

It is not clear whether the Codell Sandstone was initially a linear shelf sand-ridge deposit that was re-worked into a sheet-like geometry or whether it was originally emplaced as amorphous storm-generated sheet deposits. Many ancient shelf sand ridges were probably deposited during marine transgressions and lie on regional unconformity surfaces (Barwis, 1989). Amalgamation of storm sheets on the other hand, occurs just below sequence boundaries according to theoretical seismic stratigraphy models. Because of the terminology controversy surrounding the use of sequence boundary

versus parasequence in marine, basinal settings, it is unclear exactly what the relationship is that marks the contact between Codell and Niobrara strata. However, a few observations can be made. Parasequences generally refer to transgressive/regressive oscillations during a major cycle. In other words numerous marine flooding or ravinement surfaces are capped by transgressive deposits which are in turn capped by another minor regressive pulse of sedimentation. Since there is only one marine flooding surface contained in the Codell/Niobrara interval and the Codell/Niobrara contact is marked by a distinct lithologic break which is regional in extent and correlative over much of Colorado, the contact will be referred to as a sequence boundary (figure 69).

Storm-generated shelf sandstone intervals are common in some ancient sequences deposited in portions of the Interior Cretaceous Seaway (Walker, 1985; Clifton, 1986). The Mosby sandstone in central Montana shows strikingly similar features when compared to the Codell Sandstone in both meso and macro-scale. It is slightly older than the Codell (early Turonian) and is overlain by the Greenhorn Formation, which in this case is a normal marine limestone (Rice, 1984). Internally, the lithofacies relationships are quite similar; hummocky stratified sandstone lenses, horizontally laminated sandstone beds intercalated with shale, rippled upper surfaces of sandstone lenses, and abundant bioturbation predominantly composed of the trace fossils *Ophiomorpha, Thalassinoides, Chondrites,* and *Planolites* (Rice, 1984). The Mosby sandstone and correlative units have a sheet-like geometry, which in this case covers over 500 sq. kilometers. By comparison, the Codell Sandstone in northern Colorado is aerially contiguous for only about 80 sq. kilometers. It is likely that the extent was much larger prior to erosion associated with the Laramide uplift of the Front Range in Colorado and Wyoming.

Conclusions

After analyzing the Codell sandstone throughout the study area, several observations and conclusions can be reached. Re-statement of the objectives will help facilitate the structuring of the following conclusions:

I. Determination of the depositional system and facies relationship of the Codell sandstone in north-central Denver-Julesburg basin using all available data.

From both outcrop and core descriptions and correlations, the Codell sandstone was originally emplaced as an inner shelf deposit which underwent cannibalization as sediment supply into the basin was shut off during the subsequent transgression. The Codell sandstone represents a basinal pulse of retrogradational transgressive systems tract development during deepening of the epeiric seaway. A marine flooding surface near the top of the Codell separates normal inner shelf marine deposits from a thin condensed interval marked by the "winnowed" cap of the Codell. A sequence or parasequence boundary separates uppermost Codell from the Niobrara Formation. Internally, the bedding arrangement is extremely heterogeneous and consists of the following: randomly arranged horizontally to hummocky cross-stratified sandstone lenses, extensively bioturbated siltstone and shale intervals, and small-scale, angle-of-repose cross-bedded sandstone beds which generally occur at or near the top of the Codell sandstone.

II. Delineation of reservoir geometry, production trends and structural relationships of the Codell sandstone in the study area.

Maps developed from isopaching the Codell sandstone indicate sheet-like to broadly lobate geometries oriented in a north-west to south-east direction. Gross thicknesses do not vary significantly across the study area, however, intervals containing the

best porosity values do not necessarily correspond to the thickest Codell sandstone. This indicates that secondary diagenesis plays a major role in the development of reservoir quality zones. A series of en-echelon normal faults adjacent to a major basin axis fault system are essentially accommodation structures related to Laramide deformation of the Front Range uplift in northern Colorado and southern Wyoming. Since this basin is mature, these faults provided conduits to charge the reservoir interval with solution driven gas which produces an extremely mobile hydrocarbon environment. As the formation is porous, but fairly impermeable, any slight reversal in dip direction may trap the hydrocarbons updip from faulted zones forming combination structural/stratigraphic traps. Areas in or immediately adjacent to fault systems should be avoided as these areas have been flushed to a greater degree because of the high mobility of gaseous fluids.

III. Analysis of the compositional elements of the Codell sandstone and their effects on diagenesis and hydrocarbon recovery in the play area.

The Codell sandstone is a subarkosic arenite in composition and is composed primarily of quartz and subsidiary amounts of plagioclase feldspar and clay minerals. Clay contents are high and range up to 22% of the total composition. Primarily composed of illite and illite/smectite layered silicates, the clay fraction poses significant drilling and production problems. Fluids sensitive to minimizing the effects of swelling clays should be utilized, such as cross-linked gels, polymer emulsions and methanol/CO_2 blends. Diagenetic dissolution of carbonate cement and unstable framework constituents cause moldic porosity development. Portions of the Codell sandstone are extremely porous because of this but are fairly impermeable because of the high matrix clay content of the interval.

BIBLIOGRAPHY

Arnott, R.W.C., 1988, Deposition in an ancient storm-dominated nearshore environment, the possible preserved record of combined-flow conditions: in Shelf Sedimentation: Events and Rytthms, Programs and Abstracts: Soc. Econ. Paleon. Miner. Research Conference, 1988, vol. 1, p. 2.

Arnott, R.W.C., and Southard, J.B.,1988, Flow-duct experiments on bed forms in oscillatory and combined flow, and the origin of hummocky cross-stratification: in Shelf Sedimentation: Events and Rythms, Programs and Abstracts: Soc. Econ. Paleon. Miner. Research Conference, 1988, vol. 1, p. 3.

Asquith, D.O., 1970, Depositional topography and major marine environments, Late Cretaceous, Wyoming: Am. Assoc. Petroleum Geologists Bull., v. 54, p. 1184-1224.

Aulia, K. , 1982, Stratigraphy of the Codell Sandstone and Juana Lopez Members of the Carlile Formation (Upper Cretaceous), El Paso and Fremont Counties, Colorado: Colorado School of Mines, Golden, Colorado, M.S. Thesis, T-2589, unpub.

Barwis, J.H., 1989, The explorationist and shelf sand models: Where do we go from here?: in Morton, R.A., and Nummedal, D., eds., Shelf Sedimentation, Shelf Sequences and related hydrocarbon accumulation: Gulf Coast Section, Soc. Econ. Paleon. Mineral Seventh Annual Research Conference Proc., 1989, p. 1-14.

Barwis, J.H., and Haynes, M.O., 1979, Regional patterns of modern barrier island and tidal inlet deposits as applied to paleoenvironmental studies: in J.C. Ferm, & J.C. Horne (eds.), Carboniferous depositional environments in the Appalachian region, Univ. South Carolina, Carolina Coal Group, p. 472-498.

Barwis, J.H., and Hubbard, D.K., 1976, The relationship of flood-tidal delta morphology to the configuration and hydraulics of tidal inlet-bay sequences: GSA Abstracts with Programs, p. 128-129.

Bieber, D.W., 1983, Gravimetric evidence for thrusting and hydrocarbon potential of the east flank of the Front Range, Colorado, in Lowell, J.D., ed., Rocky Mountain Foreland Basins and Uplifts, Rocky Mountain Assoc. Geologists, 1983, p. 245-255.

Boczar-Karakiewicz, B., and Bona, J.L., 1986, Wave-dominated shelves: A model of sand-rich formation by progressive infragravity waves: in Knight, J.R., and McLean, J.R., eds., Shelf Sands and Sandstones: Canadian Soc. Petroleum Geologists, Memoir 11, p. 163-180.

Bourgeois, J. and Smith, J.D., 1984, Paleohydraulic significance of hummocky cross-stratification: in Sedimentology of Shelf Sands and Sandstone Symposium - Programs and Abstracts: Canadian Soc. Petroleum Geologists, p. 27.

Boyles, J.M., and Scott, A.J., 1982, A model for migrating shelf-bar sandstones in Upper Mancos Shale (Campanian), northwestern Colorado: Am. Assoc. Petroleum Geologists Bull., v. 66, p. 491-508.

Butman, B., Noble, M., and Folger, D.W., 1979, Longterm observations of bottom currents and bottom sediment movement on the Mid-Atlantic Continental Shelf: Jour. Geophys. Research, no. 84, p. 1187-1205.

Cacchione, D.A., 1988, Sediment patterns and small-scale morphology on the northern California continental shelf: Measurements, estimates, and causes: in Shelf Sedimentation: Events and Rythms, Programs and Abstracts: Soc. Econ. Paleon. Miner. Research Conference, 1988, vol. 1, p. 9.

Chronic, J., 1957, Boulder Measured Section, in McKee, E.D., ed., Colorado Measured Sections, A symposium: Rocky Mountain Assoc. Geologists.

Clayton, J.L., and Swetland, P.J., 1980, Petroleum generation and migration in the Dever Basin: Amer. Assoc. Petroleum Geologists, v. 64, no. 10, p. 1613-1633.

Clifton, H.E., 1986, Interpreting paleoenergy levels from sediment deposited on ancient wave-dominated shelves: in Knight, J.R. and McLean J.R., eds., Shelf Sands and Sandstones: Canadian Soc. Petroleum Geologists, Memoir 11, p. 181-190.

Csanady, G.T., 1982, Circulation in the coastal ocean: Reidel Pub. Co., London, 280 p.

Dane, C., Kauffman, E., and Cobban, W. 1968, Semilla sandstone, a member of the Mancos shale in the southeastern part of the San Juan basin, New Mexico: USGS Bull., No. 1254-F, p. F1-F21.

Elliott, T., 1987, Tidally produced sigmoidal cross-bedding in Cretaceous shelf bodies, Western Interior basin, U.S.: Abstracts, Soc. Econ. Paleon. & Miner. Annual Midyear Meeting, Austin, TX, v. 4, p. 25.

Erslev, E.A., Rogers, J.L., and Harvey, M., 1988, The northeastern Front Range revisited: Horizontal compression and crustal wedging in a classic locality for vertical tectonics: in Holden, G.S., ed., Geological Soc. America Field Trip Guidebook,1988, Professional Contributions-Colorado School of Mines, no.12, p. 122-133.

Evetts, M.J., 1976, Microfossil biostratigraphy of the Sage Breaks Shale (Upper Cretaceous) in northeastern Wyoming: The Mountain Geologist, v. 13, p. 115-134.

Fassett, J.E., 1976, What happened during late Cretaceous time in the Raton and San Juan basins; with some thoughts about the area in between: New Mexico Geo. Soc. Annual Field Conf. Guidebook No. 27, Guidebook of Vermejo Park, notheastern New Mexico, p. 185-190.

Fenneman, N.M., 1905, Geology of the Boulder District: U.S. Geological Survey Bull., no. 265, 101 pp.

Field, M.E., Cacchione, D.A., Drake, D.E., and Tate, G.B., 1988, Deposition and preservation of storm and flood beds on the shelf: the Northern California storm of February 1986: in Shelf Sedimentation: Events and Rythms - Program and Abstracts: Soc. Econ. Paleon Miner. Research Conference, 1988, vol. 1, p. 19.

Gallagher, J., Jr., and Tauvers, P.R., 1988, Tectonosynthem analysis of northwestern South America: ARCO Oil and Gas Company Exploration Research Letters, no. 11, p. 4.

Gelfenbaum, G., and Smith, J.D., 1986, Experimental evaluation of a generalized suspended-sediment transport theory: in Knight, R.J., and Mclean, J.R., eds., Shelf sands and sandstones: Canadian Soc. Petroleum Geologists, Memoir 11, p. 133-144.

Glenister, L.M. and Kauffman, E.G., 1985, High resolution stratigraphy & depostional history of the Greenhorn regressive hemicyclothem, Rock Canyon anticline, Pueblo, Colorado: in Fine-grained deposits & biofacies of the Cretaceous Western Interior Seaway: Evidence of cyclic sedimentary processes, Soc. Econ. Paleon. Miner. Field Trip No. 9, Guidebook No. 4, p. 170-183.

Gorsline, D.S., and Swift, D.J.P., 1977, Shelf Sediment Dynamics: A national overview: Report of workshop held in Vail, CO., Nov. 2-6, 1976.

Greenwood, B., and Sherman, D.J., 1986, Hummocky cross-stratification in surf zone: flow parameters and bedding genesis: Sedimentology, v. 33, p. 33-45.

Gries, R., 1983, North-south compression of Rocky Mountain Foreland Structures in Lowell, J.D., ed., Rocky Mountain Foreland Basins and Uplifts, Rocky Mountain Assoc. Geologists, 1983, p. 9-32.

Hann, M., 1981, Petroleum potential of Niobrara formation in the Denver basin, Colorado: Colorado State University, Fort Collins, Colorado, M.S. thesis, 260 p.

Harms, J.C., Southard, J.B., and Walker, R.G., 1982, Structures and sequences in clastic rocks: Soc. Econ. Paleo. Miner. Short Course no. 9, not sequentially paged.

Hart, G.F., et al., 1989, Shelf sandstones of the *Robulus* zone, offshore Louisiana: in Morton, R.A., and Nummedal, D., eds., Shelf sedimentation, shelf sequences and related hydrocarbon accumulation, Seventh Ann. Res. Conf., Gulf Coast Section, Soc. Econ. Paleon. & Miner., 1989, p. 117-141.

Hattin, D.E., 1975, Stratigraphic study of the Carlile-Niobrara (Upper Cretaceous) unconformity in Kansas and northeast Nebraska: in Caldwell, W.G.E., ed., 1975, The Cretaceous System of the Western Interior of North America: Geological Assoc. Canada, Special Pub., no. 13, p. 195-210.

Hayes, M.O., 1967, Hurricanes as Geologic agents: Case studies of Hurricane Carla 1961 and Cindy 1963: Texas Bureau Econ. Geology, Report Investigations no. 61, p. 1-56.

Henderson, J., 1908, The Foothills Formations of North Central Colorado: Colorado Geological Survey, 1st report, p. 145-188.

Hobday, D.K., and Morton, R.A., 1984, Lower Cretaceous shelf storm deposits, northeast Texas: in Tillman, R.W., and Siemers, C.T., eds., Siliclastic Shelf Sediments: Soc. Econ. Paleon. Miner. Special Pub. No. 34, p. 205- 213.

Hubbard, R.J., 1988, Age and significance of sequence boundaries on Jurassic and early Cretaceous rifted continental margins: Am. Assoc. Petroleum Geologists , v. 72, no. 1, p. 49-72.

Hunter, R.E., and Clifton, H.E., 1981,Cyclic deposits and hummocky cross-stratification of probable storm origin in upper Cretaceous rocks of the Cape Sebastian area, southwestern Oregon: Jour. Sed. Petrol., v. 52, p. 127-143.

Jacob, A.F., 1983, Mountain Front Thrust, Southeastern Front Range and northeastern Wet Mountains, Colorado, in Lowell, J.D., ed., Rocky Mountain Foreland Basins and Uplifts, Rocky Mountain Assoc. Geologists, 1983, p. 229-244.

Johnson, H.D., 1978, Shallow Siliclastic Seas: in Reading, H.G., ed., Sedimentary Environments and Facies: Blackwell Scientific Pub., Oxford, p. 207-258.

Kachel, N.B., and Smith, J.D., 1986, Geological impact of sediment transporting events on the Washington continental shelf: in Knight, J.R., and McLean, J.R., eds., Shelf Sands and Sandstones: Canadian Soc. Petroleum Geologists, Memoir 11, p. 145-162.

Kauffman, E.G., 1969, Cretaceous marine cycles of the Western Interior: The Mountain Geologist, v. 6, p. 227-245.

Kauffman, E.G., 1977, Geological and biological overview, Western Interior Cretaceous Basin, in Kauffman, E.G., ed., Cretaceous facies, fauna, and paleoenvironments across the Western Interior Basin: The Mountain Geologist, v. 14, nos. 3 & 4, p. 75-100.

Kennedy, C.L., 1983, ed. Codell Sandstone, D-J Basin's New Objective, Petroleum Frontiers, v. 1, no. 1, p. 4-34.

Kennett, J. P., 1982, Marine Geology: Prentice-Hall, Inc., Englewood Cliffs, 534 p.

Kreisa, R.D., 1988, Shelf Sedimentation Events: An industry point of view: in Shelf Sedimentation events and rythms - Programs and Abstracts: Soc. Econ. Paleon. Miner. Research Conference, 1988, vol. 1, p. 25.

Krutak, P.R., 1970, Origin and depositional environment of the Codell Sandstone member of the Carlile Shale (Upper Cretaceous) southeastern Colorado: The Mountain Geologist, v. 7, p. 185-204.

LeMasurier, W., 1970, Structural study of a Laramide Fold involving shallow-seated basement rock, Front Range, Colorado: Geological Soc. America Bull., v. 81, p. 421-434.

Lowell, J.D., 1983, Foreland Deformation, in Lowell, J.D., ed., Rocky Mountain Foreland Basins and Uplifts, Rocky Mountain Assoc. Geologists, 1983, p. 1-8.

Lowman, B.M., 1977, Stratigraphy of the Upper Benton and Lower Niobrara Formations, Boulder County, Colorado: Colorado School of Mines, Golden, Colorado, M.S. Thesis, T-1926, unpub.

Luternauer, J.L., 1986, Character and setting of sand and gravel bed forms on the open continental shelf off Western Canada: in Knight, R.J., and Mclean, J.R., eds., Shelf sands and sandstones: Canadian Soc. Petroleum Geologists, Memoir 11, p. 45-55.

Madsen, O.S., and Grant, W.D., 1976, Quantitative description of sediment transport by waves: Proceedings 15th Coastal Engineering Conference, p. 1093-1112.

Martin, A.K., and Flemming, B.W., 1986, The Holocene shelf sediment wedge off the south and east coast of South Africa: in Knight, R.J., and Mclean, J.R., eds., Shelf sands and sandstones: Canadian Soc. Petroleum Geologists, Memoir 11, p. 27-44.

McGookey, D.P., *et al,* 1972, Cretaceous System: in Mallory, W.W., ed., Geologic Atlas of the Rocky Mountain Region: Rocky Mountain Assoc. Geologists, p. 190-228.

McLane, M.J., 1982, Upper Cretaceous coastal deposits in south-central Colorado--Codell and Juana Lopez Members of the Carlile Shale: Am. Assoc. Petroleum Geologists Bull., v. 66, no. 1, p. 71-90.

McLane, M.J., 1983, Codell and Juana Lopez in south-central Colorado in Mid-Cretaceous Codell Sandstone Member of the Carlile Shale, eastern Colorado-Spring Field Trip Guidebook, Rocky Mountain Section, Soc., Econ., Paleon., Miner., p. 49-66.

Merewether, E.A., Cobban, W.A., and Cavanaugh, E.T., 1979, Frontier Formation and equivalent rocks in eastern Wyoming: The Mountain Geologist, v. 16, no. 3, p. 67-101.

Merewether, E.A., and Cobban, W.A., 1983, Mid-Cretaceous biostratigraphic units, unconformities, and diastrophism: Am. Assoc. Petroleum Geologists, V. 67, no.3, p. 513.

Miall, A.D., 1986, Eustatic sea level changes interpreted from seismic stratigraphy: a critique of the methodology with particular reference to the North Sea Jurassic record: Am. Assoc. Petroleum Geologists Bull., v. 70, p. 131-137.

Morton, R.A., 1979, Subaerial storm deposits formed on barrier flats by wind-driven currents: Sedimentary Geology, no. 24, p. 105-122.

Morton, R.A., 1981, Formation of storm deposits by wind-forced currents in the Gulf of Mexico and the North Sea: in Nio, S.D., Shuttenhelm, R.T.E., and van Weering,

T. C.E., eds., Holocene Marine Sedimentation in the North Sea Basin: Int. Assoc. Sedimentologists, Spec. Pub. no. 5, p. 385-396.

Morton, R., and Jirik, L.A., 1989, Origin, depositional pattern and reservoir characteristics of middle Miocene shallow-marine sandstones, offshore south Texas: in Morton, R.A., and Nummedal, D., eds., shelf sedimentation, shelf sequences and related hydrocarbon accumulation, Gulf Coast Section, Soc. Econ. Paleon. Mineral., Seventh Annual Research Conf. Proc., 1989, p. 143-161.

Myrow, P.M., and Southard, J.B., 1988, Combined-flow model for vertical stratification sequences: in Shelf Sedimentation: Events and Rythms, Programs and Abstracts: Soc. Econ. Paleon. Miner. Research Conference, 1988, vol. 1, p. 29.

Niedoroda, A., Swift, D.J.P., and Thorne, J.A., 1989, Modeling shelf storm beds: contrals of bed thickness and bedding sequence: in Morton, R.A., and Nummedal, D., eds., Shelf sedimentation, shelf sequences and related hydrocarbon accumulation, Gulf Coast Section, Soc. Econ. Paleon. Mineral., Seventh Annual Research Conf. Proc., 1989, p. 15-36.

Nittrouer, C.A., *et al.*, 1986, Association of sand with mud deposits accumulating on Continental Shelves: in Knight, R.J., and Mclean, J.R., eds., Shelf sands and sandstones: Canadian Soc. Petroleum Geologists, Memoir 11, p. 17-25.

Nottvedt, A., and Kreisa, R.D., 1987, Model for the combined-flow origin of hummocky cross-stratification: Geology, v. 15, p. 357-361.

Nummedal, D., and Fischer, I.A., 1978, Process-Response models for depositional shorelines: the German and Georgia Bights: Proc. 16th Conf. Coastal Eng. II, p. 1215-1231.

Nummedal, D., Swift, D.J.P., and Kofron, B., 1989, Sequence stratigraphic interpretation of Coniacian strata in the San Juan basin, New Mexico: in Shelf sedimentation, shelf sequences and related hydrocarbon accumulation, Gulf Coast Section, Soc. Econ. Paleon. Mineral., Seventh Annual Research Conf. Proc., 1989, P. 175-202.

Nummedal, D., *et al.*, 1980, Geologic response to hurricane impact on low profile Gulf Coast barriers: Trans. Gulf Coast Assoc. Geological Soc., V. XXX, p. 183-195.

Payton, C.E., 1977, Seismic stratigraphy - application to hydrocarbon exploration: Am. Assoc. Petroleum Geologists Memoir 26, 516 p.

Perrodon, A., 1988, Dynamics of oil and gas accumulations: in Beaumont, E.A., and Foster, N.H., eds., Geochemistry: Am. Assoc. Petroleum Geologists, Treatise of Petroleum Geology, Reprint series no. 8, p. 3-26.

Pinel, M.J., 1977, Stratigraphy of the upper Carlile and lower Niobrara Formations (Upper Cretaceous), Fremont and Pueblo Counties, Colorado: Colorado School of Mines, Golden, Colorado, M.S. Thesis, T-1938.

Pinel, M.J., 1983a, Stratigraphy of some of the Carlile Shale and Niobrara Formation near Morrison, Colorado, in Mid-Cretaceous Codell Sandstone member of Carlile

Shale, eastern Colorado-Spring Field Trip Guidebook, Rocky Mountain Section, Soc., Econ., Paleo., and Miner., p. 14-25.

Pinel, M.J., 1983b, Stratigraphy of the upper Carlile Shale and lower Niobrara Formation, (Upper Cretaceous), Fremont and Pueblo Counties, Colorado: in Mid-Cretaceous Codell Sandstone member of the Carlile Shale, eastern Colorado-Spring Field Trip Guidebook, 1983: Rocky Mountain Section, Soc. Econ. Paleon. Miner., p. 67-95.

Porter, K.W., 1976, Marine shelf model, Hygiene Member of Pierre Shale, Upper Cretaceous, Dever Basin, Colorado: in Studies in Colorado Field Geology: Colorado School Mines Prof. Contr. No. 8, p. 251-263.

Reisser, K.O., 1976, Petrography and Diagenesis of the Codell Sandstone member of the Carlile Shale (Upper Cretaceous), southcentral Colorado: M.S. thesis, University of Nebraska, Lincoln, Nebraska, unpub.

Rice, D.D., 1988, Shelf sedimentation and Turonian (Late Cretaceous) sea-level fall, northeastern Wyoming and southwestern South Dakota: in Shelf Sedimentation: Events and Rythms, Programs and Abstracts: Soc. Econ. Paleon. Miner Research Conference, 1988, vol. 1, p. 35.

Rice, D.D., 1984, Widespread, shallow-marine, storm-generated sandstone units in the Upper Cretaceous Mosby Sandstone, Central Montana: in Tillman, R.W., and Siemers, C.T., eds., Siliclastic Shelf Sediments: Soc. Econ. Paleon. Miner. Special Pub. No. 34, p. 143-161.

Rice D., and Threlkeld, C., 1983, Character and origin of Natural Gas from upper Cretaceous Codell Sandstone, Denver Basin, Colorado: in Mid-Cretaceous Codell Sandstone member of the Carlile Shale, eastern Colorado-Spring Field Trip Guidebook, 1983,: Rocky Mountain Section, Soc. Econ. Paleon. Miner., p. 96-100.

Ritchie, J.G., 1986, Thermal maturity of Codell Sandstone - Carlile Shale interval (Cretaceous) in part of Denver basin, Colorado: Am. Assoc. Petroleum Geologists Bull., abstract, vol. 70, no. 8, p. 1052-1053.

Scott, G.R., and Cobban, W.A., 1965, Geologic and biostratigraphic map of the Mancos shale between Jarre Creek and Loveland, Colorado: U.S. Geological Survey Misc. Geol. Inv. Map I-439.

Snedden, J.W., 1985, Origin & sedimentary characteristics of discrete sand beds in modern sediments of the central Texas shelf: unpub. Ph.D. dissert, Louisiana State University, Baton Rouge, LA, 247 p.

Snedden, J., and Nummedal, D., 1989, Sand transport kinematics on the Texas continental shelf during Hurricane Carla, September 1961: in Morton, R.A., and Nummedal, D., eds., Shelf sedimentation, shelf sequences and related hydrocarbon accumulation, Gulf Coast Section, Soc. Econ. Paleon. Mineral., Seventh Annual Research Conf. Proc., 1989, p. 63-76.

Sternberg, R.W., 1972, Predicting initial motion and bedload transport of sediment in the marine environment: in Swift, D.J.P., *et al.*, eds., Shelf sediment transport, Dowden, Hutchinson, and Ross, Stroudsburg, PA., p. 61-82.

Sterns, D.W., 1978, Faulting and forced folding in the Rocky Mountain foreland, in Matthews, V. III, ed., Laramide folding associated with basement block faulting in the western United States., Geological Soc. America, Memoir 151, p. 1-38.

Swift, D.J.P., 1976, Coastal Sedimentation: in Marine Sediment Transport and Environmental Management, Stanley, D.J., and Swift, D.J.P., eds.,: Wiley and Sons, New York, p. 255-310.

Swift, D.J.P., and Rice, D.D., 1984, Sand bodies on muddy shelves: A model for sedimentation in the Western Interior Cretaceous Seaway in North America: in Tillman, R.W., and Siemers, C.T., eds., Siliclastic Shelf Sediments: Soc. Econ. Paleon. Miner., Special Pub, no. 34, p. 43-62.

Swift, D.J.P., and Niedoroda, A.W., 1985, Fluid and sediment dynamics on continental shelves: in Tillman, R.W., Swift, D.J.P., and Walker, R.G., eds., Shelf Sands and Sandstone Reservoirs: Soc. Econ. Palon. Miner. Short Course Notes, no. 13, p. 47-133.

Tillman, R.W., 1985a, A spectrum of shelf sands and sandstones, in Tillman, R.W., Swift, D.J.P., and Walker, R.G., eds., Shelf Sands and Sandstone Reservoirs: Soc. Econ. Paleon. Miner., Short Course Notes No. 13, p. 1-46.

Tillman, R.W., 1985b, The Tocito and Gallup Sandstones, New Mexico, a comparison: in Tillman, R.W., Swift, D.J.P., and Walker, R.G., eds., Shelf Sands and Sandstone Reservoirs: Soc. Econ. Paleon. Miner., Short Course Notes No. 13, p. 403-463.

Tillman, R.W., and Martinsen, R.S., 1984, The Shannon shelf ridge complex, Salt Creek Anticline area, Powder River Basin, Wyoming: in Tillman, R.W., and Siemers, C.T., eds., Siliclastic Shelf Sediments: Soc. Econ. Paleon. Miner., Special Pub. No. 34, p. 85-142.

Tweto, O., 1975, Laramide (Late Cretaceous-early Tertiary) Orogeny in the southern Rocky Mountains, in Curtis, B.F., ed., Cenozoic history of the southern Rocky Mountains: Geological Soc. America, Memoir 144, p. 1-44.

Vail, P.R., 1987, Seismic stratigraphy interpretation using sequence stratigraphy. Part 1: Seismic stratigraphy interpretation procedure: in Bally, A.W., ed., Atlas of Seismic stratigraphy , vol. 1, Am. Assoc. Petroleum Geologists Studies in Geology, no. 27, p. 1-10.

Van Wagoner, J.C., *et al.*, 1988, An overview of the fundamentals of sequence stratigraphy & key definitions: in Sea-Level changes: An integrated approach, Soc. Econ. Paleon. Miner. Special Pub. No. 42, p. 39-45.

Vincent, C.E., 1986, Processes affecting sand transport on a storm-dominated shelf: in Knight, R.J., and Mclean, J.R., eds., Shelf sands and sandstones: Canadian Soc. Petroleum Geologists, Memoir 11, p. 121-132.

Walker, R.G., 1984, Shelf and shallow marine sands: in Walker, R.G., ed., Facies Models, 2nd Edition: Geoscience Canada, Reprint Series No. 1, p. 141-170.

Walker, R.G., and Eyles, C., 1988, Geometry and facies of stacked shallow-marine sandier upward sequences dissected by erosion surface, Cardium formation, Willesden Green, Alberta: AAPG Bull., v. 72, No. 12, p. 1469-1494.

Warner, L.A., 1956, Tectonics of the Colorado Front Range: Geologic Record, Rocky Mountain Section, Am. Assoc. Petroleum Geologists, p. 129-144.

Weimer, R.J., 1960, Upper Cretaceous Stratigraphy, Rocky Mountain Area: Am. Assoc. Petroleum Geologist Bull., v. 44, no. 1, p. 1-20.

Weimer, R.J., 1978, Influence of Transcontinental Arch on Cretaceous Marine Sedimentation: a preliminary report, in Pruit, J.D., and Coffin, P.E., eds., Rocky Mountain Assoc. Geologists Symposium, Energy Resources of the Denver Basin, p. 211-222.

Weimer, R.J., 1983, Relation of unconformities, tectonics, and sea level changes, Cretaceous of Denver basin and adjacent areas in Reynolds, M.W., and E.D. Dolly, eds., Mesozoic paleogeography of west-central United States: Soc. Econ. Paleo. and Min., Rocky Mountain Section Sp Pub.

Weimer, R.J., and Sonnenberg, S.A., 1983, Codell Sandstone, A new exploration play, Denver Basin: in Mid-Cretaceous Codell Sandstone member of the Carlile Shale, eastern Colorado-Spring Field Trip Guidebook: Rocky Mountain Section, Soc. Econ. Paleon. Miner., p. 26- 48.

Wright, J.D., and Fields Jr., R.A., 1988, Production characterisitcs and economics of the Denver Julesburg Basin Codell/Niobrara Play: Soc. Petroleum Engineers: Jour. Petroleum Technology, Nov. 1988, p. 1457-1468.

APPENDIX

Cross-section A-A' -- Plate 2

Well Location & Formation Tops		Thickness
1. NeSeSw 1-2N-66W		
Niobrara -	7183'	267'
Carlile -	7450'	60'
Greenhorn -	7510'	212'
Graneros -	7722'	
2. Nw/4 25-3N-66W		
Niobrara -	7273'	210'
Carlile -	7483'	64'
Greenhorn -	7547'	223'
Graneros -	7770'	
3. SeSe 7-3N-65W		
Niobrara -	7090'	253'
Carlile -	7343'	57'
Greenhorn -	7400'	223'
Graneros -	7623'	
4. NwNw 9-4N-65W		
Niobrara -	6813'	307'
Carlile -	7120'	59'
Greenhorn -	7179'	241'
Graneros -	7420'	
5. NwNwSe 15-5N-65W		
Niobrara-	6905'	305'
Carlile-	7210'	61'
Greenhorn-	7271'	248'
Graneros-	7519'	

Well Location & Formation Tops		Thickness
6. SeSe 21-6N-65W		
Niobrara -	6745'	325'
Carlile -	7070'	50'
Greenhorn -	7120'	250'
Graneros -	7370'	
7. NeNe 4-6N-65W		
Niobrara -	6820'	300'
Carlile -	7120'	50'
Greenhorn -	7170'	240'
Graneros -	7410'	
8. SwNe 2-6N-64W		
Niobrara -	6700'	299'
Carlile -	6999'	46'
Greenhorn -	7045'	247'
Graneros -	7292'	
9. SeSe 26-7N-63W		
Niobrara -	6497'	277'
Carlile -	6774'	37'
Greenhorn -	6811'	244'
Graneros -	7055	
10. SwSw 2-7N-63W		
Niobrara -	6600'	304'
Carlile -	6904'	26'
Greenhorn -	6930'	263'
Graneros -	7193'	
11. NeSe 33-8N-63W		
Niobrara -	6683'	300'
Carlile -	6983'	27'
Greenhorn -	7010'	268'
Graneros -	7278'	

Well Location & Formation Tops		Thickness
12. SwNe 14-8N-62W		
Niobrara -	6652'	294'
Carlile -	6946'	22'
Greenhorn -	6968'	282'
Graneros -	7250'	
13. SwNw 35-9N-61W		
Niobrara -	6445'	305'
Carlile -	6750'	40'
Greenhorn -	6790'	282'
Graneros -	7072'	
14. NeSe 5-9N-61W		
Niobrara -	6440'	343'
Carlile -	6793'	17'
Greenhorn -	6810'	290'
Graneros -	7100	
15. SeNe 28-10N-60W		
Niobrara -	6410'	383'
Carlile -	6793'	47'
Greenhorn -	6840'	287'
Graneros -	7127'	
16. SwNw 11-10N-60W		
Niobrara -	6765'	370'
Carlile -	7135'	55'
Greenhorn -	7190'	246'
Graneros -	7410'	
17. NeNw 30-11N-59W		
Niobrara -	6560'	310'
Carlile -	6870'	65'
Greenhorn -	6935'	305'
Graneros -	7240'	

Well Location & Formation Tops		Thickness
18. NeNe 7-11N-59W		
Niobrara -	6620'	238'
Carlile -	6858'	92'
Greenhorn -	6950'	304'
Graneros -	7254'	
19. SeSe 35-12N-59W		
Niobrara -	6345'	245'
Carlile -	6590'	76'
Greenhorn -	6664'	306'
Graneros -	6970'	
20. SeNe 23-12N-59W		
Niobrara -	6383'	253'
Carlile -	7723'	87'
Greenhorn -	6710'	310'
Graneros -	7020'	
21. SeSeNw 20-12N-58W		
Niobrara -	6186'	284'
Carlile -	6470'	110'
Greenhorn -	6580'	288'
Graneros -	6868'	

Cross-section B-B'

Well Location & Formation Tops		Thickness
1. SeNwSw 9-4N-66W		
Niobrara -	6910'	340'
Carlile -	7250'	52'
Greenhorn -	7302'	233'
Graneros -	7535'	
2. SwSw 25-4N-65W		
Niobrara -	6765'	285'
Carlile -	7050'	62'
Greenhorn -	7112'	233'
Graneros -	7345'	
3. NeSwSw 32-4N-64W		
Niobrara -	6723'	279'
Carlile -	7002'	60'
Greenhorn -	7062'	228'
Graneros -	7290'	
4. NwSeSe 25-4N-64W		
Niobrara -	6522'	282'
Carlile -	6804'	54'
Greenhorn -	6858'	235'
Graneros -	7093'	
5. SwNeNe 28-4N-63W		
Niobrara -	6494'	281'
Carlile -	6775'	55'
Greenhorn -	6830'	242'
Graneros -	7072'	
6. NwNw 35-4N-60W		
Niobrara -	5540'	314'
Carlile -	5854'	43'
Greenhorn -	5397'	239'
Graneros -	6136'	

Well Location & Formation Tops		Thickness
7. NeNe 18-4N-59W		
Niobrara -	5400'	300'
Carlile -	5700'	60'
Greenhorn -	5760'	250'
Graneros -	6010	
8. NwSe 36-4N-59W		
Niobrara -	5780'	300'
Carlile -	5480'	68'
Greenhorn -	5548'	237'
Graneros -	5785'	
9. SeNw 33-4N-58W		
Niobrara -	4982'	308'
Carlile -	5290'	66'
Greenhorn -	5356'	234'
Graneros -	5590'	
10. NwSe 27-4N-57W		
Niobrara -	4668'	314'
Carlile -	4982'	71'
Greenhorn -	5053'	237'
Graneros -	5290'	
11. NwNeSw 18-4N-56W		
Niobrara -	4570'	340'
Carlile -	4910'	87'
Greenhorn -	4997'	210'
Graneros -	5202'	
12. NeNe 26-4N-56W		
Niobrara -	4342'	338'
Carlile -	4680'	80'
Greenhorn -	4760'	242'
Graneros -	5002'	

Well Location & Formation Tops		Thickness
13. NeSe 17-4N-55W		
Niobrara -	4128'	351'
Carlile -	4479'	111'
Greenhorn -	4590'	230'
Graneros -	4820'	
14. SwNe 34-4N-55W		
Niobrara -	4212'	328'
Carlile -	4540'	104'
Greenhorn -	4644'	236'
Graneros -	4880'	

Lithology relationships across basin axis

Codell Sandstone and Fort Hays Limestone

North-central Denver-Julesburg Basin, Colorado

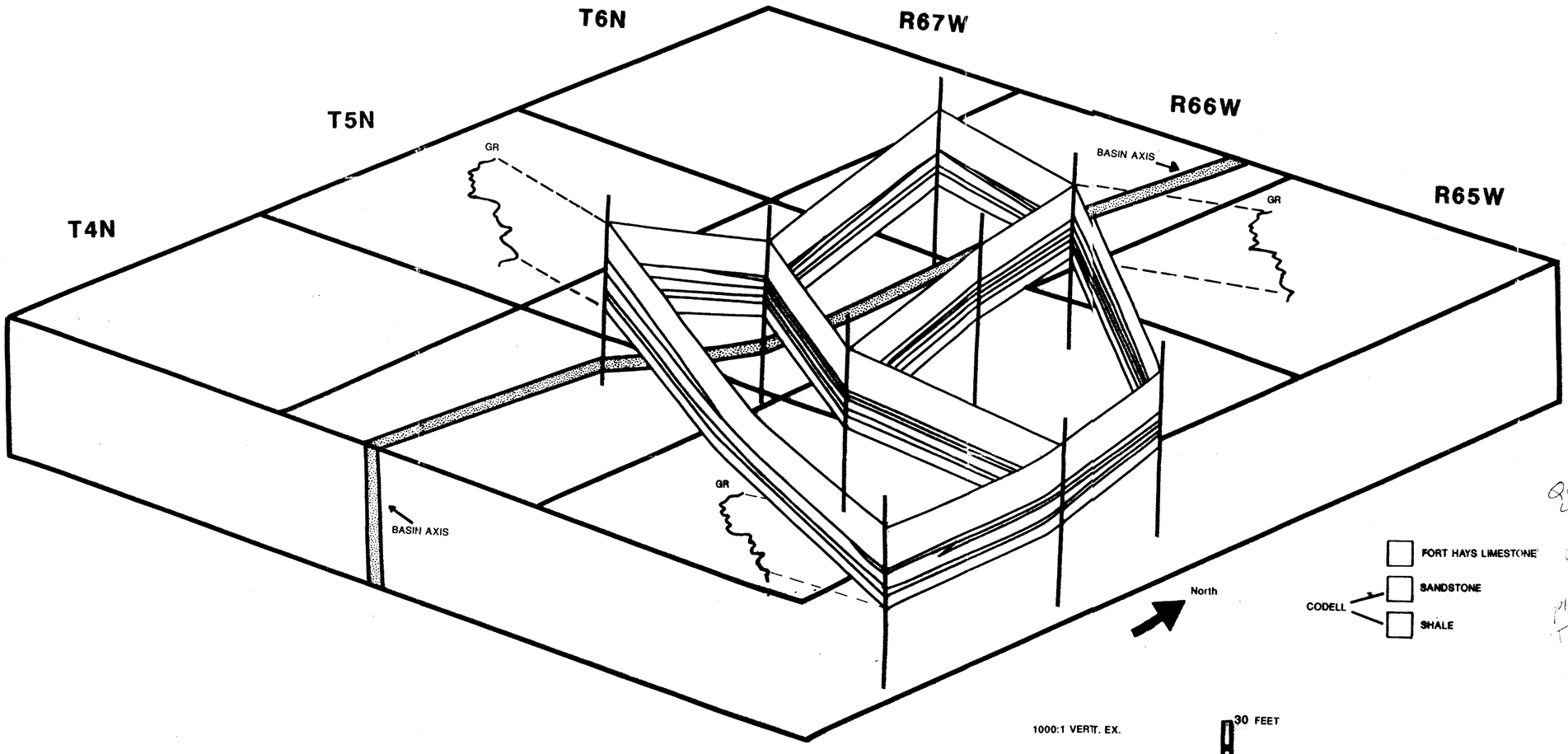

PLATE I

Codell Sandstone and Fort Hays Limestone

Fence Diagram

By D. Caraway,

Jan. 1988

A

Southwest

A'

Northeast

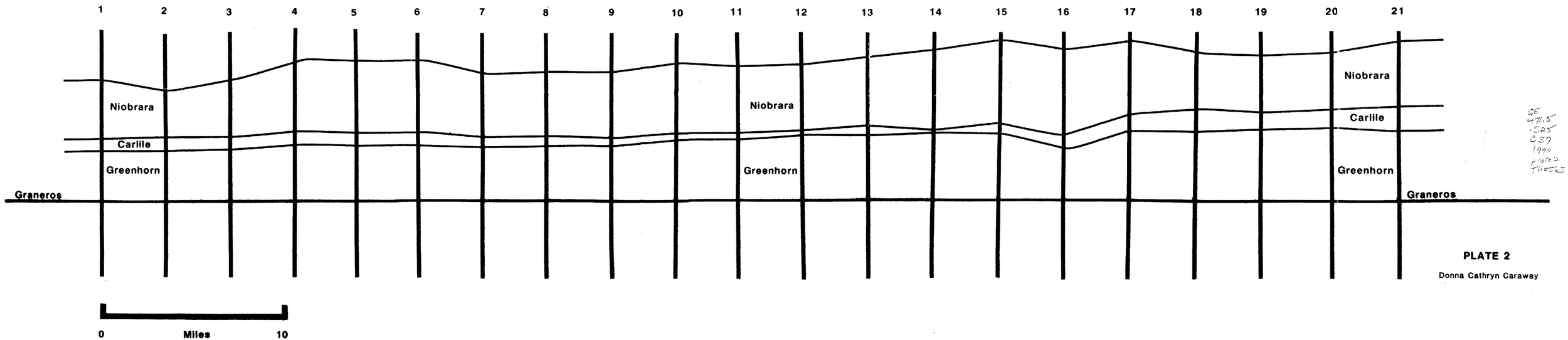

PLATE 2

Donna Cathryn Caraway

B

West

B'

East

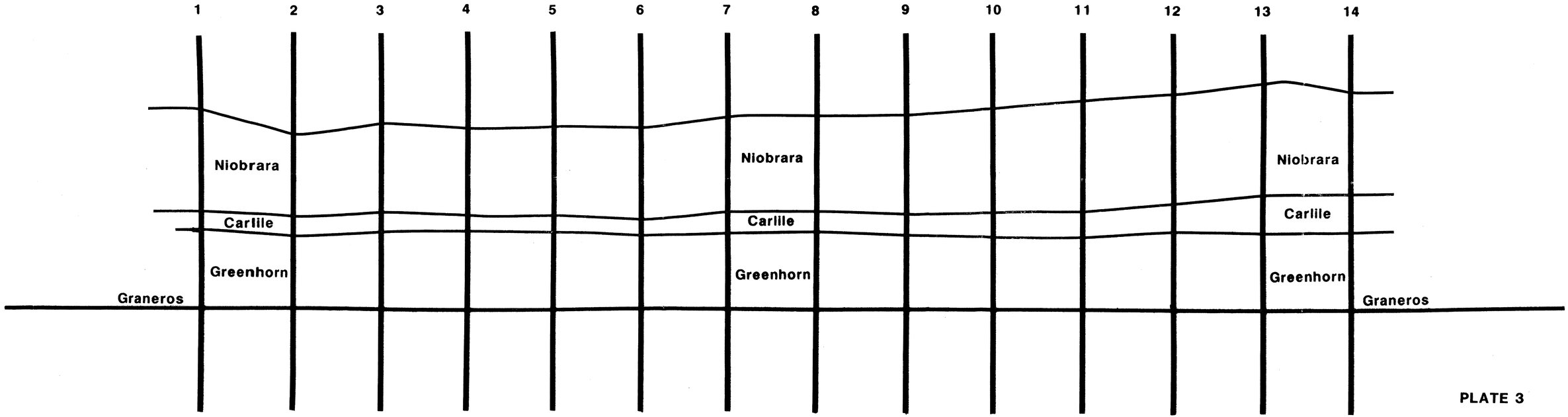

0 Miles 10

PLATE 3

Donna Cathryn Caraway